CRANFIELD UNIVERSITY

PHILIP JAMES DICKSON

GAS/LIQUID SEPARATION WITHIN A NOVEL AXIAL FLOW CYCLONE SEPARATOR

School of Mechanical Engineering

PhD Thesis

CONFIDENTIAL

CRANFIELD UNIVERSITY

SCHOOL OF MECHANICAL ENGINEERING
Department of Turbomachinery & Engineering Mechanics

PhD THESIS

Academic Year 1997-8

PHILIP JAMES DICKSON

GAS/LIQUID SEPARATION WITHIN A NOVEL AXIAL FLOW CYCLONE SEPARATOR

Supervisors:

Professor Robin Elder	Cranfield University
Mr Gerry McNulty	BHR Group Limited
Mr Sacha Sarshar	BHR Group Limited
Dr. David Ellix	Amerada Hess

CONFIDENTIAL

ABSTRACT

Cyclone separators have been described in detail and, although substantial research has been performed on solid / gas devices, the use of cyclones for gas / liquid separation has been comparatively ignored; this is particularly true for higher concentrations of liquid and for degassing applications. Consequently no generic models are available which will predict separation efficiency or pressure drop for all designs of cyclone.

A novel design of axial flow cyclone called WELLSEP was examined for the purpose of degassing. This design was not believed to be optimal and no design criteria or performance prediction models were available for it. An experimental programme was therefore produced and executed to investigate changes in geometry and the affect of fluid dynamics. Changes to the length, vortex finder and swirl generator were examined first and then one design was selected and tested over a number of liquid flow rates, Gas Void Fractions (GVFs) and liquid extractions.

Data was collected from the experiments which assisted in the development of semi-empirical models for the prediction of pressure drop and separation efficiency. These models could be used in the design of WELLSEP.

Geometric and fluid dynamics changes have both been shown to influence the performance of the tested cyclone. The principal conclusions that have been drawn from this research are:

- Of the tested designs, the design based upon a 30mm vortex finder diameter, settling chamber length of three times the diameter of the cyclone and a four start helix gave the optimum separation efficiency over the greatest range of conditions.

- The separation efficiency is affected by the superficial liquid velocity and the liquid extraction but not the GVF.

- The dimensionless pressure drop coefficient (Euler number) is a function of liquid extraction and GVF. It may also be a function of the superficial liquid velocity but it is

unproven by this research.

Separation :

"The process of forming a unit by itself,
not joined or united with others"

- Oxford English Dictionary

ACKNOWLEDGEMENTS

I would like to express my appreciation to all of my supervisors, for all of their help and guidance throughout this PhD. Many thanks also to all of my friends and colleagues at Caltec and BHR Group, who provided friendship, support and assistance which aided in my persistence up to the submission of this thesis.

Mostly I would like to thank Rachel Keitch for her support throughout the 'darkest' times of this PhD, and also my gratitude to my closest friends and my family for their faith, encouragement and foresight.

My special thanks to Martyn Witton for his assistance in completing this thesis and providing a fresh view on the subject.

DEFINITION OF TERMS

This thesis may refer to various terms which are defined below:

Classifier - A device designed to separate one solid from another. This is usually used with solids of differing particle size.

Critical liquid extraction - This is the point at which if the liquid extraction was increased, some gas would be present in the liquid removal line. A liquid extraction lower then this would still result in pure liquid being removed.

GVF - Gas Void Fraction, which is the also referred to as gas holdup.

Liquid extraction - Defined as the flow rate through the liquid removal line to the liquid feed flow rate.

Purge flow - This is the flow which carries the particle through the underflow. It is usually associated with solid particles as they require a transportation medium.

Re-entrainment - This is the process of separated particles in the outer radius becoming reintroduced (re-entrained) into the gas flow. This is a phenomenon which is undesirable if good separation is required.

Residence time - This is the time in which the mixture to be separated remains within the separator in order for satisfactory separation to occur.

Sharpness of separation - A measure of the effectiveness of separation of one substance from another.

Sharpness of cut - This refers to the ability of a classifier to separate one solid from another.

Throughput - This relates to the volume of flow which the separator can handle. It is proportional to the size of the separator - the bigger the separator the higher the throughput.

Turndown ratio - Defined as the ratio between the minimum and maximum gas flow at a certain minimum separation efficiency.

NOMENCLATURE

a	Gas inlet height	m
b	Gas inlet width	m
D	Diameter of cyclone	m
d_{50}	Cut diameter	m
Dx	Diameter of vortex finder	m
E_T	Total efficiency	-
Eu, ξ	Euler number	-
g	gravitational acceleration	ms^{-2}
H_g	Gas holdup	-
H_L	Liquid holdup	-
K	Drag per unit relative velocity per unit mass	$kgm^{-1}s^{-1}$
K_m	Stokes Cunningham Correction Path	-
Lb	Length of cyclone	m
Lv	Length of swirl generator	m
m	Mass of particle	kg
M	Feed mass flow rate	kgs^{-1}
Mc	Mass recovery	kgs^{-1}
N	Avagadro's number	-
P	Pressure	Pa
Qg	Gas volumetric flow rate	m^3s^{-1}
Ql	Liquid volumetric flow rate	m^3s^{-1}
r	Radial position	m
R	Radius	m
R	Gas Constant	$Jmol^{-1}K^{-1}$
Re	Reynolds number	-
S	Swirl number	-
Stk	Stokes number	-
Stk_{50}	Stokes number based upon d_{50}	-
t	time	s

T	Residence time	s
T	Temperature	K
u	Velocity component	ms^{-1}
U_r	Radial velocity	ms^{-1}
U_T	Tangential velocity	ms^{-1}
v	Velocity	ms^{-1}
v_m	Mixture or two phase velocity	ms^{-1}
v_{Sg}	Superficial gas velocity	ms^{-1}
v_{SL}	Superficial liquid velocity	ms^{-1}
x_g	Mass median of solids size distribution	m
X_m	Length of path	m
ΔP	Pressure drop or change	Pa, Bar
ε_h	Hydraulic efficiency	-
μ	Viscosity	Pa.s
ρ	Density	Kgm^{-3}
ρ_m	Mixture density	Kgm^{-3}
ϕ	Angle of fixed rotor blade to the axial direction	-

LIST OF FIGURES

LIST OF TABLES

CHAPTER ONE

1 INTRODUCTION

Cyclone separators have been used for many years on applications in the gas cleaning and mining and mineral industries. However their use has only recently been in oil and gas process engineering. Cyclone design, particularly for axial flow cyclones, has not yet been fully optimised for this application and is the basis for the work in this thesis.

Good separation of hydrocarbon oil, gas and its associated byproducts (water and sand) is an essential part of the oil production process. It can take place on land, top sides (offshore platforms) or subsea, although subsea applications are currently not as common as they may be in the future. Separation is also required in processes such as metering and transportation of the fluids, as well as arriving at the final stage of each separated phase. However, definite scope exists for improvement upon the conventional method used with gravity separators. Gravity separators are usually large, heavy devices which have high residence times. This may be acceptable on land-based oil production sites but on offshore platforms where size and weight is restricted, it is not.

With transportation, sand and other harmful byproducts can damage process equipment and therefore need to either be removed, or bypass the equipment. This means that some form of separation is required. Once separated these damaging byproducts could ideally be discharged subsea and not transported to the surface, but environmental laws prevent this. Instead they can be reinjected either into part of the subsea reservoir, or into the pipework downstream of the process equipment, and refined on the surface. Mixing these separated, harmful byproducts back into the cleaned flow may seem strange, but subsea pipework is very expensive and this way may be more economical than two pipes. Subsea removal of the byproducts is the most preferable method, as transportation of the un-required items is avoided. However, for this to occur extremely good separation is needed so that minimal amounts of oil or gas are lost with the byproducts once they are disposed.

Pumping multiphase mixtures, such as oil, gas and water, presents an additional challenge. The presence of gas in liquid can cause pumps to deprime or function less efficiently. However, removing gas upstream of a rotodynamic pump or jet pump can prevent this from occurring. Unlike sand, the gas is not a waste product and it is also required to be transported to the surface. Again, due to the high cost of subsea pipes, the separated gas/liquid mixture is usually reintroduced to the boosted flow downstream of the pumps and subsequent separation is performed on the surface.

Metering of the multiphase flow to determine the quantity of oil and gas production is another essential process. It is not only required for good management of the reservoir, but is also required for legal reasons such as government taxation. Some current multiphase flow meters firstly separate the phases before metering them independently. Such meters would also benefit from small, high efficiency, separators with low residence times.

Multiphase flow complicates the issue of separation quite dramatically. As well as all the initial problems with designing separators, there is also the problem that the flow may not be in a steady state. This means that at one moment in time, high volumes of gas (with a little liquid) could pass through the separator and the next high volumes liquid (with a small amount gas) will need to be separated. Velocities of the fluids entering the separator may also not be constant and a situation with pulsating flow can also arise. Therefore a separator potentially has to cope with constantly changing upstream conditions and still operate efficiently.

The size and weight of a separator are also important, particularly when it is to be installed on the platform of an offshore oil rig. This is because space is limited and supporting infrastructure is expensive. Therefore a smaller separator would be beneficial but not if it is at the detriment of its separation efficiency. Maintenance and reliability are other key factors which need to be considered in separator design, particularly in subsea applications. High costs are incurred if essential equipment on the sea bed malfunctions or requires servicing, and therefore moving parts are to be avoided as much as possible. The

downtime caused by maintenance problems also has financial implications as it can halt production.

Many hydrocarbon wells are abandoned before all of the oil has been removed. This is because the water production becomes too high with an ageing well and it is no longer economically viable to continue production. If good and reliable subsea separation techniques can be used then more of the oil in wells like these can be retrieved.

Cyclones are devices which use centrifugal force to separate and are usually small with a high separation efficiency. Previously they have been used in a number of other industries for well over a century yet have only really been considered in the oil and gas industry more recently. Unlike conventional gravity separators, cyclones are much smaller devices with low residence times. The size and weight problems have been mentioned before, but the residence time can be an important safety issue; this is because a separator with a low residence time does not need a large vessel storing the volatile hydrocarbons. Although many designs of cyclones have been available for some time, they also have limitations, particularly with pulsating gas/liquid flows. Therefore, an improvement in the design of cyclone separators is also in needed.

To tackle some of these problems a novel cyclonic separator known as WELLSEP has been designed by CALTEC. Its initial purpose was to remove gas from gas/liquid mixtures (degas) in order to improve the performance of pumps suffering from depriming, but its use is not only restricted to degassing. A number of other functions, such as gas/solid separation and demisting are also possible with the device, but it is the intention of this research project to investigate degassing. Even with the research narrowed down to just degassing there are still many different multiphase flow combinations which the separator may encounter.

The original design of WELLSEP is based on an understanding of the fluid dynamics of gas/liquid mixtures. It has been tested over a limited range of operating conditions, but

needs to be developed further for it to work efficiently over a wider range of phase fractions and flow rates.

The first chapters of this thesis will discuss various mechanisms of separation, but will focus upon cyclonic devices. The mathematical models previously derived by other authors will be introduced and appraised for their relevance to this application. The structure of the report will be in the form shown in Fig 1:

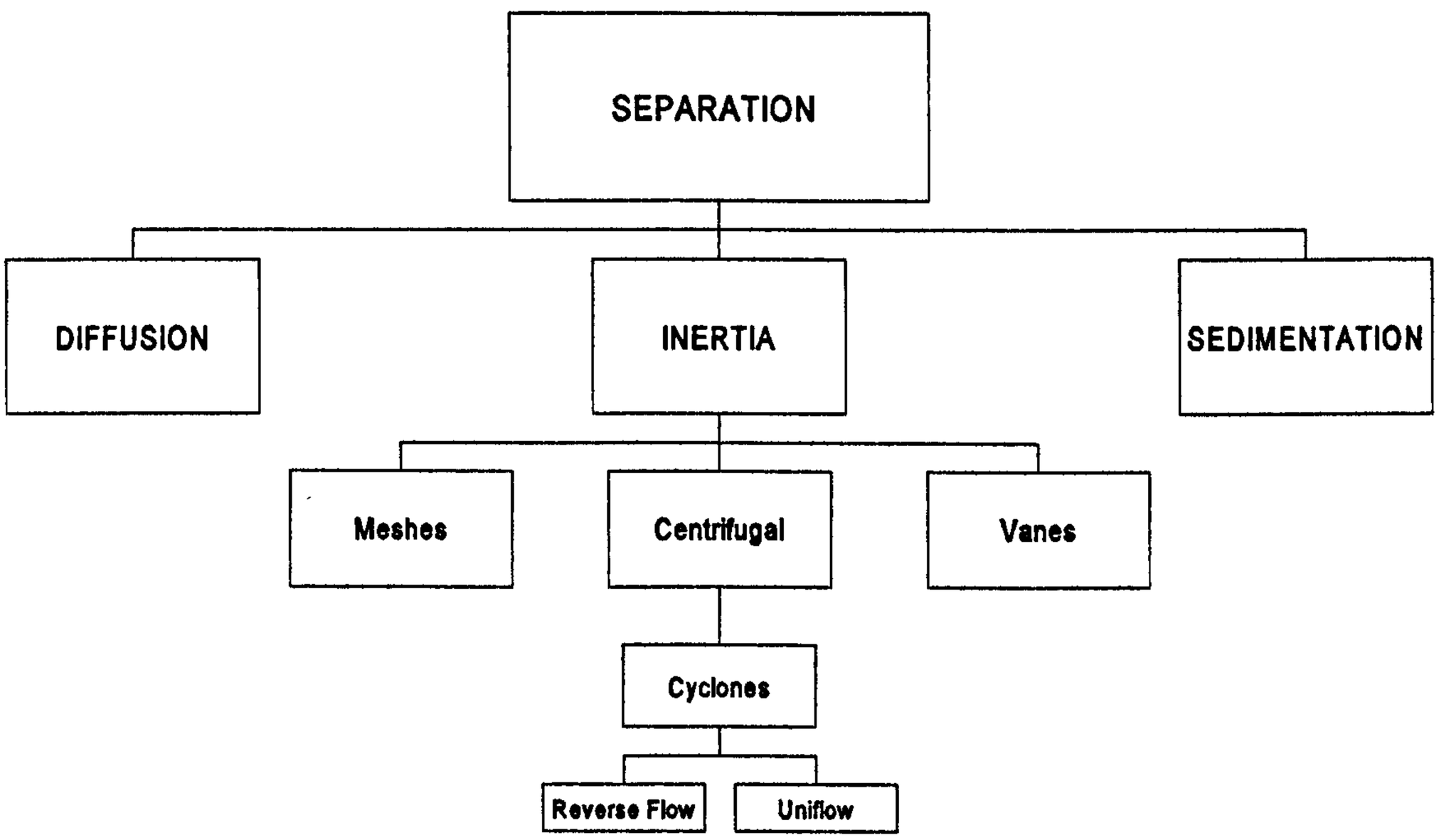

Figure 1: Structure of Theory Chapters

1.1 SEPARATION THEORY

1.1.1 Overview of the Section

This chapter briefly describes some of the processes and theories of separation. It provides a background to the subject of separation and then more specifically focuses on oil and gas separation.

The topic of separation is large and to discuss each method in detail would divert from the area of cyclones which is the most relevant to the work carried out in this research project. Therefore, this section briefly covers the main mechanisms of separation. Chapter two describes the different types of two phase flow regimes under which a separator might be expected to operate.

1.1.2 Mechanisms of Separation

Any separation process relies on the fact that the substances to be isolated are different in some way. Various designs of separators are available but the majority work upon three main principles or mechanisms:

i) Sedimentation or Gravity Settling.
ii) Diffusion.
iii) Inertia.

The correct combination of any of the above systems will enable satisfactory phase separation for almost any application.

Two other separation methods are ultrasonic agglomeration and the use of electrostatic forces. Although these have been applied successfully and could offer advantages, their

use is of less importance to present gas/liquid separation technology in the oil and gas industry. Consequently these two subjects will not be described any further in this report.

1.1.2.1 Sedimentation or Gravity Settling

Consider a mixture of solid, liquid and gas, with density decreasing respectively. Left to settle in a tank, the solid would fall and the gas would rise through the other two-phases. This is the simplest and most fundamental of all separation mechanisms, and upon which gravity settling depends. This method of separation, however, does have its limitations. It cannot always separate smaller particle sizes, and usually requires a large vessel to store the mixture. The mixture must be allowed to settle undisturbed for some time (known as the residence time) before the individual phases are satisfactorily separated. It therefore follows that two common applications of this mechanism are:

i) Where the separation of smaller particles is not essential.

ii) In bulk separators, where another separator is employed downstream (compound separators) to remove the smaller particles.

1.1.2.2 Diffusion

This method is more commonly used in the separation of mixtures with low liquid concentrations and small particle diameter ($d_p < 1\mu m$). In these cases the small particles move randomly under Brownian motion and obey the equation:

$$X_m = \sqrt{\frac{4RTK_m t}{3\pi^2 \mu N D_p}} \qquad 1.1.2.2$$

where

X_m = length of path

K_m = Stokes Cunningham Correction Path; varies between 1- 5 depending on temperature and particle diameter.

N = Avagadro's number

R = Gas constant

t = time

D_p = Particle diameter

The effects of diffusion are very small and will only noticeably influence particles with diameters less than 0.5 μm.

1.1.2.3 Inertia

The principle of changing flow direction to create, or increase, forces acting on particles is used with the inertia method. It is usually employed to remove smaller particles than are required by sedimentation alone. Different ways of achieving this include:

i) Meshes.

ii) Vanes.

iii) Centrifugal Force.

1.1.2.3.1 Meshes

This method is generally used on gas/liquid mixtures, and works in the following way. When an obstruction, such as a wire mesh, is introduced into a flow it changes its direction. This can similarly be seen with a bridge support pier in a river. The gas can more readily change its direction to pass around the wire, whilst the heavier liquid droplets cannot, and impinge on the surface. The droplets form films on the wires and coalesce with each other, like rain droplets on a window. Once enough droplets have coalesced, gravity causes them to flow down towards a liquid removal line.

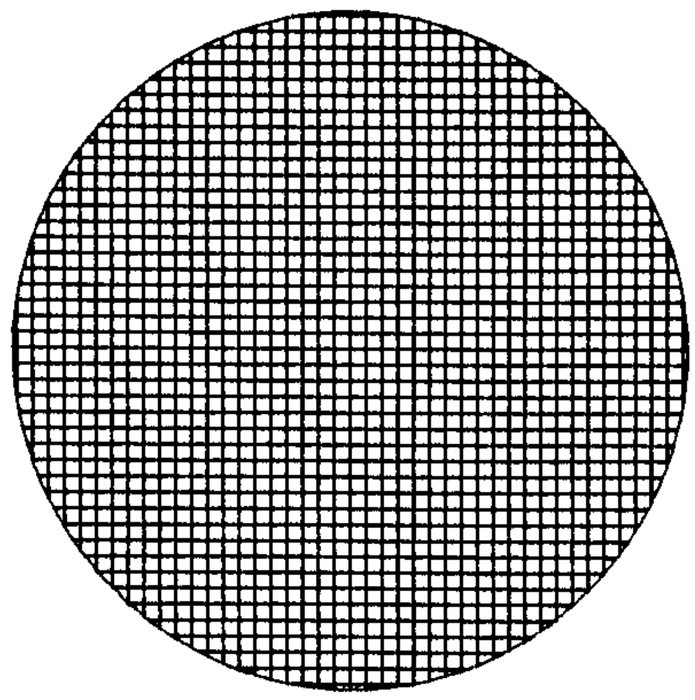

Figure 1.1-1 : Typical cross section of a mesh

1.1.2.3.2 Vanes

A typical vane-type separator has a series of meandering parallel plates throughout. The principle of separation can be seen in Fig 1.1-2. As the gas/liquid mixture flows between the plates, it is turned sharply by the bends in the plates. This causes the liquid droplets, which cannot change direction as easily as the gas, to impinge (as was seen with meshes).

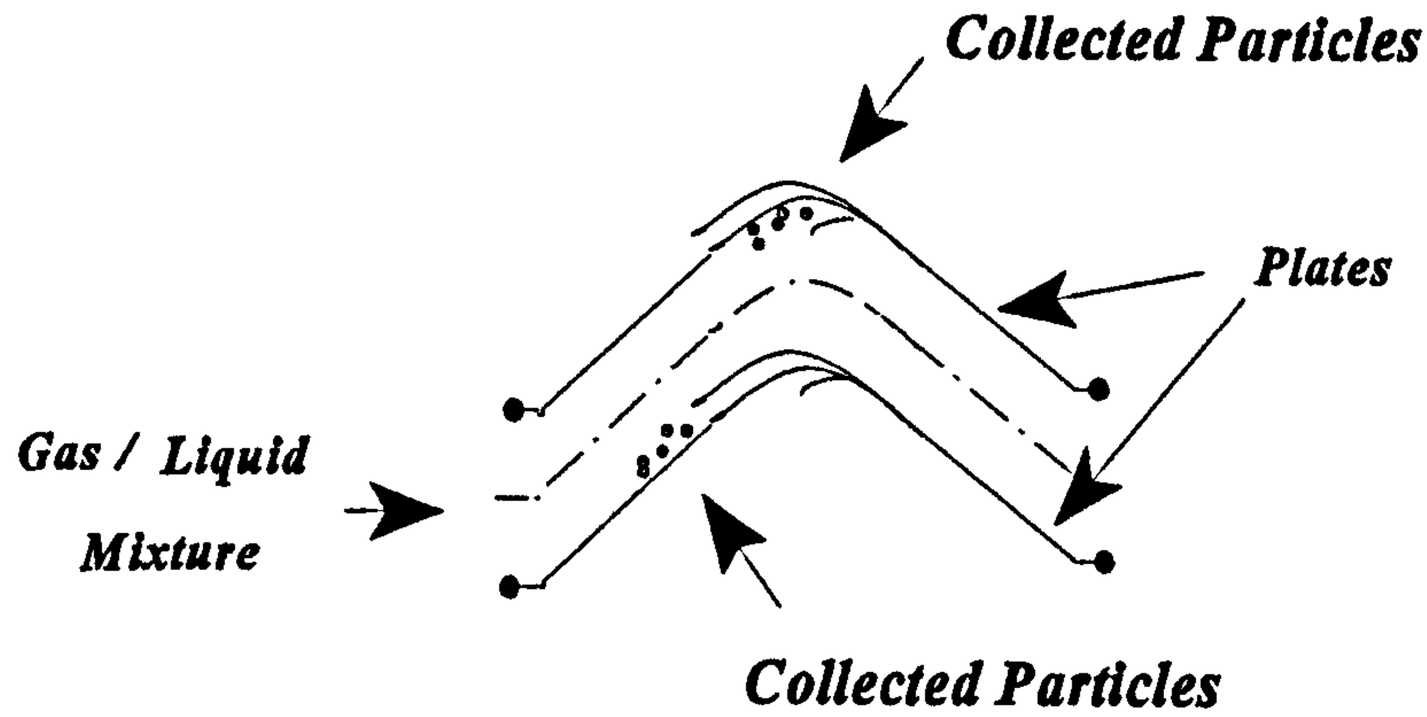

Figure 1.1-2 : Principle of Vane Separation

This continues until enough droplets have combined to give them sufficient weight to fall out of the gas stream.

1.1.2.3.3 Centrifugal Force

Probably the most exciting and ingenious method of separation is the centrifugal force mechanism. This is an inertial method that changes the direction of the particles to a circular or spiral path and hence exerts a centrifugal force on them. It is this force which causes the particles to separate. The effect is similar to the approach of a gravitational force, but the magnitude generated is often much greater. This can lead to reduced residence times without hindering the separation efficiency.

One complication is that creating high centrifugal forces leads to high turbulence, which causes shearing of the particles. The particle diameter may be decreased by this and, in turn, the efficiency of the separator reduced. Clearly a balance between the centrifugal force and the turbulence must be sought.

The centrifugal force required for this method may be generated by an external mechanical device (as with centrifuges) or by the fluids (the method normally used by cyclones). Some devices also use a combination of external mechanical and fluid energy to create the centrifugal force required for separation.

1.2 CYCLONES

The most common separator that implements centrifugal force is known as a cyclonic separator. A spiralling gas vortex differentiates it from other centrifugal separators. Cyclonic separators are simple, maintenance free, and inexpensive devices, which can be constructed from a wide range of materials. This makes them ideal for use in hostile environments. Phillips and Deakin (1991) compiled a list of the different materials from which the cyclones can be made.

Although there are many variations in the design of cyclonic separators, they all operate under a common principle. A spinning, pressurised, fluid mixture is introduced into the cyclone. The mixture consists of two or more different substances of different density which is spun to generate the centrifugal force. This causes the substances to separate radially with the most dense substance on the outside and the least at the centre, forming a core.

The merits of these devices are assessed in the table 1.2.

Advantages	Disadvantages
They are simple and cheap to purchase, install and run and require little maintenance.	Sensitive to fluctuations in pressure, flow rate & feed concentration.
No moving parts - which is reduces maintenance problems.	Prone to abrasion- particularly in the separation of solids.
High efficiency.	Shear produced in hydrocyclonic separation can prevent coalescence, which normally assists separation.
Low pressure losses.	Low throughput - although they can be manifolded
They are compact, saving space, and giving low residence times.	-
Can be installed horizontally or vertically with no effect on their performance.	-
Operate at higher pressure with no drop in efficiency	-

Table 1.2 : Advantages and Disadvantages of Cyclones

Cyclonic separators are extremely versatile and have many different applications. They can be used to:

a) Clarify liquids.

b) Concentrate slurries.

c) Classify solids.

d) Separate two immiscible liquids.

e) Degas liquids.

f) Demist gases.

The use of cyclonic separators has been extensively applied to the separation of dusts from gas streams, which is reflected in the literature reviewed. It should be remembered that some of the designs and processes being referred to in this report, are for this purpose. Nevertheless, they may be applicable to some cases of gas/liquid separation.

The technology used for dust/gas separation can be applied to gas/liquid separation for the following reason. In demisting or degassing processes, droplets or bubbles are considered as "particles" of liquids or gas, and the separation process involved is similar to solid/gas. Many of the designs and mathematical models derived are therefore comparable for both liquid and solid separation from gas streams. However the similarity between the different types of two-phase separation ends upon the collection of the substances, as the "particles" have different static and dynamic characteristics. Comparison between gas/liquid and gas/solid separation will also start to break down once the concentrations of gas or solid in the liquid become large. This is because the liquid will no longer be a finite particle but a continuous phase.

The way in which the mixture is removed governs which of the two following groups cyclones are sub-divided into:

i) Reverse Flow Cyclones - Also referred to as "return flow" or "hydrocyclones".

Here the mixture enters typically a conical body tangentially and the less dense phase forms a core in the centre which travels to the bottom of the cyclone where it reverses its direction. It then travels in the opposite direction and exits through the top of the cyclone. Reverse flow cyclones are described in more depth in section 1.2.1.

ii) Axial Flow Cyclones - Also referred to as "straight through" or "uni-flow".

The axial flow cyclone has the mixture enter at one end, where it is spun by the

presence of a swirl generator (a fixed physical object designed to create a swirl).

As the mixture travels along the cyclone length it separates and the separated mixture leaves at the other end. Axial cyclones will be dealt with more fully in section 1.2.2.

Axial flow cyclones are the most relevant topic to the research work performed in this project, however there are areas of overlap with reverse flow cyclones and they will therefore be discussed first.

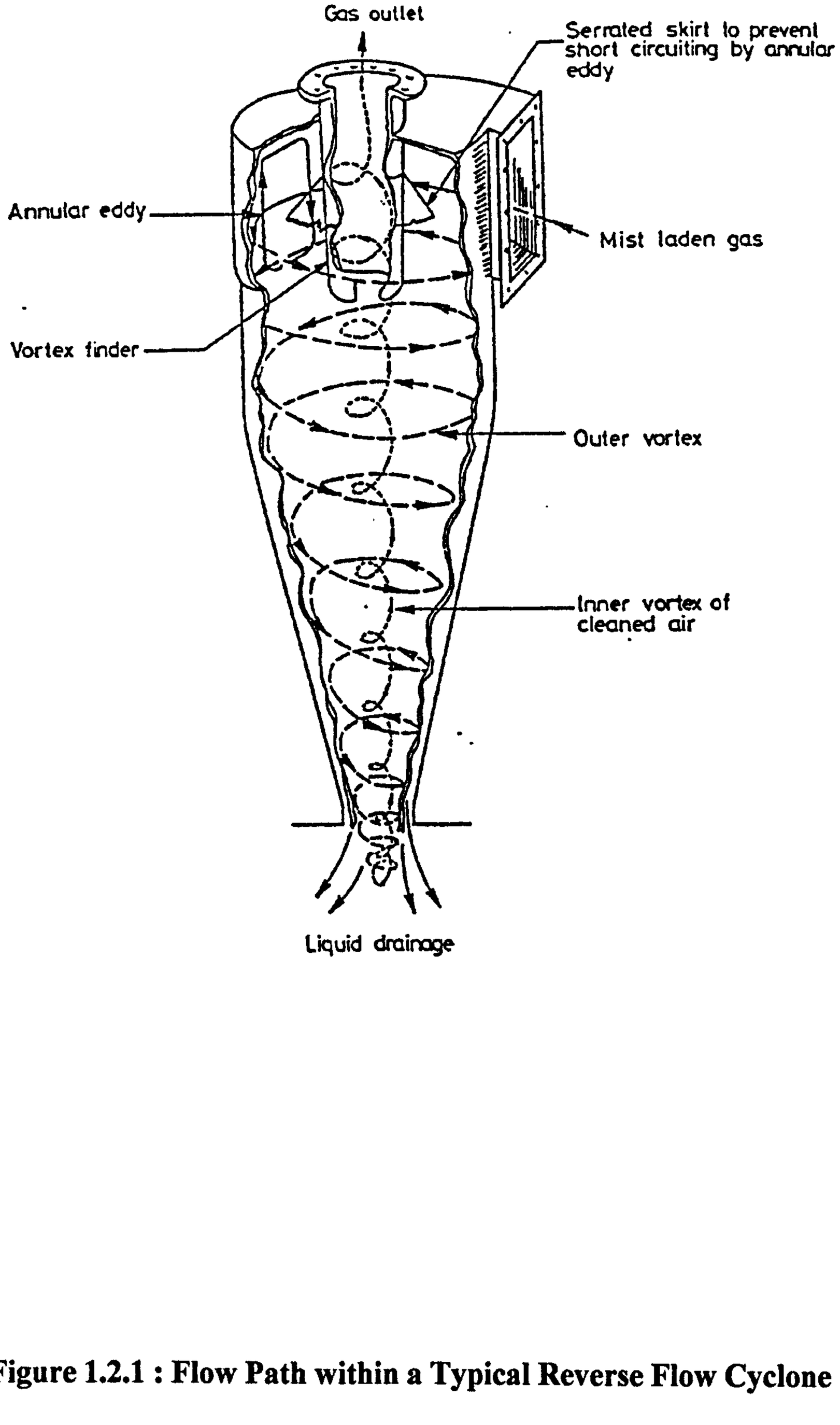

Figure 1.2.1 : Flow Path within a Typical Reverse Flow Cyclone

1.2.1 Reverse Flow Cyclones

The principle and basic design of reverse flow cyclones has been used for more than 100 years, but significant application in industry was not found until after the Second World War.

A typical arrangement of a reverse flow cyclone is illustrated in Fig 1.2-1. The flow enters the device tangentially - at the top of the device, and spirals down into a conical section. Just at the exit point (at the bottom) the flow separates - with some exiting through the "underflow" at the bottom and some reversing direction to flow back up towards the "overflow" exit (at the top). Two vortices are thus created (outer and inner) that spiral in opposite directions. This is one of the main differences between reverse and axial flow cyclones.

Initial applications of reverse flow cyclones centred on gas cleaning (removing particles from a gas stream). Solid/liquid reverse flow cyclones are used widely and more recently their use has been extended to gas/liquid and even liquid/liquid separation. Liquid cyclones are often referred to as hydrocyclones for the separation of liquid and solids, and are presently in common use. The name comes from "Hydraulic Cyclone" and has been conveniently shortened. Their principal use is in the separation of solids from liquids, typically in mining and mineral washing processing, although more recently they have been applied to other phases. Investigations by many researchers have been carried out and an abundance of experimental, theoretical, empirical, design and performance literature is available. Despite much research, the flow field and separation process within reverse flow cyclones are not fully understood. For this reason, research is still active on these devices. A number of theories have been suggested to describe the behaviour in reverse flow cyclones but as of yet there is no single model which will predict both the separation efficiency and pressure drop.

1.2.2 Axial flow cyclones

A typical axial flow cyclone design is shown in Fig 1.2-2. The flow path through the device is illustrated along with the characteristic dimensions.

The flow enters the cyclone to the left of the swirl generator which causes the fluid to spin. The flow then passes along the length of the settling chamber and the denser phase is forced to the outer radius; this is due to the centrifugal force, which is induced by the spinning flow. The denser phase passes through the lighter phase to the outer annulus in the same way that it would if left to settle under the gravitational force in a conventional separator.

The lighter phase exits through the vortex finder (Dx) and the denser phase through an outlet in the outer annulus at the same end. The fact that the flow is not reversed means that there can be a lower pressure drop than a reverse flow cyclone, but this can lead to a reduction in separation efficiency as found by Umney (1948).

The purge flow is shown to be through the outer annulus, which would be the case if the denser phase was wanted to be discarded (as with gas cleaning). However if the less dense phase is to be removed then the purge flow would exit through the vortex finder (in the central annulus).

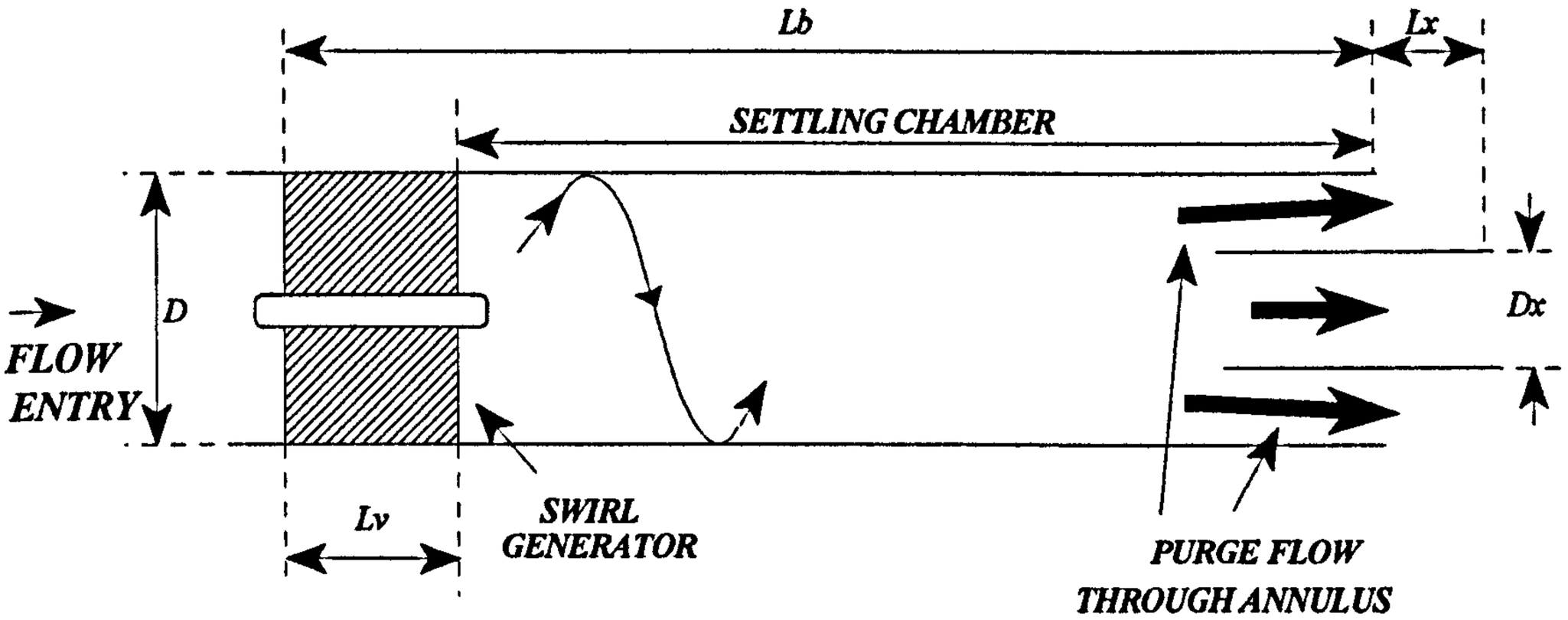

Figure 1.2-2 : Typical Axial Flow Cyclone Arrangement

Axial (or uniflow) cyclones have not been as widely used as the reverse flow type. Consequently, less research into these devices and their performance has been conducted; this would seem to indicate that their design has not been fully optimised. In fact many are only used as a primary 'bulk' separator which is followed by a high efficiency reverse flow cyclone to remove smaller particles. Axial flow cyclones can be more easily manifolded together into multi-cyclones due to their cylindrical body as opposed to the traditional conical shape of a reverse flow cyclone; this may also be helpful for use of cyclones downhole in oil and gas applications or in space restricted areas. The fact that both phases are exhausted from the cyclone at the same end can also reduce external pipework.

A change in any of the variables, shown in Fig 2.1-1, can affect the performance of the device, and the impact of this is discussed below.

1.2.2.1 Body Diameter

A reduction in the body diameter will result in an increase in the centrifugal force generated within the separator - as with all cyclones. The opposite is also true and the cyclone should therefore be sized accordingly. However too small a diameter will reduce the throughput and can result in trapped particles of dirt or wax blocking the flow, hence reducing the reliability of the device.

Jackson (1963) tested an axial cyclone with an angled settling chamber (ie increasing the diameter in the direction of flow). This is presumably to avoid the re-entrainment of particles back into the gas flow. The removal of solid particles, where particles can bounce off the wall of the cyclone and become re-entrained into the central core, is more likely to be affect this.

1.2.2.2 Cyclone Length

Daniels (1957) observed an increase in efficiency with an increase in length (L_b). A

length/diameter ratio approaching 5:1 was found to give the optimum efficiency, although higher ratios were not tested. Stenhouse & Trow (1985) also tested different settling chamber lengths and found that an optimum L_b/D of approximately 2.43 was achieved. The separation efficiency deteriorated above and below this. It should also be noted that both tests were undertaken with solids and gas.

The pressure drop across the cyclone is also affected by the settling chamber length, according to Plekhov (1971). He found the lowest drop to occur when $1.0 \leq L/D \leq 1.3$ for the design of cyclone he tested.

1.2.2.3 Swirl Generators

To generate the required swirling flow within axial cyclones, a number of approaches have been tried. Fig 2.1-2 illustrates some of the methods found by Jackson (1963). Explanations for the designs shown seem to be lacking, and can only be found for the D.C.P. cyclone. This states that there is a large boss, in the centre of the vanes, to reduce the annulus around them. Higher velocities, and hence greater centrifugal forces will be caused in this area. Immediately after the vanes is a region of greater cross sectional area into which the gas flow expands. The velocity of the particles is not expected to reduce as rapidly as the gas and hence they should remain at the outer radius. This phenomenon was also experienced in the work of Nieuwstadt et al. (1995).

An extension of the vanes (within the swirl generator) beyond the point at which the swirl has been generated is not recommended by Smith (1961). Steeper vanes were also found to produce a more pronounced vortex, but an angle of 45° to the axis was concluded to be the optimum.

Violent spins were reported by Daniels (1957) and Alden (1959) to cause problems with coarser particles bouncing from the outside walls back into the gas core. This obviously led to a reduced collection efficiency.

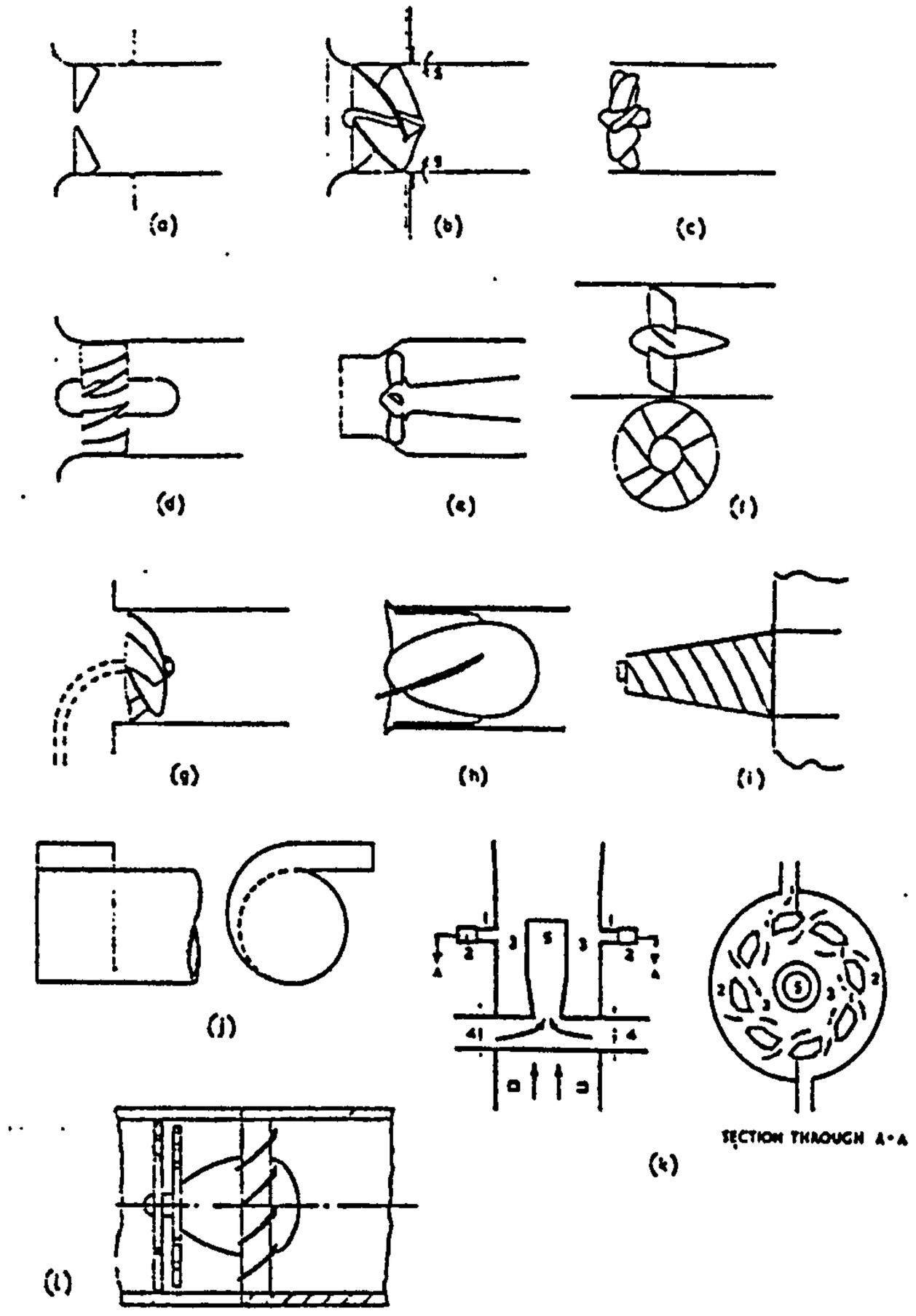

FIG. 4. VARIOUS FORMS OF CYCLONE INLET VANES.

(a) Ludgate (Sturtevant Engineering Co., Ltd.).
(b) Sirocco (Davidson & Co., Ltd.).
(c) Holmes-Rothemuhle (W. C. Holmes & Co., Ltd.).
(d) Multivortex (James Howden & Co., Ltd.).
(e) Cyclogalax (Ventil).
Tornado Cyclogalax (Keith Blackman, Ltd.).
(f) Alden (1959)
(g) Axial flow dust separator (Prat-Daniels (Stroud), Ltd.).
(h) D.C.P. Turbocell (Dust Control Processes, Ltd.).
(i) Cellular axial separator (Lasserre 1962).
(j) Tangential inlet cyclone (Daniels 1957).
(k) Turbine type jet spinner (Green & O'Driscoll 1959).
(l) Coalescent in-line separator (Kelburn Engineering Co., Ltd.).

Figure 1.2-3 : Various Forms of Cyclone Inlet Vanes. (Jackson 1963)

Swanborn (1988) also tested a number of swirl generating elements (shown in figure 1.2-4) and characterised their performance in terms of swirl number (S), hydraulic efficiency (ε_h) and pressure drop coefficient, (ξ) - which is the dimensionless pressure drop or Euler number. His results are shown in table 2.1.3. The first two values should be as high as possible whilst the pressure drop coefficient should be as low as possible.

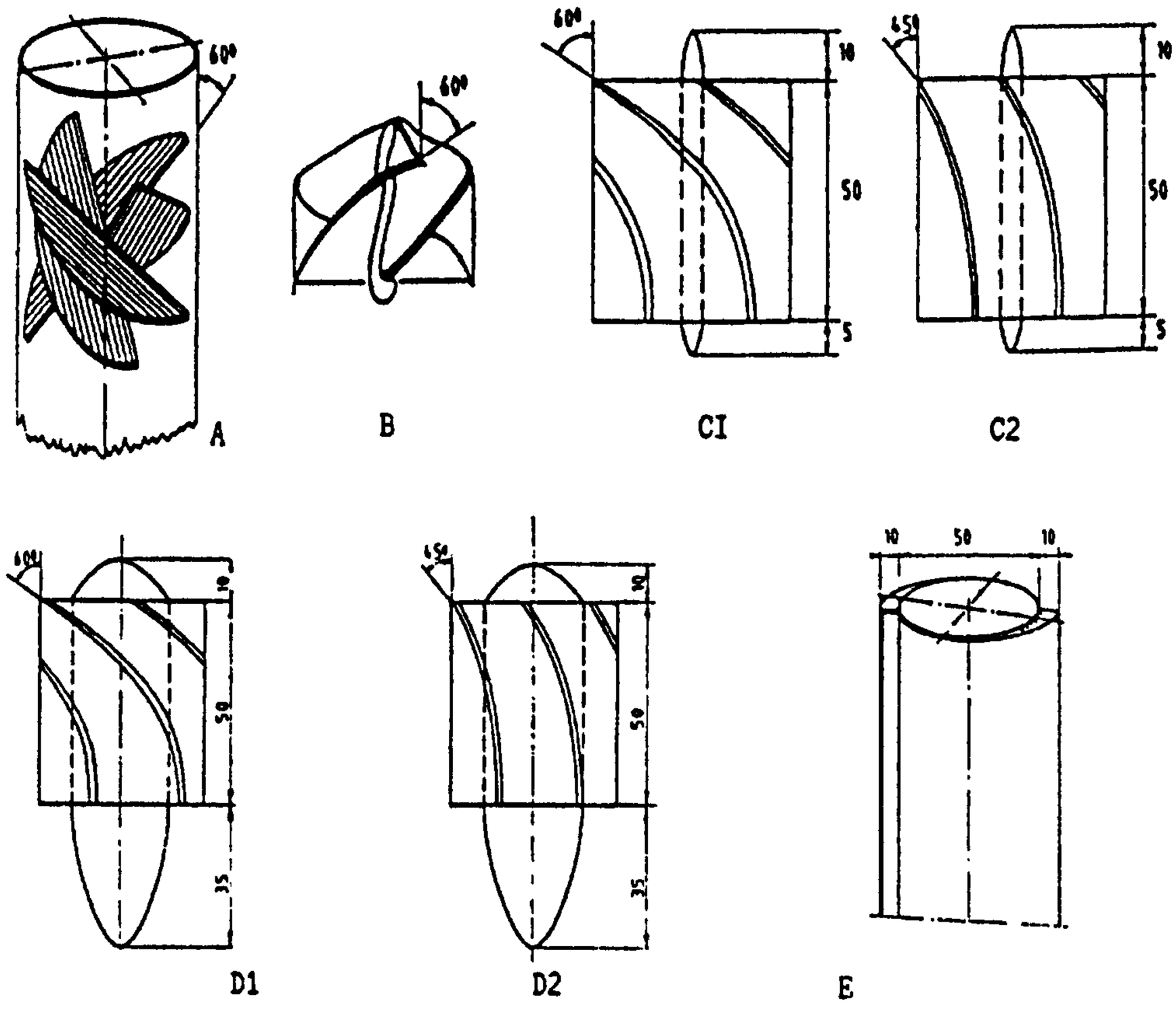

Figure 1.2-4 : Swirl Elements Used By Swanborn (1988)

Swirl Element	Swirl Number (S)	Hydraulic Efficiency (ε_h)	Pressure drop Coefficient (ξ)
A	1.0	0.4	12.2
B	1.2	0.5	6.1
C_1	0.8	0.6	3.2
C_2	0.5	0.9	1.1
D_1	2.0	0.7	9.1
D_2	1.2	0.9	2.7
E	1.1	0.8	5.6

Table 2.1-a : Characteristics of Swirl Elements Tested by Swanborn (1988)

1.2.2.4 Vortex Finder Diameter

Svarovsky (1984) states that the size of the vortex finder diameter on a reverse flow cyclone affects just about every performance characteristic. Although Svarovsky is not referring to axial cyclones, this is still applicable, as found by Stenhouse & Trow (1985) and Daniels (1957). Both authors found that the efficiency increased considerably as the vortex finder diameter was reduced. A higher pressure drop was also recorded but then it has long been recognised that there is a trade off between pressure drop and efficiency.

1.2.2.5 Exit Configuration

Once the separated mixture leaves the cyclone, it can be subjected to various processes. It is at this stage that the difference between solid/gas and liquid/gas separation becomes most apparent. Dust is often collected in a hopper directly from the exit, but liquid can be taken off through another pipe. Both solid and liquid particles can exit the axial flow cyclone coaxially or radially.

The coaxial exit is pretty straight forward and is illustrated in figure 1.2-2. The purged flow exits through an outer annulus. Radial exits on the other hand can be of different forms. Swanborn (1988) tested cyclones with both coaxial and radial exits. He found that at higher liquid concentrations the coaxial discharge suffered from heavy re-entrainment just before the vortex finder. The radial slits tested by Swanborn are in the outer body, along the length of the settling chamber (after the swirl generator). Figures 1.2-5 & 1.2-6 show cross sections through the body of the cyclones tested by Swanborn. He found that the tangential slits (figure 1.2-5) provided a much more efficient discharge than the radial slots (figure1.2-6). With the radial slots, droplets were observed to jump across them.

Another design of radial exit is for an involute arrangement to be employed at the end of the settling chamber. This can reduce the swirl from the flow after the separation has taken place and can offer pressure recovery.

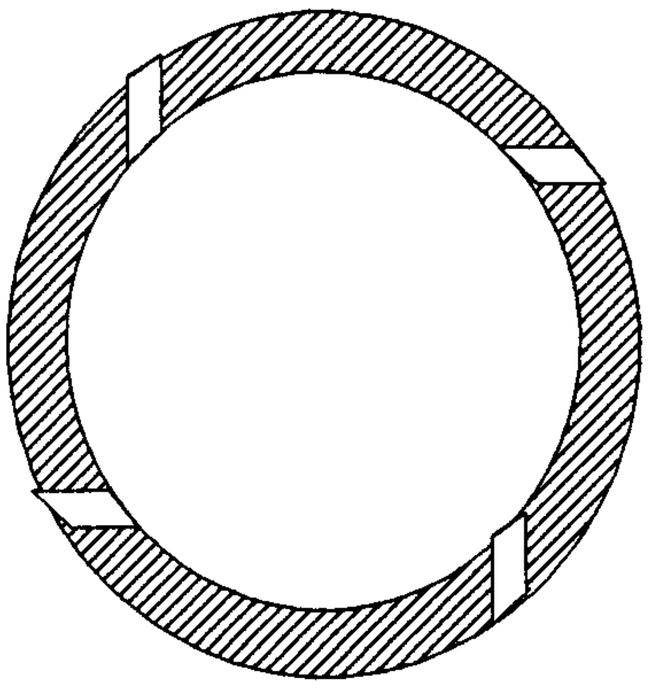

Figure 1.2-5 : Slits at a tangent

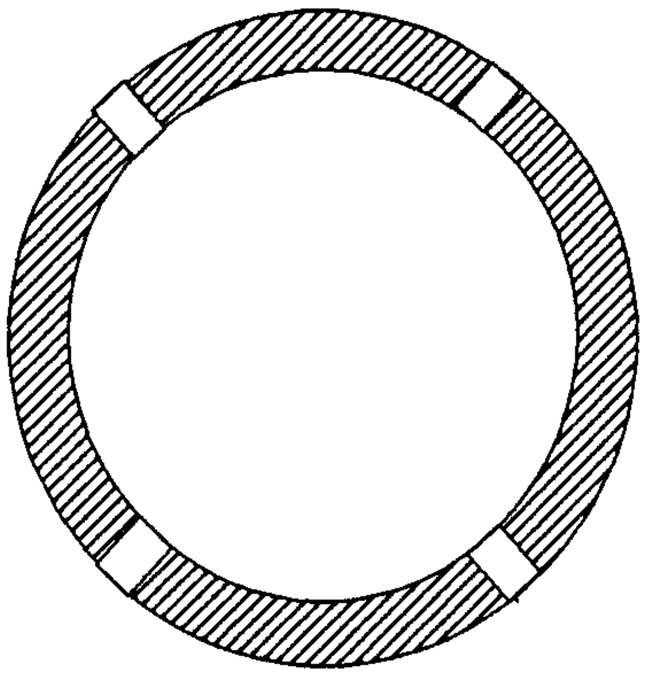

Figure 1.2-6 : Radial slits

Axial cyclones, in the past, have not shown as high a separation efficiency as reverse flow cyclones; they are therefore often succeeded by one of the three following recirculation systems:

(Note that the explanation given is in terms of solid/gas separation)

No recirculation - The solids are removed and collected in a hopper. No gas is purged with the solid, it just exits through the vortex finder and no further process is performed.

Partial recirculation - Most of the gas is removed through the vortex finder, but some is purged with the solids. The heavier particles fall from the purged stream and are collected in a hopper straight from the annulus outside the vortex finder. Smaller particles are carried in the purged flow and are then separated in a high efficiency separator.

Total recirculation - The purge gas carries all of the collected solids (coarse and fine) to another separator. The main gas flow exits through the vortex finder.

1.3 PERFORMANCE

The performance of separators is usually categorised by the pressure drop across them and their separation efficiency. Various ways of expressing the separation efficiency are used, depending upon the purpose of the separator. Dimensionless numbers are preferred (wherever possible) to describe both the pressure drop and separation; this is because scaling can be performed with dimensionless numbers.

1.3.1 Separation Efficiency

Although 100% separation is the goal for which to aim, it is rarely possible in cyclonic devices as well as many other separators. For gas/liquid separation there would normally be some gas in the underflow and some liquid in the overflow (referring to reverse flow cyclones). This is common with hydrocyclones used to separate solid from liquid. Even if all of the solid is removed through the underflow, it can be accompanied by an equal

amount (or more) of liquid.

It is usually expected, in areas outside of separation, that efficiency is given as one term. This relates the output as a percentage of the input. However, in the case of two-phase separation, there are two outputs, and hence two terms are necessary. For gas cleaning cyclones, only one term is given but a purge flow rate should also be stated.

1.3.2 Criteria Based on Recovery

Total Efficiency (Mass Recovery)

$$E_T = \frac{M_C}{M} \qquad 1.3.2$$

The above formula (1.3.2) expresses the total efficiency (E_T) as the rate of mass recovery in the underflow (Mc) over the feed flow of particles (M).

For this method to give a real understanding of which phase (liquid and gas) goes where, two terms should be given (one for each phase). As long as there is no accumulation they can be given in any two of the three lines (feed, overflow and underflow), and the other line can be calculated by a mass balance. This is illustrated in Fig 1.3-1 and Fig.1.3-2.

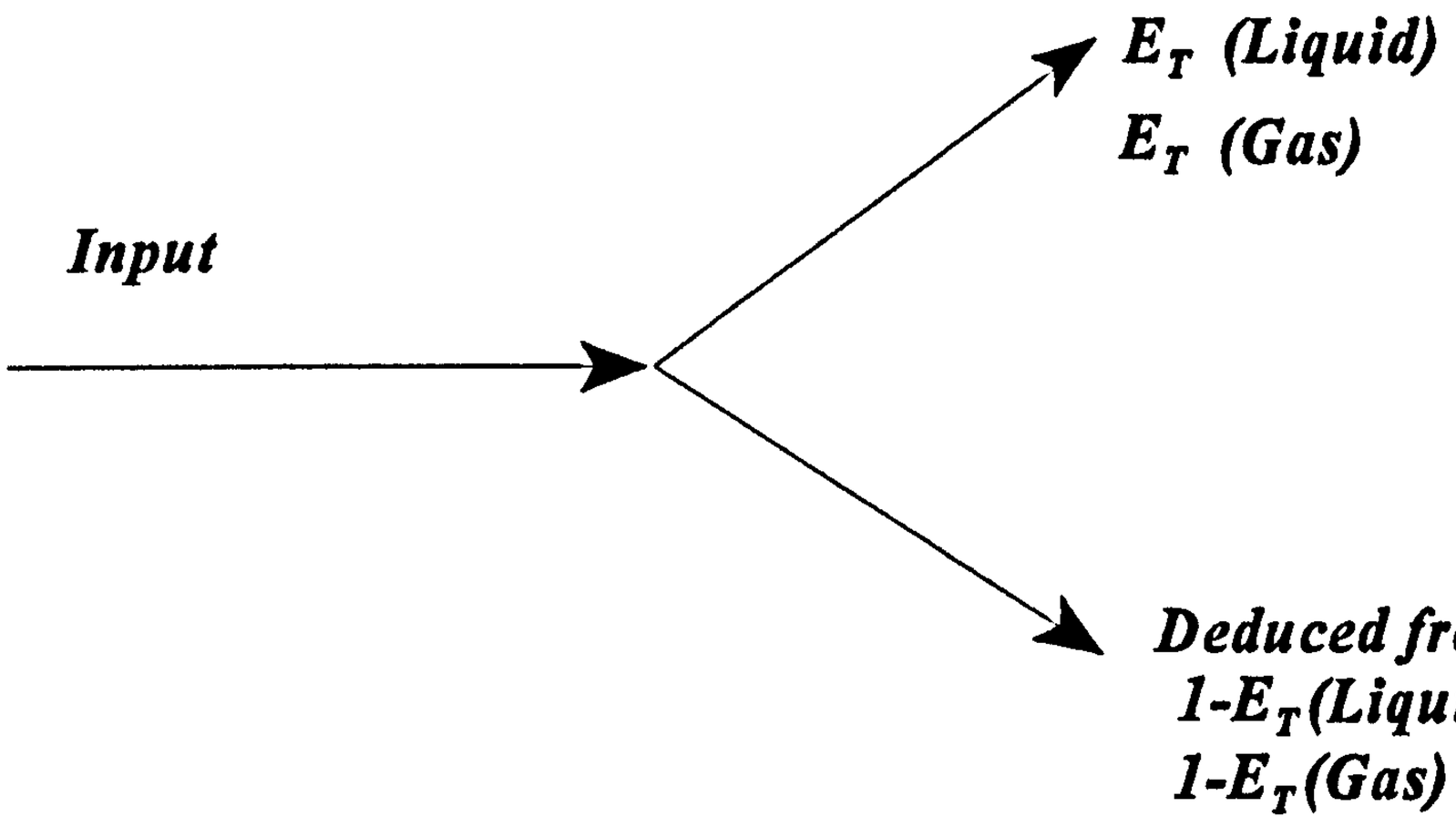

Figure 1.3-1 : Efficiency of Liquid and Gas given in one Outlet

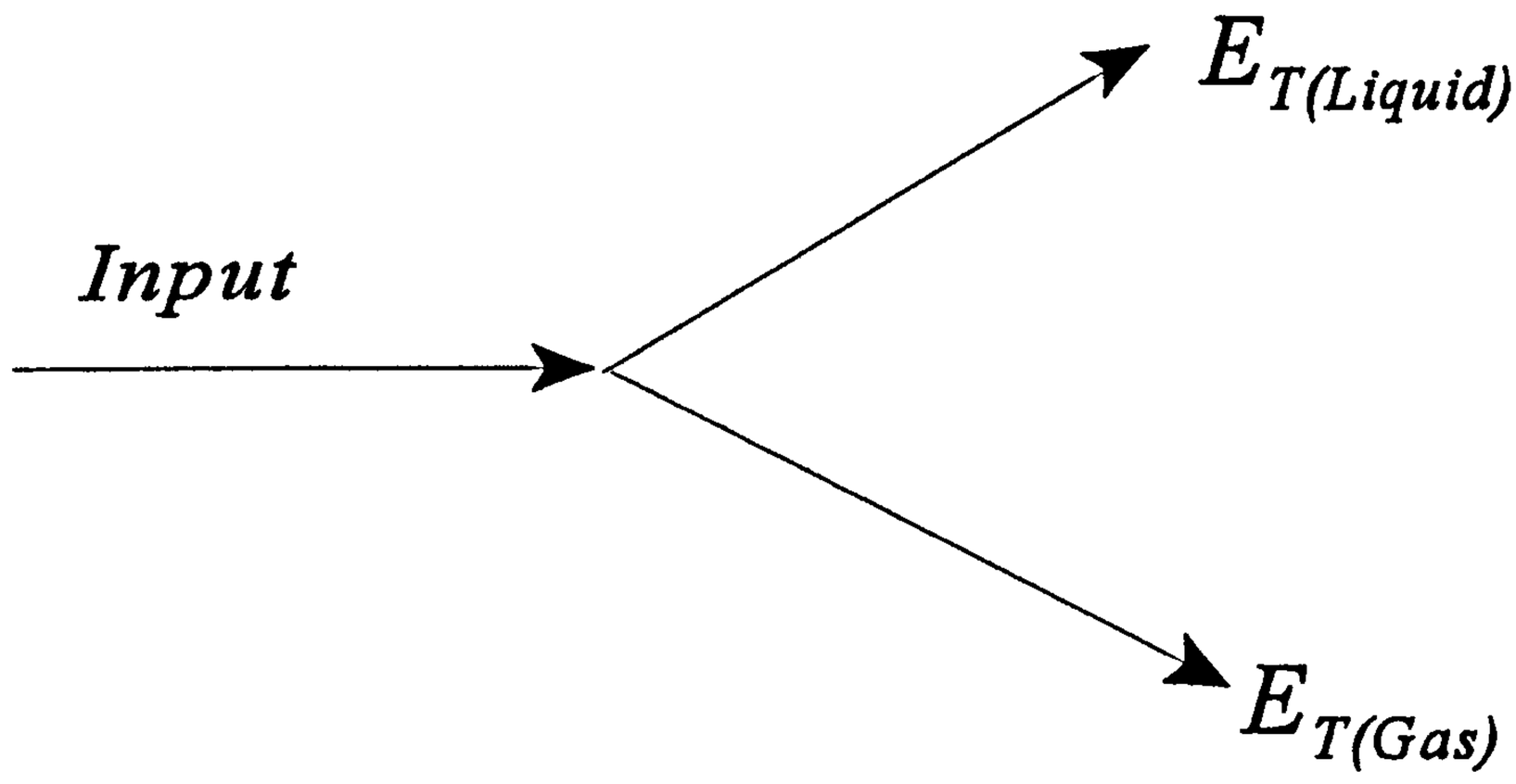

Figure 1.3-2 : Efficiency of Liquid given in one Outlet and Gas in Another

1.3.3 Cut diameter (d_{50})

The cut diameter is the size of particle that has an equal chance (50%) of being collected or escaping. Anything larger will also be collected, but smaller particles will not. It is a convenient method for comparing different units for a specific application but cannot be used as an accurate measure of the cyclones overall performance; this is because there is no precise indication of how it performs at other particle diameters.

1.3.4 Grade Efficiency Curve

Probably the most comprehensive description of a cyclones' collection efficiency is given by the grade efficiency curve. The performance is described over a range of particle sizes and not just one (as with the cut diameter approach). If compared with the inlet size distribution, an overall efficiency can also be calculated. Unfortunately, the grade efficiency curves are not easy to obtain - particularly for small particle sizes (<2μm). The inlet size distribution is also often unknown. This is a particular problem when dealing with liquid droplet sizes, and it will not be relevant if the concentration of liquid is high as there will be a continuous phase rather than dispersed droplets.

1.3.5 Pressure Drop (ΔP)

The pressure drop across a cyclone is the second important performance characteristic. It has long been recognised that it is inversely proportional to the separation efficiency but no detailed description of their exact relationship is given. The ideal situation would be total separation efficiency with no pressure drop, but in practise this is not possible.

The Euler number or loss coefficient is the preferred dimensionless number to characterise the pressure drop and is written:

$$\frac{\Delta P}{\frac{1}{2}\rho v^2} = \xi\ (Eu) \qquad 1.3.5$$

This is the static pressure drop divided by the dynamic pressure, where the characteristic velocity, v, is normally taken as the inlet velocity.

For cases of particle separation from gas streams in which there is a low loading of particles, the Euler number (Eu) is constant when plotted against the Reynolds number

(Re) (Loxham 1976). In the case of hydrocylones (reverse flow cyclone separating solid from liquid) there is an initial drop in Eu as Re increases and then a linear increase in Eu with increase Re (Svarovsky 1984).

1.4 APPLICATIONS

Many applications for cyclonic separators exist and it is usually this application which tailors their designs. Each particular function is often given a name, but these may vary with the industry in which they are used. As the possible manipulations of cyclonic devices is vast, only those used for gas/liquid separation are listed.

1.4.1 Scrubbing or Demisting

Normally associated with the thorough separation of liquids from gas flows, scrubbing can also refer to the removal of solids. Dehydration refers specifically to the removal of water from the gas. The term "demisting" is also used for the removal of liquid mists from gas flows, and this process is used in cleaning domestic gas.

Van Dongen and Ter Linden (1958) propose the following uses of a reverse flow cyclone separator designed by Ter Linden:

- Catalytic cracking feed preparation by vacuum flashing
- Distillation columns
- Thermal cracking - eg for separation of pitch from vapour
- Reduction of entrainment from a propane evaporator
- Pre-cleaner for improving heavily loaded scrubbers

In some metering applications (eg. turbine meters) the removal of mists from gas streams is essential for accurate mensuration. This application can also benefit from cyclone separators.

1.4.2 Degassing

This term is used for the total separation of gas bubbles from liquid flows, and this process is used where a pure liquid free from gas is required. This could be for maximising the efficiency of pumps and avoiding de-priming. Other applications are in the degassing of crude oil and for a number of processes in the chemical industry.

Bandyopadhyay *et al* (1994) describes a case in which hydrogen bubbles are needed to be separated from a sodium hydroxide electrolyte in an aqueous silver oxide battery.

Gas removal from roadside fuel pumps is an application suggested by Massingberd-Mundy *et al* (1992); the aim being to conform with new standards on gas volumes in petrol and diesel. However the results of their study illustrated that the cyclone used was not satisfactory.

1.5 MODELLING

This section will mention some of the empirical, semi-empirical, and theoretical models which have been developed for reverse flow cyclones. The limitations of the models will be discussed and the needed areas of understanding will be made apparent.

Visualisation and qualitative reports are widely available on cyclones. A number of researchers have also presented both mathematical and empirical models. However a generic model applicable to all geometric configurations of all cyclones (including both axial and reverse flow cyclones) has not been developed. Ideally a totally universal model would be available with factors which account for any geometry or flow possibilities amongst any phase. Realistically, however, this is a long way off and will not be possible until more understanding is available

The models that have been derived attempt to describe one of the two performance

characteristics, separation efficiency or pressure drop. Both theoretical models (which are based upon fundamental fluid mechanics) and empirical models (which are based upon experimental data) exist to describe both separation efficiency and pressure drop. Although neither of these types of model can be used universally, the empirical models tend to be more accurate than the theoretical ones, but are limited to one geometric design. The theoretical models, on the other hand, attempt to predict more generally to a number of designs, but their accuracy is usually limited to the cyclone used by the researcher when deriving their model. If this is the case then an empirical model which can provide a more accurate solution is just as useful but will not help towards the solution of one day having a totally generic model.

Various scaling methods have also been used in the past. Usually these consist of dimensionless numbers and can give good predictions for one particular cyclone of fixed geometric proportions. Unfortunately they also only tend to be applicable to one particular design and are not accurate in their prediction of pressure drop or efficiency for different geometric ratios. They use either the Stokes number (Stk) to scale on efficiency or the Euler number (Eu) to scale the pressure drop. Although this approach does not attempt to understand the fluid mechanics involved, it is applicable for the design of a separator to a customers needs. Experimental data is needed for scaling the design in this method.

1.5.1 Separation Efficiency and Flow Modelling

To gain an understanding of how separation takes place within a cyclone, many researchers have first attempted to describe the flow field created. It is then usually assumed that small particles are influenced by this flow field, and even follow the path of the streamlines. This seems a reasonable assumption for cases with one dispersed phase within another continuous one. However, when concentrations of both phases are high, the models start to break down.

The first attempts at modelling flows within a cyclone were based upon solid particle

trajectories within reverse flow cyclones. Stern (1937) based his predictions on a laminar flow with no eddies. Seillan (1929), Lissman (1930) and Barth (1932) all assumed that vortices formed obeying the equation:

$$U_T \alpha r^{-n} \qquad 1.5.1$$

Where U_T = tangential velocity, r = radial position and $-1 \leq n \leq 1$ (where "forced" and "free" vortex is represented by n=-1 and n=1 respectively; anywhere in between represents a combination vortex).

1.5.1.1 Forced Vortex

This is shown by a fixed body of rotation (eg. a revolving record). If a line was drawn from the centre to the radius, it would not change shape as the body revolved. It is depicted by the equation:

$$U_T \alpha r \qquad 1.5.1.1a$$

or

$$\frac{U_T}{r} = const \qquad 1.5.1.1b$$

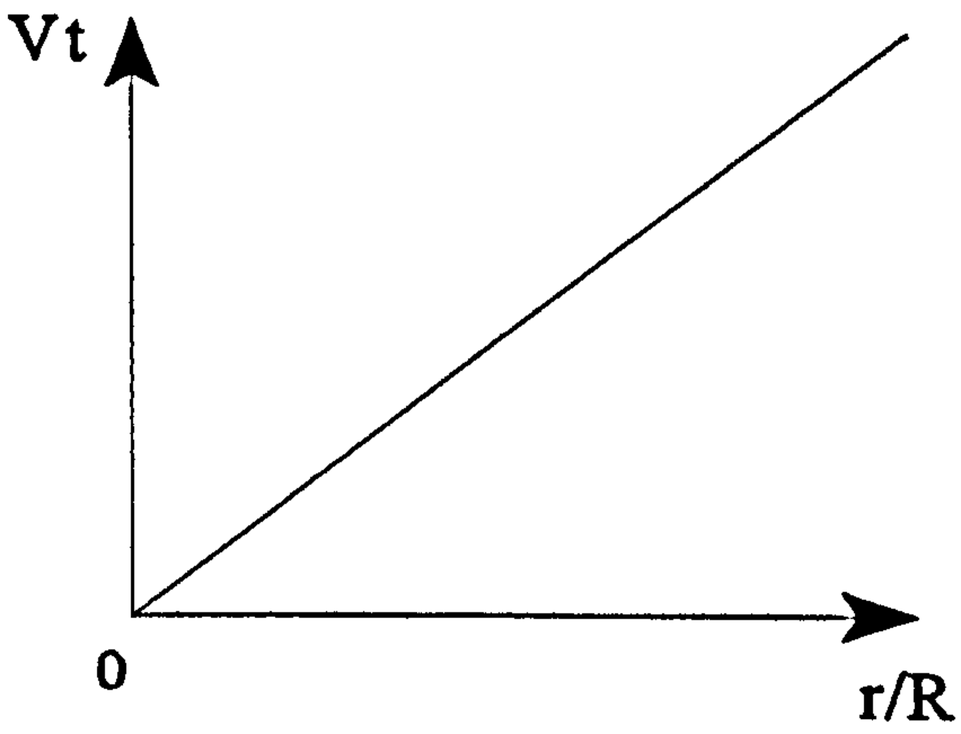

Figure 1.5-1 : Forced Vortex Tangential Velocity Profile

1.5.1.2 Free Vortex

A free vortex occurs when the tangential fluid velocity decreases from a maximum in the centre to a minimum radius. This is described by the Helmholtz equation for ideal separation:

$$U_T \alpha r^{-1} \qquad 1.5.1.2a$$

or

$$U_T r = const. \qquad 1.5.1.2b$$

With a free vortex a core usually forms in the middle, like water flowing down a plug hole.

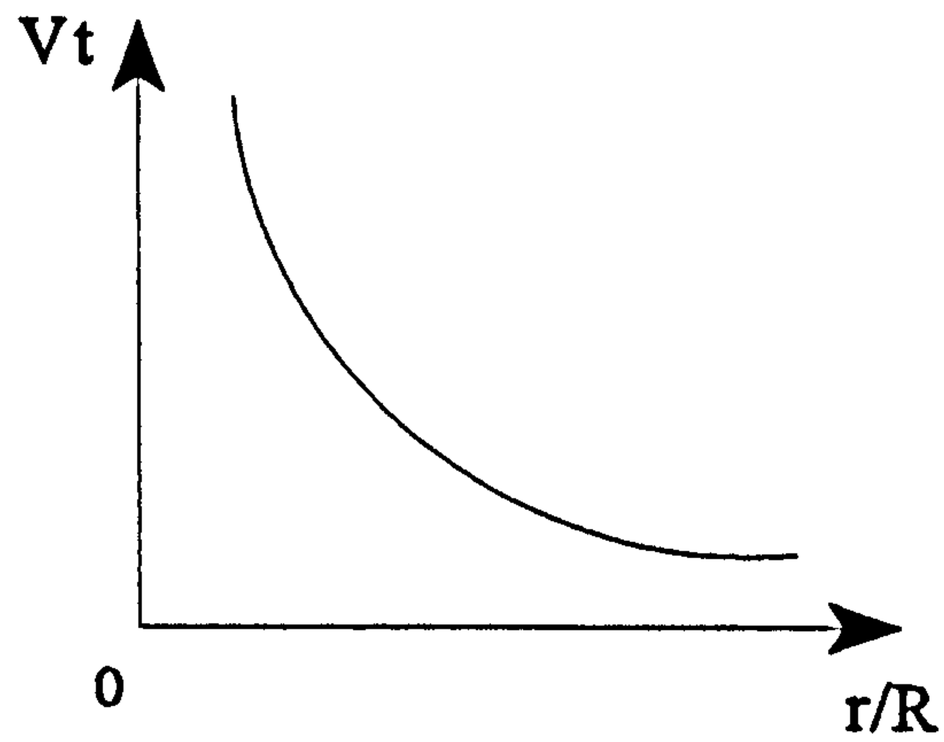

Figure 1.5-2 : Free Vortex Tangential Velocity Profile

1.5.1.3 Combined Vortex

Another possible vortex formation is where a combination of a free and a forced vortex is generated across the diameter of a cyclone. This usually occurs with a forced vortex in the central region and a free vortex outside of that. For this case the tangential velocity profile is shown in figure 1.5-3.

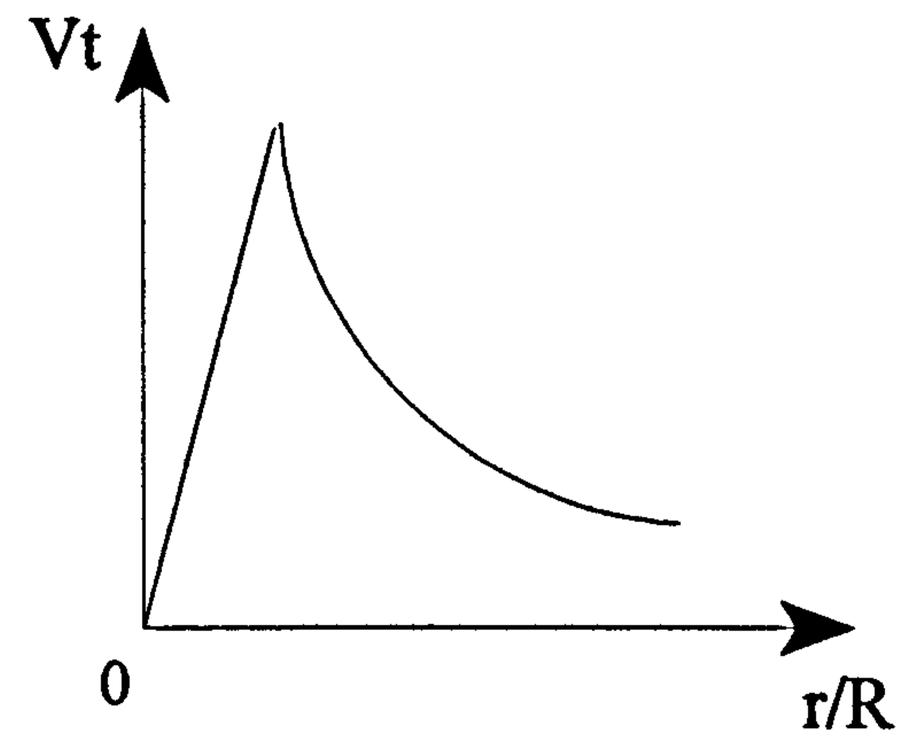

Figure 1.5-3 : Combined Vortex Velocity Profile

1.5.2 Reverse Flow Cyclones

Svarovsky (1996) has identified seven fundamental categories into which the physical models can be grouped:

i) Simple Fundamental Theories.
   - Equilibrium Orbit Theory.
   - Residence Time Theory.

ii) Turbulent two-phase Theory.

iii) Crowding Theory.

iv) Regression Models

v) Dimensionless Group Models

vi) Analytical Flow Models

vii) Numerical Simulations of Flow

Some of these apply specifically to reverse flow cyclones and others also apply to axial flow cyclones. Results varying from entire grade efficiency curves to just qualitative statements (in the case of crowding theory) are produced.

Most of the theories were derived for use with low concentration (less than 1%) of solid particles in a liquid flow, but modifications have since been made to allow for higher concentrations. Whenever possible, the final correlation is given in terms of dimensionless numbers (eg. Stk, Eu, Re).

1.5.2.1 Equilibrium Orbit Theory

According to this concept, originally proposed by Driessen (1951) and Criner (1950), particles of a given size attain an equilibrium radial orbit position where their terminal velocity (u_r) is equal to the radial velocity of the liquid (v_r). There is therefore a balance between the centrifugal and drag forces that, if Stokes' law is assumed, is governed by:

$$u_r = \tau \frac{v_t^2}{r} \qquad 1.5.2.1.1$$

where

$$\tau = \frac{\Delta \rho x^2}{18\mu} \qquad 1.5.2.1.2$$

Some correlations suggested by authors such as Bradley (1965) and Yoshioka & Hotta (1955) conclude that there is little or no affect on $Stk_{50}Eu$ by a change in the inlet diameter.

No account of the particle residence time in the cyclone is made in this theory, and all particles may not have reached their equilibrium orbit. An allowance for turbulence, which may also affect particle separation, has also been omitted.

Nevertheless, the theories based upon this approach are usually quite accurate at predicting cyclone performance at low concentrations. The results given by the proposers are also reproducible under similar conditions.

1.5.2.2 Residence Time Theory

Unlike the equilibrium orbit theory, equilibrium conditions are assumed not to occur in the residence time theory. Instead the possibility of a particle reaching the cyclone wall within the residence time available is considered. Rietema (1961) first suggested this theory and assumed a homogeneous distribution of all particles across the inlet. The cut size is stated as the size of particle which, if entering precisely in the centre of the inlet pipe, will just reach the wall in residence time T.

1.5.2.3 Turbulent Two-Phase Theory

The other theories do not take into account the affect of turbulence. Turbulent two-phase theory does, although it is not a theory in itself but more an adaption of other models including an affect for turbulence.

Rietema (1961) investigated its effect on tangential velocity profiles and concluded that turbulent diffusion may be neglected in residence time theory. Schubert and Neesse (1980) proposed a turbulent two-phase model as below:

$$Stk_{50} \cdot \sqrt{Eu} = 0.5676 \cdot k_d^2 \cdot \frac{\ln\left[0.91\left(\frac{D_o}{D_u}\right)^3\right]}{(1-c)^3 \cdot \sqrt{\rho}} \qquad 1.5.2.3.1$$

where

$$k_d = \left[220 x_g \left(\frac{\Delta\rho}{D}\right)^{0.5}\right]^m \qquad 1.5.2.3.2$$

and

x_g = mass median of solids size distribution

m = 5D for D<0.1m and m=0.5 for D≥0.1m

d_{50} = particle diameter size which stands a 50% chance of being collected

Stk_{50} = Stokes number based on d_{50}

They compared results from this expression to many published experimental ones and found it to be better for umbrella discharge than for rope discharge. Umbrella and rope discharge refer to the patterns generated within the flow and are characterised by their visual appearance (ie. Rope discharge looks like a rope).

1.5.2.4 Crowding Theory

Generally this theory attempts to allow for the underflow diameter's influence on the cut

size. It states that the cut size is a function of the capacity of the underflow orifice and of the particle size distribution of the feed, and was initiated crudely by Fahlstrom (1960). Bloor, Ingham and Laverack (1980) refined the theory creating a mathematical model of the flow which predicts particle trajectories within a cyclone.

1.5.2.5 Regression Models

Regression models are derived by performing lots of tests on various designs of cyclone. Lynch et al (1968, 1974,1975 and 1978) and Plitt (1976) performed such tests and obtained empirical models not in dimensionless form. The results were therefore only valid for the tests performed.

Svarovsky (1996) doesn't seem to favour this method but if the purpose is give an accurate description of one specific cyclone's performance then there is at present no better way of achieving this. Theoretical models attempt to describe the performance of all cyclone designs but none can currently perform that task accurately. This method is also useful for illustrating the operation range of one cyclone design more fully.

1.5.2.6 Dimensionless Group Models

The intention of the dimensionless group models is to be able to scale a cyclone of fixed geometric proportions to a number of sizes. One method uses an experimental constant called the cyclone number and predictions of better reliability are produced. This method can be used to calculate the required diameter of a cyclone for a given application, if the cut size and underflow concentration are specified. It is an ideal method for computational cyclone selection which is commercially used.

1.5.2.7 Analytical Flow Models

Mathematical solutions of the fundamental fluid mechanics are performed to provide analytical models. The pioneers of this method are Bloor and Ingham (1975) who have

published a number of papers on the subject. A number of assumptions were initially made, one of which (regarding the uniform distribution of momentum) Bloor himself later disproved.

This method has more recently been used less, in favour of numerical simulations.

1.5.2.8 Computational Fluid Dynamics

Computational Fluid Dynamics (CFD) is the process by which a computer attempts to solve the Navier-Stokes equations in order to predict a flow pattern. CFD is becoming more popular in many areas of modelling, especially with the power of computers increasing and consequently processing time being reduced. Many commercial packages are now widely available. Predictions made through CFD can eliminate the need for expensive experimental programmes. However, models created in this way do have to be calibrated initially against some experimental results and therefore do not completely rule out testing. An additional advantage of this form of modelling is that conditions which are not easy to simulate on a test rig can be more easily set up on a CFD package.

Often this method produces colourful velocity profile patterns, and can fool people into believing anything that is suggested by it. That is not to say that this technique cannot produce a good model of what is actually occurring with the fluids but that care should be taken when interpreting the results.

1.5.3 Axial Flow Cyclones

As with the reverse flow cyclones the attempts at modelling axial flow cyclones endeavour to predict one or both of the performance characteristics (separation efficiency or pressure drop). Once again, there is no comprehensive model for predicting separation efficiency and/or pressure drop for every design of axial flow cyclone.

1.5.3.1 Separation efficiency

Umney (1948) was the pioneer of describing particle collection mechanisms, and he used a residence time method which predicts the time it would take for a particle to reach the cyclone wall. With reference to Fig 1.5-6, he considered the forces acting on a particle P to be centrifugal acceleration and drag. For a particle whose cylindrical co-ordinates are given by (r,θ), these are described as in equilibrium (at time t) by,

in the radial direction:

$$-mK\frac{dr}{dt} = m\left[\frac{d^2r}{dt^2} - r\left(\frac{d\theta}{dt}\right)^2\right] \qquad 2.2.1.1$$

where m = mass of particle

K = drag per unit relative velocity per unit mass

and in the tangential direction:

$$-mK\left[\frac{rd\theta}{dt} - U_T\right] = m\left[\frac{rd^2\theta}{dt^2} + 2.\frac{dr}{dt}.\frac{d\theta}{dt}\right] \qquad 2.2.1.2$$

The minimum length of a cyclone could be determined, from these equations, by finding the time it took for a particle to move from r_1 to r_2.

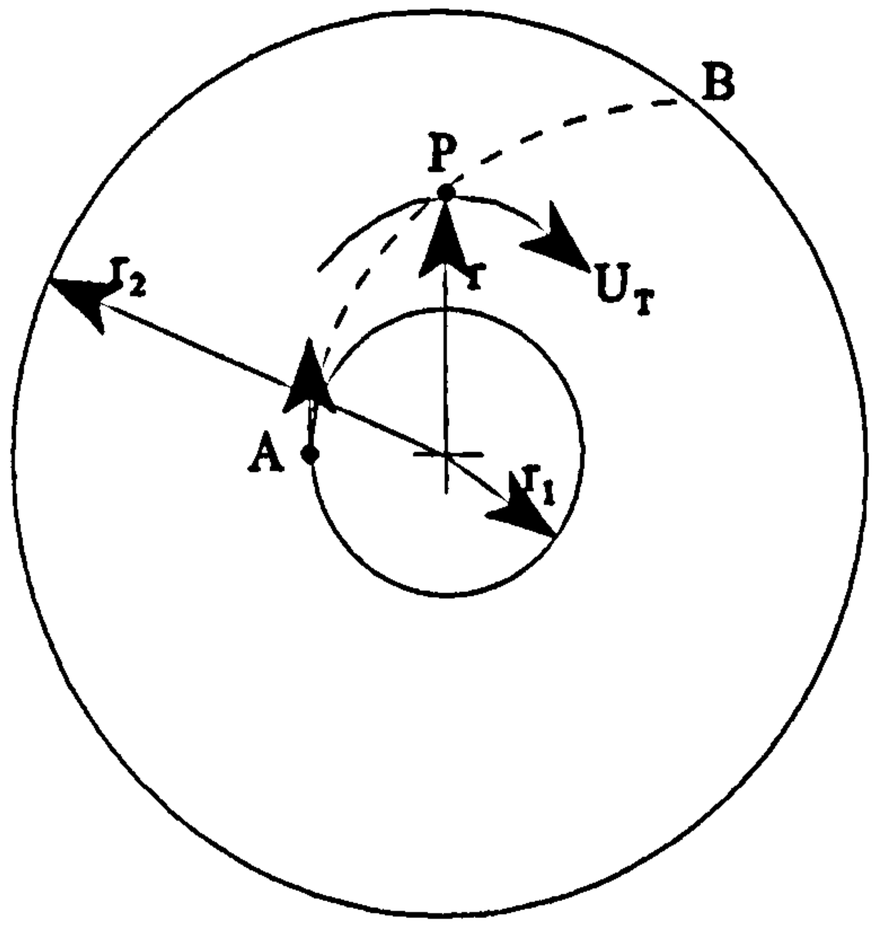

Figure 1.5-6 : Particle Motion in a Centrifugal Field

A similar method was described by Stenhouse and Trow (1979), but they presumed a forced vortex occurred. By assuming that the gas and particle tangential velocities are equal they produced a method of predicting the minimum size of particle which could be separated:

$$\eta = 1-\left(\frac{r_1}{r_2}\right)^2 = 1 - \left[\exp\left(- \frac{2\rho_p U_o d_p^2 l_b (\cot\phi)^2}{9\mu D^2}\right)\right] \qquad 2.2.1.3$$

where D = diameter of cyclone

l_b = length of cyclone

U_o = axial velocity

ϕ = angle of fixed rotor blade to the axial direction

The methods of both Umney and Stenhouse and Trow over predict the collection efficiency. However, the latter does provide a closer prediction.

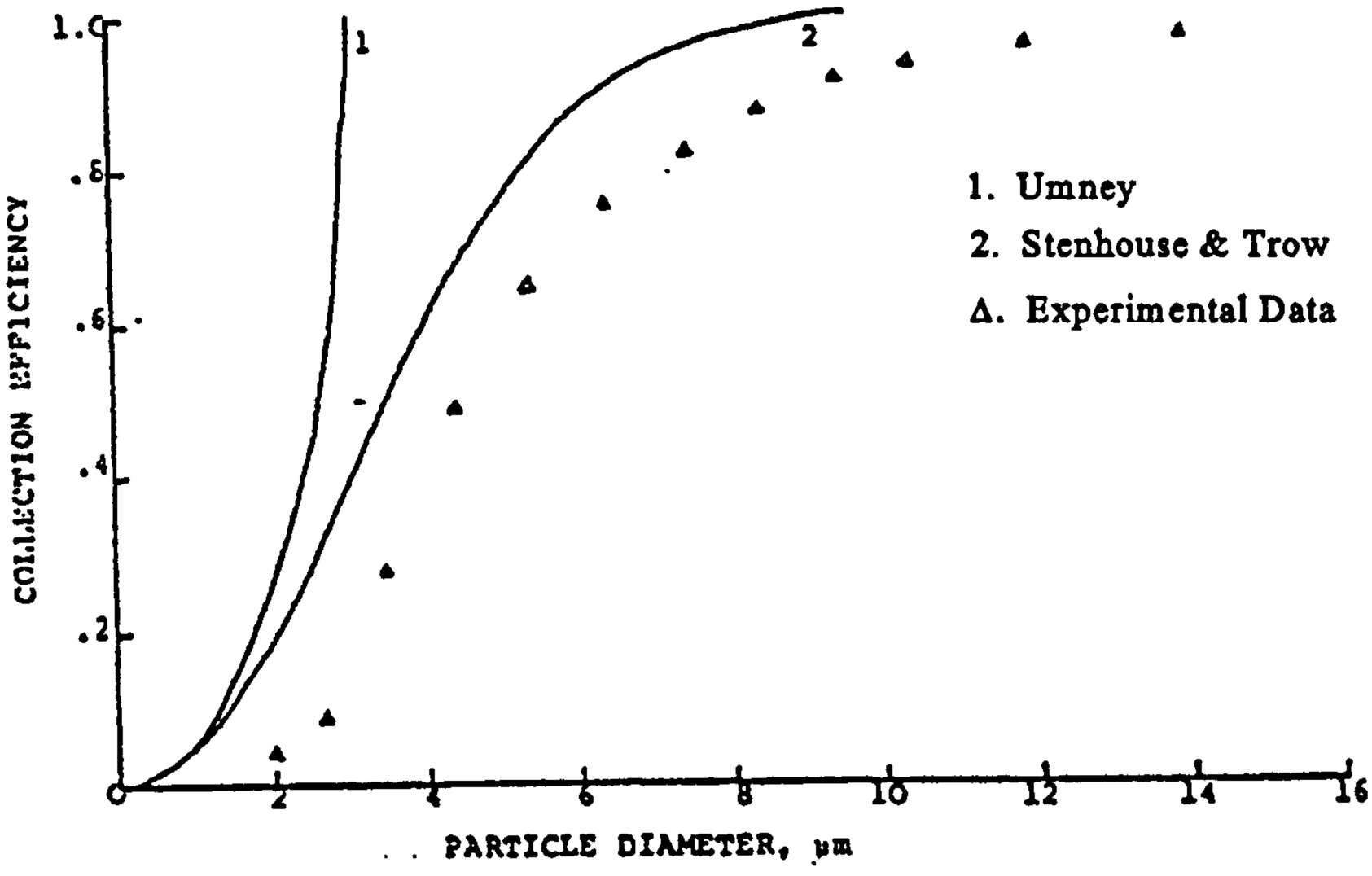

Figure 1.5-7 : Results of Umney and Stenhouse & Trow compared to Experimental Data

Neither of the methods account for turbulence or the purged flow, although Stenhouse and Trow stated that turbulence was negligible in the collection region. The experimental data is given by Stenhouse & Trow (1979).

1.5.4 Pressure drop prediction

Pressure drop prediction is important for the assessing the implication of using a cyclone separator (ie. to determine the loss in energy to the system in which it is going to be installed). Most cyclone research has been centred around the prediction of separation efficiency and modelling particle behaviour. However, the pressure drop has been recognised to have some form of relationship with separation efficiency. If this relationship can be found, then the efficiency can be found indirectly be first predicting the pressure drop.

Strauss (1975) listed the following factors which affect the pressure difference across a cyclone:

1. Loss to kinetic energy in the swirling flow
2. Frictional losses on the wall of the cylinder
3. Loss as the gas expands on entering the cyclone chamber (reverse flow cyclones)
4. Additional frictional losses in the swirling flow in the exit line
5. Frictional losses in the entrance pipe
6. Loss in static head between inlet and outlet and losses due to the swirl generator (axial flow cyclones).

Factors one and two are considered by most models to be the most important in determining the cyclone pressure drop.

As with separation efficiency, models have been established to predict the pressure drop across cyclones. Both empirical and theoretical models have also been developed but once again the empirical, and semi-empirical models are more accurate, with the same limitations.

Modelling attempts to predict the dimensionless pressure drop coefficient (Euler number), and many theories for predicting this have been formulated for reverse flow cyclones. However only Plekhov (1971) has been found to have attempted this for axial flow cyclones.

1.5.4.1 Empirical Models

Shepperd and Lapple (1939) suggested that the Euler number (Eu) was related to the inlet and outlet geometry of a reverse flow cyclone by:

$$Eu = K\frac{ab}{D_x^2} \qquad 1.5.3.1.1$$

a = Gas inlet height

b = Gas inlet width

D_x = Vortex finder (gas outlet) diameter

where K is equal to 16 for standard tangential inlets and 7.5 for tangential inlets which extend into the cyclone body, and v in the Euler number is the inlet velocity.

This prediction assumes that there is no swirl in the vortex finder. A more detailed expression was given by First (1949) which allows for the loss in spin energy as the gas travels down the cyclone :

$$Eu = \frac{ab}{D_x^2}\left[\frac{24}{\left[\frac{h(H-h)}{D^2}\right]^{\frac{1}{3}}}\right] \qquad 1.5.3.1.2$$

Note that this is essentially the same as the model of Shepperd and Lapple but the constant K has been broken down into details of the cyclone geometry.

Casal and Martinez-Benet (1983) correlated the work of Shepperd and Lapple (1940), Stairmand (1949), Caplan (1977) and Parker et al (1981) to the cyclone's geometric shape to produce the following equation:

$$\xi_i = 11.3\left(\frac{ab}{D_x^2}\right)^2 + 3.33 \qquad 1.5.3.1.3$$

ξ_i = Eu = Euler number (dimensionless pressure drop)

Interestingly, this gives the pressure drop coefficient in terms of (ab/D_x^2) to the power of two rather than one in the previous equation.

1.5.4.2 Theoretical Models

Many current expressions for pressure drop are based upon Bernoulli's equation applied to a consider a small element of gas moving through the cyclone. Researchers such as Stairmand (1949), Alexander (1949), Barth (1956), Muschelknautz (1970) all have offered models in this way, but none are very accurate.

Muschelknautz based his equation upon Barth's but assumed that the major part of the pressure drop was in the vortex finder. Based upon the axial velocity in the vortex finder his expression is

$$\xi_e + 2+3\left(\frac{V_x}{W_x}\right)^{\frac{4}{3}}+\left(\frac{V_x}{W_x}\right)^2 \qquad 1.5.3.2.1$$

Ogawa (1987) used a semi-empirical relationship involving intricate fluid mechanics combined with experimental findings.

Muschelknautz's model over-predicts the pressure drop but still provides the best theoretical model, however Shepperd and Lapple's empirical model is simple yet effective.

1.5.4.3 Axial flow cyclones

Among with other aspects of axial flow cyclones, the pressure drop across them has been somewhat overlooked. This is particularly true for gas/liquid separation, especially for high concentrations of liquid.

Plekhov (1971) suggested an empirical model that related the Euler number as:

$$Eu = (5.2m^{-1.4} + \zeta_k)\left(10\ \frac{L}{G}+1\right)^{-0.08} \qquad 2.2.2.1$$

where

m = ratio of the area of inlet slots to the cross sectional area of the sleeve (body diameter) ie. ab/D.

L = Liquid feed in kg/h

G = Gas feed in kg/h

ζ_k = Coefficient of hydraulic resistance of an internal ring at the outlet.

And the above must lie between the range of: $0 \leq L/G \leq 0.06$, $0.4 \leq m \leq 1.2$, $0 \leq \zeta_k \leq 3$, and Re = 20000.

This axial cyclonic separator had a scroll inlet to create the swirl and not a swirl generator; it is therefore not apparent if this holds true for an axial cyclone separator with a swirl generator. The above pressure drop expression is also very limited as it is only valid for high GVFs. In other words it only holds true for the separation of liquid droplets from a gas stream.

1.6 Conclusion

The subject of cyclones is extremely large and diverse, as the applications can range from two phase to multi-phase separation of materials of different densities. To cover in depth all of the research across these different applications would be a mammoth task and therefore this literature review has only scraped the surface of all possibilities of cyclonic application. Authors such as Bradley (1965) and Svarovsky (1984) are recommended as sources of further reading on reverse flow cyclones. However there has been no book which I have encountered providing anything as thorough on axial cyclones. The work of Umney (1948) and Daniels (1957) is the best starting point for axial cyclones and other work by Alden (1959), Smith (1961), Jackson (1963), Strauss (1966) and Stenhouse & Trow (1985) has investigated axial flow cyclones further.

As the subject of axial flow cyclones is neglected compared to that of reverse flow cyclones, the same is true for the topic of gas/liquid separation compared to that of gas/solid. Probably the most commonly referred to work on gas/liquid separation is that of Ter Linden (1958) but the separator investigated in this case is more like a reverse flow cyclone than an axial flow cyclone. Nebrensky et al (1980) also developed a gas/liquid cyclone separator for degassing crude oil, which also works in a similar manner to a reverse flow cyclone. More recently work at the Universities of Delft and Tulsa (USA) have concentrated on the separation of gas/liquid. The research at Tulsa by Marti et al. (1996) is with a device which has a tangential inlet like a reverse flow cyclone but with a cylindrical body as opposed to a conical one. Researchers at Delft Swanborn (1988) and Nieuwstadt et al. (1995) have made the most relevant attempts to this research. They have both used axial flow cyclones but have concentrated on mist extraction and not high concentrations of liquid. There have been no attempts to incorporate the phenomenon of multiphase flow either.

Many researchers strive for one generic design equation that will predict separation efficiency and pressure drop for all possible cyclone designs and configurations. There is

currently no model which will predict both separation efficiency and pressure drop for every possible configuration of reverse flow cyclone and axial flow cyclone. This gap in the understanding of cyclones needs to be filled but is a long way off. Many models can be found (empirical, theoretical, or semi-empirical) on both separation efficiency and pressure drop, but these concentrate on reverse flow cyclones and their accuracy can be limited.

Most models on axial flow cyclones have been in the area of gas/solid separation or mist extraction (the removal of liquid droplets from a gas stream) and are limited to low concentrations of solid or liquid.

Pressure drop modelling has also been virtually ignored in comparison to separation efficiency models, even though it has been recognised by many as being related to the separation efficiency. Plekhov (1971) seems to be the principal researcher into the pressure drop on axial flow cyclones and nothing has been found since. His model has great restrictions, especially in terms of the liquid to gas ratio ($L/G \leq 0.06$) which would make his model unsuitable for degassing. Therefore a model to predict pressure drop is sought as an objective of this research.

The use of cyclone separators within the oil and gas industry is also a much more recent occurrence. Although they have been used successfully in other industries for some time and can offer definite advantages over gravity separators, their application has only been attempted in this field relatively recently. However, their use in this industry is now of interest to many companies faced with the challenge of extracting and processing oil and gas. With these big companies now investigating more economical methods of hydrocarbon production, their popularity has risen. This is due to the fact that cyclones are small, efficient, low maintenance separators which can be used in hostile conditions and have a low residence time. In fact if they are to be used in downhole applications they may be capable of re-activating previously abandoned reservoirs.

CHAPTER TWO

2 TWO PHASE FLOW

This chapter describes the different types of two phase flow which is introduced to give the reader an idea of possible flow regimes which the separator may expect. From a review of previous work and assessing the main factors affecting separator performance, a plan of research is presented.

2.1 Two Phase Flow

Gas/liquid separation in the oil and gas industry can be much more challenging than conditions which may occur in other industries. Most of the work described so far has dealt with constant gas flows containing less than about 5% of liquid or solid particles by volume. In these cases only one stable flow regime will occur. However, in offshore pipelines much more varied two phase or multiphase flow conditions may arise.

Figure 2.1-1 shows some of the possible flow patterns which may occur with two phase gas/liquid flow. Prediction of flow pattern occurrence has been attempted by many researchers over the years of whom Taitel and Duckler (1976) are recognised as producing a fairly reliable, semi-theoretical derivation of the flow regimes.

The flow patterns are a function of gas velocity, liquid velocity and the inclination of the pipeline (in addition to physical properties of the fluids). Models which have been derived to predict the flow pattern, pressure and temperature profiles, and gas / liquid ratio are not very accurate and are often limited to an angle of pipeline inclination. Prediction of expected conditions at process equipment is therefore difficult. Pipework before a separator may well have travelled through a combination of horizontal, inclined and vertical pipes, especially if it follows the contours of the seabed, and it is therefore difficult to predict the flow regime conditions upstream of a separator.

It is more likely that the slug regime will cause the biggest problem due to its pulsating

conditions where at one moment the pipe will have mostly gas and at the next moment mostly liquid. Unfortunately the slug regime is the most likely one to develop and can have a dramatic effect upon the separation efficiency of a cyclone separator.

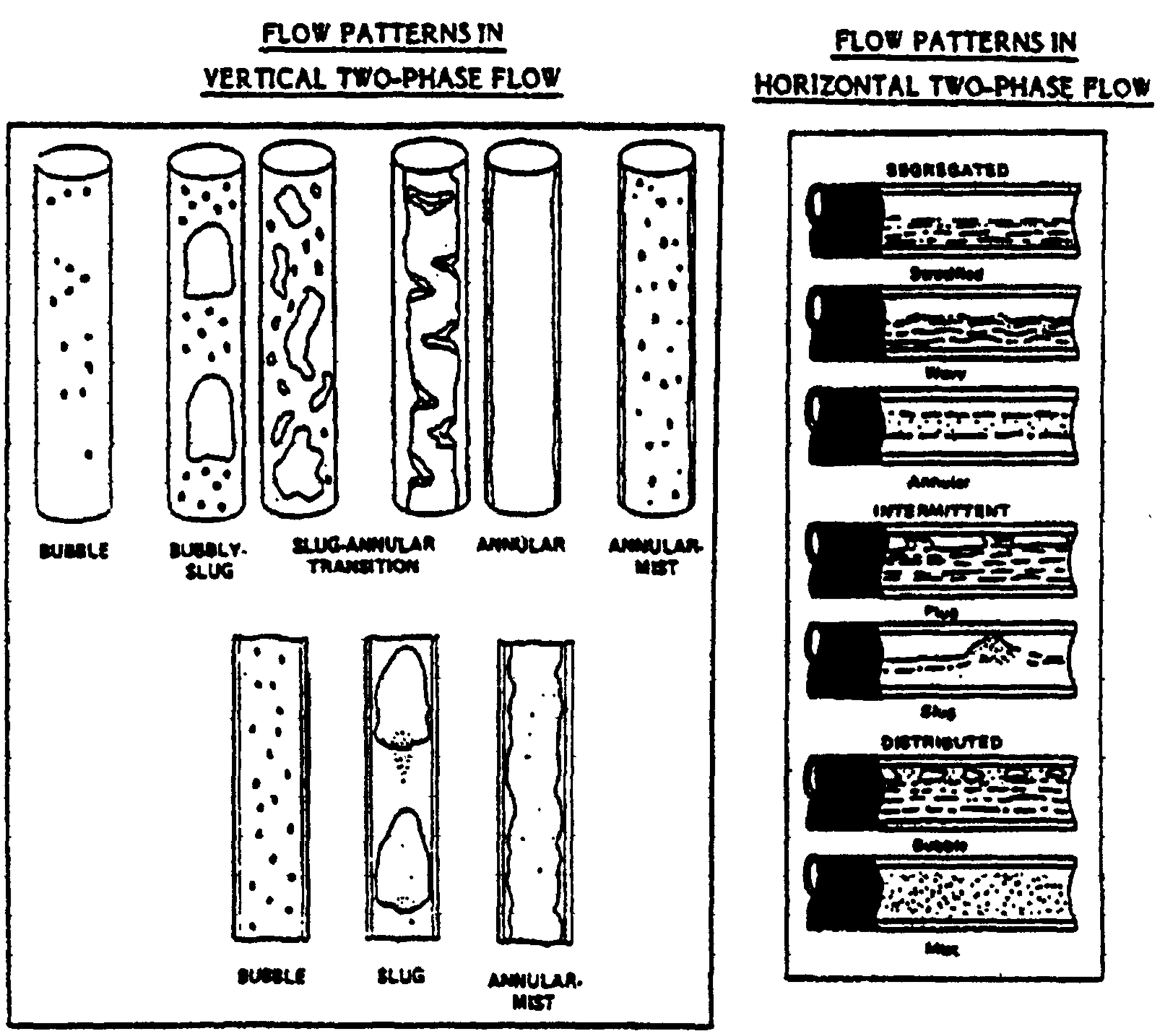

Figure 2.1-1 : Flow Regimes

2.1.1 Dimensionless Numbers in Two Phase Fluids

As described in section 1.3, the performance characteristics of cyclones are usually given in some dimensionless form. Two phase flow complicates the calculation of fluid properties (such as density, viscosity and also the calculation of velocities) used in the Reynolds and Euler numbers.

$$Eu = \frac{\Delta P}{\frac{1}{2}\rho_m v_m^2} \qquad Re = \frac{\rho_m v_m D}{\mu_m}$$

ρ_m = mixture density

v_m = mixture velocity (based upon "no slip" conditions - ie. The gas flow does not "slip" over the liquid phase and travel faster)

μ_m = mixture viscosity

The calculation of the two phase (or mixture) density, velocity and viscosity for the above dimensionless numbers, may therefore be misleading. Brill & Beggs (1984) suggest the following for the calculation of two phase density, viscosity and velocities:

To calculate some of the two phase parameters, the liquid holdup must be known. Therefore this will be defined first.

2.1.2 Liquid Holdup

Liquid holdup is defined as the ratio of the volume of a pipe segment occupied by liquid to the volume of the pipe segment. That is

$$H_L = \frac{Volume\ of\ liquid\ occupying\ a\ pipe\ segment}{Volume\ of\ pipe\ segment} \qquad 2.3.2.1$$

Liquid holdup is a fraction which varies from zero to one, corresponding to all gas and all liquid respectively. One method for measuring liquid holdup is to isolate a segment of the flow stream between two quick closing valves and to physically measure the liquid trapped. The remainder of the pipe segment is therefore occupied by gas and this is referred to as the gas holdup or Gas Void Fraction (GVF).

$$H_g = 1 - H_L = GVF \qquad 2.3.2.2$$

2.1.3 No-Slip Liquid Holdup

No-slip holdup, sometimes called liquid input content is defined as the ratio of the volume of liquid in a pipe segment divided by the volume of the pipe segment which would exist if the gas and liquid travelled at the same velocity (no slippage). It can be calculated directly from the known gas and liquid flow rates by

$$\lambda_L = \frac{q_L}{q_L + q_g} \qquad 2.3.3.1$$

where q_L and q_g are the in-situ liquid and gas flow rates respectively. The no-slip gas holdup or GVF is defined as

$$\lambda_g = 1 - \lambda_L = \frac{q_g}{q_L + q_g} \qquad 2.3.3.2$$

2.1.4 Two Phase or Mixture Density

Three equations for two phase density are used by various investigators in two phase flow:

$$\rho_s = \rho_L H_L + \rho_g H_g \qquad 2.3.4.1$$

$$\rho_n = \rho_L \lambda_L + \rho_g \lambda_g \qquad 2.3.4.2$$

$$\rho_k = \frac{\rho_L \lambda_L}{H} + \frac{\rho_g L \lambda_L}{H} \qquad 2.3.4.3$$

2.1.5 Mixture Viscosity

The following equations have been used to calculate two-phase viscosity:

$$\mu_s = \mu_L H_L + \mu_g H_g \qquad 2.3.5.1$$

$$\mu_n = \mu_L \lambda_L + \mu_g \lambda_g \qquad 2.3.5.2$$

2.1.6 Superficial Velocity

The superficial velocity is defined as the velocity which that phase would exhibit if it flowed through the total cross section of the pipe alone.

2.1.6.1 Two Phase Velocity

The two phase velocity is the sum of the gas and liquid superficial velocity.

$$Superficial\ liquid\ velocity = v_{sL} = \frac{q_L}{A} \qquad 2.3.6.1.1$$

$$Superficial\ gas\ velocity = v_{sg} = \frac{v_g}{A} \qquad 2.3.6.1.2$$

$$v_m = v_{sL} + v_{sg} = \frac{q_L + q_g}{A} \qquad 2.3.6.1.3$$

2.2 Summary of Chapter

Two phase and multiphase flow is an entire subject area of its own and this thesis makes no attempt to fully tackle the problems associated with handling such flow phenomenons or the modelling of it. Instead, in this chapter the reader has been introduced to the subject and possible flow conditions under which a separator may be expected to operate have been illustrated. The key terms relating to multiphase flow have been defined along with the calculation of certain dimensionless two phase numbers which have been used in subsequent chapters in this thesis.

CHAPTER THREE

3 DESCRIPTION OF RESEARCH PROJECT

WELLSEP is a novel axial cyclone separator which is designed to degas liquids (the engineering drawings are shown in Appendix A). The original design was based more upon experience than experimental data and the optimum dimensions are unknown. No design guide has been developed for the separator and it is the intention of this research project to satisfy these requirements. The behaviour of pressure drop across WELLSEP will also be examined.

3.1 Formulation of research objectives

The literature shows a lack of work on the subject of axial flow cyclones. The previous research has been mostly on the topic of gas cleaning, which involves the removal of dust particles from a gas stream. Other work has stated that there are similarities between the removal of dust particles and liquid droplets, and continued to investigate in this form of separation in axial flow cyclones. However there seems to be little tackled for the case of high dust or liquid loadings. The models derived from these studies also tend to be specific only for the design of separator tested (or other geometrically similar designs), and are not generally transferable to other designs.

It has been the intention of this research project to investigate the affect of geometric parameters such as length and vortex finder diameter, which have been shown to affect the performance of other cyclones, on the performance of the axial cyclone WELLSEP. Along with this, the affect of flow parameters, such as flow rate, GVF and pressure drop were investigated. As two different objectives were sought, the tests have been split up. The first tests have investigated the geometric changes and second set explored the affects of the fluids.

3.1.1 Geometry Tests

The first priority was to review the original design of WELLSEP. This was to assess the possible variations in the geometric design. The next step was to list these along with the fluid parameters (see section 3.5.1.2) which could also be varied. An extensive list was produced, of which a restricted number had to be selected due to time and financial constraints.

3.1.1.1 Original Design

The original separator was developed and patented by E.G.Arato, W.L.Loh and M.M Sarshar of CALTEC, a division of the BHR Group in Cranfield, Beds.

It is a variation of an axial cyclonic separator designed to "degas" the liquid phase of a gas/liquid mixture. Centrifugal force is generated by the presence of a four start helix and a gas core is formed in the centre of the settling chamber (just downstream of the helix). The liquid is forced to the outer radius where it is tapped off, at right angles to the input flow direction, through an involute chamber. This is a "scroll" type exit which has an increasing radius as one travels in a radial direction. The gas is picked up by a vortex finder and forced through the overflow gas outlet.

The overall length L_b is 444 mm with a length to diameter ratio (L_b /D) of 5.92 (internal diameter = 75 mm), and vortex finder to diameter ratio (D_x /D)of 0.6. Many of the dimensions were arbitrarily selected and the optimum design is unknown.

3.1.1.2 Selection of Possible Geometric Test Variables

As stated before, the possible test variables can be divided into the two groups - Geometric and Fluid parameters. The geometric ones identified for variation on WELLSEP are listed here and the fluid ones in 3.1.2.

All of the dimensions shown in Fig 1.2-2 can be varied. Additionally the following were also considered:

- Angling the involute chamber.
- The number of starts on the helix.
- Pitch of the blades on the helix.
- The degree to which the vortex finder protrudes.
- Angle of the settling chamber.
- Abruptness of start on the helix.

3.1.1.3 Justification of Chosen Separator Parts

The possible combination of all of the variables in section 3.1.1.2 would result in too many tests for the time and finances available, and a selection was therefore made. The chosen geometric variables to be tested were : Helix (2 & 4 Start), Settling chamber length, Vortex finder diameter, and their choice is justified below:

Helix (2 Start)

The original four start helix was designed to provide a full 360° turn over a length of 1-1.5 pipe diameters. Four starts was an arbitrary number and a two start helix may provide a lower pressure loss without drastically reducing the separation efficiency. Even if the separation efficiency is somewhat affected, applications exist for separators in which a low pressure loss is more of a priority than separation efficiency. The engineering drawing of the two start helix is shown in Appendix A.

Settling Chamber Length

As discussed in section 1.2.4 the length has a noticeable affect on the performance of cyclonic separators. Therefore three lengths which have length to body diameter ratios of 1.2, 1.8, and 2.0 were manufactured (from perspex to allow for visual observation). These can be connected end to end to produce a combination of seven different lengths, but only the L/D ratios of 1.2, 3, and 5 were tested.

Vortex Finder Diameter

The size of the vortex finder must affect the performance of a cyclone separator as if it were to have a diameter of zero (ie. Not exist), then all of the flow must report to the other exit.

Experiments were performed with three sizes of vortex finder diameter (D_x) which have a diameter (D_x) to body diameter ratio of 0.4, 0.6, and 0.8 (ie.30 mm, 45 mm, 60 mm).

The chosen variables were:

- Settling chamber lengths to body diameter ratios of 1.2, 3, and 5 (this length refers to the length between the downstream end of the swirl generator housing and the upstream end of the outer block of the involute).

- Vortex finder internal diameter to internal body diameter ratios of 0.4, 0.6 and 0.8.

3.1.2 Fluid Tests

A separator used for the separation of gas/liquid in the oil & gas industry is likely to experience some of the two phase flow conditions discussed in chapter 2. Therefore the separator must be tested over some of these conditions, or at least the harsher slug or semi-slug conditions in order to provide a better test of its capability.

The following variables which are associated with the fluid may affect the WELLSEP's performance:

- Density (and density difference)
- Flow rate (both gas and liquid)
- Pressure
- Gas Void Fraction (GVF)

$$GVF = \frac{GasFlowRate}{TotalFlowRate} = \frac{Q_g}{(Q_g + Q_l)}$$

- Viscosity
- Back pressure on both the liquid and gas outlets (which controls the flow split).

The GVF (which is a function of gas and liquid flow rates) and back pressure on the outlets were tested. To alter the density and viscosity would involve the use of another fluid which was decided against.

3.2 Experimental Plan

As the geometry and fluid tests both had their individual objectives, their experimental procedure's varied and are therefore described separately.

3.2.1 Geometry Tests

The aim of the geometry tests was to investigate changes in the geometry over a range of conditions. If all of the possible geometric configurations (18) were tested against a multitude of flow conditions, a large number of tests would have to have been performed. To minimise the tests, a spread was completed as shown in the following test matrix:

Ql (l/s)													
13	■						■						■
12													
11													
10													
9													
8													
7	■						■						■
6													
5													
4													
3													
2													
1	■						■						■
	0.5						16						31
												Qg(l/s)	

Figure 3.2-1 : Test Matrix

The shaded areas indicate the points at which the tests were performed. Instead of testing every point over the capable range of the rig and instrumentation only the extreme points were tested and those in the mid point of the range.

3.2.2 Fluid Tests

The objectives of these tests were:

- To select one design of WELLSEP (based upon the results of the geometry tests) and to test it over a broader set of conditions. The liquid flow rates will be 3, 5, 7, 9, and 13 l/s (13 l/s is the maximum obtainable from the rig). At each liquid flow rate GVF's ranging from 50% - 90% (in steps of 10%) will be tested. The separator should be tested to allow for some gas carry under and the amount of liquid extraction (Q_{L3}/Q_{L1}) should be noted.

- To investigate the relationship between the separation efficiency, pressure drop and flow split, over the range tested.

- To examine the affect of the liquid flow rate and the GVF.

- In order to establish some means of scaling, the Euler number (dimensionless pressure drop) should be measured over the range of conditions and its relationship with Reynolds Number, Flow Rates, and flow splits should be compared.

For gas cyclones the Euler number does not appear change with Reynold's number (Loxham 1976) and for hydrocyclones the Euler number increases with increasing Reynold's number (Svarovsky 1984).

3.3 Summary of Chapter

Axial flow cyclones have been discussed in this chapter and previous work on geometric variations has been illustrated. The geometric design and fluid parameters were both considered to have an affect on the performance of axial flow cyclones and it was decided to investigate the two separately.

Daniels (1957), Stenhouse (1985) and Plekhov (1971) have all stated that the length of an axial flow cyclone affects the performance characteristics, and it was decided to vary this geometric parameter on WELLSEP. The vortex finder and swirl generator have also been reported by various workers to influence the performance characteristics and were therefore also selected as test variables. Other less important variables were listed as influential, but were not chosen due to cost, time and practical constraints.

The fluids being separated were also believed to influence the separation process in axial flow cyclones. Gas and liquid flow rates, and back pressure on the outlets of WELLSEP (which controls the flow split) were chosen to be tested over the range permitted by the rig.

To reduce the number of tests required yet still achieve the required objectives, some experimental design was carried out and the test matrix shown in figure 3.2-1 was drawn up.

CHAPTER FOUR

4 THE WELLSEP TEST RIG

In order to carry out the experimental part of this research project, a test rig was required. The project was given a fixed budget and therefore expenditure had to be kept to a minimum. To reduce costs, an existing rig used for a previous project called WELLCOM was chosen. The WELLCOM rig originally incorporated WELLSEP, but needed modification to allow further testing of WELLSEP. This section describes: the test facility used for the experimental programme, the modifications made to the rig, the components of WELLSEP and explains how the experiments were performed.

4.1 Description of facility

The test facility, used for the purpose of testing WELLSEP, was a modified version of the WELLCOM rig. The original rig (shown schematically in Figure 4.1-1) was designed with flexibility in mind and was capable of separate testing on each of the three main components on the WELLCOM rig (ie. WELLSEP, commingler and jet pump). However, the need for the commingler and jet pump no longer exists and the jet pump has been replaced with a pipe to allow better control downstream of WELLSEP. The low pressure line will also not be required for the WELLSEP testing. Instead the high pressure liquid and gas lines will be used (see Figure 4.1-1, which indicates the chosen flow path through the rig). The rig can therefore be simplified in terms of a Process Flow Diagram (PFD), as shown in Figure 4.1-2, and the water will be pumped by the Worthington Simpson 2DDM4 pump (pump number A15464A).

Due to the fact that the rig was originally designed for other tasks, there may be parts of the rig that have no use for this project, but the existing rig was used to reduce project costs. The rig consists of 2" and 3" PVC-glas pipework which is transparent to allow visual observation. Various ball and gate valves are used to control the flow rate and path through out the rig and the flow split through WELLSEP. The instrumentation will be described in section 4.2.

Water is supplied from a tank (2.4m x 1.2m x 1.2m, with baffle to settle the flow before it re-enters the pump) by a Worthington Simpson pump (Pump curve in Appendix B) and ultimately returns to the tank to form a closed loop. This prevents the continuous requirement of fresh water. The liquid flow rate is controlled by adjusting the bypass valve V_{A1}, and valve V_{A2}. Metering of the liquid flow rate is performed by a magnetic flow meter before the gas is injected into the line.

Compressed gas is supplied by an ML30 compressor hired from Rent Air (Compressor details in Appendix B). The compressor supplies compressed air to an accumulator to help provide a more stable gas supply. From the accumulator the gas flows into the rig downstream of the pumps via a metering section. The metering section consists of two turbine flow meters in parallel with pressure and temperature readings being taken at the same point. Two meters are required here to cover the range required, and they were installed in accordance to BS 7405 : 1991. To avoid any back-flow of the liquid into the gas line, the gas pressure must be maintained higher than that of the liquid. Gas pressure is varied by a regulator which is positioned upstream of the metering section.

Once the gas is injected into the liquid line, the mixture flows through about 15 metres of pipe before it reaches WELLSEP. This was an existing feature of the rig but also provided good conditions for the development of slug or semi-slug flow regimes.

A "T" junction is positioned upstream of the separator which allows flow to bypass the separator. This had the intention of pre-conditioning the flow on the WELLCOM project, but will not be used for these tests.

A vertical separator has also been added downstream on one of the axial separation lines of WELLSEP, to assist in mensuration of the two phase flow. The vertical separator is essentially a cylindrical tank, constructed of perspex of a low pressure rating and mounted vertically. It has two exits - one at the bottom for liquid removal and one at the top for the separated gas. A series of mist extraction plates are placed in the top of the vertical

separator - just before the gas exit. The liquid exit from the vertical separator has a valve between it and the water tank (to which the liquid returns). This valve can be closed and the time taken for the liquid to rise a certain level can be recorded to give an averaged liquid flow rate. A turbine meter on the gas outlet records the gas flow but proved to be unreliable for the fluctuating flow regimes generated by the multiphase fluids. However, this turbine meter could be used in the commissioning procedure to verify the input gas flow meters.

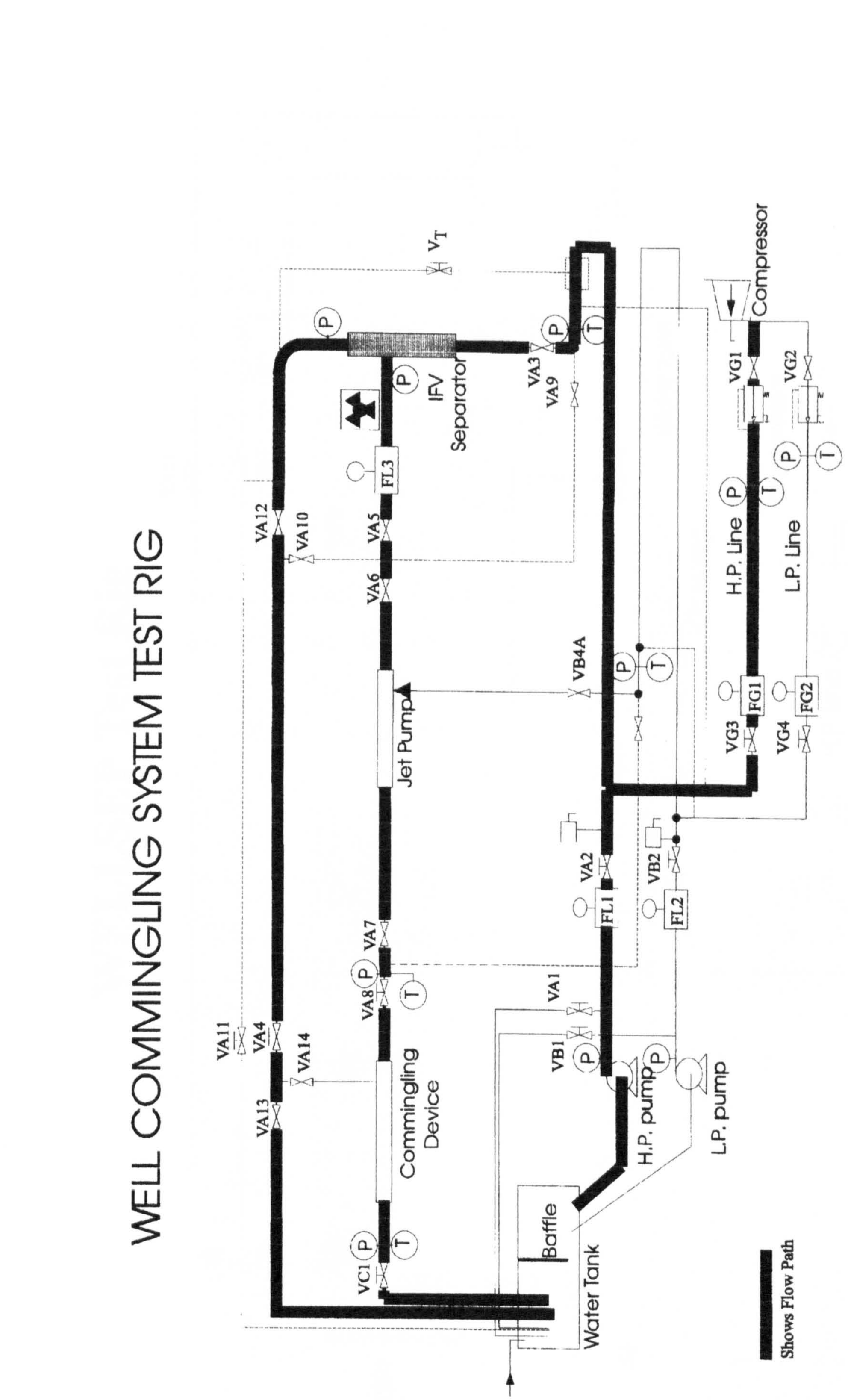

Figure 4.1-1 : Process Flow Diagram of the WELLCOM rig

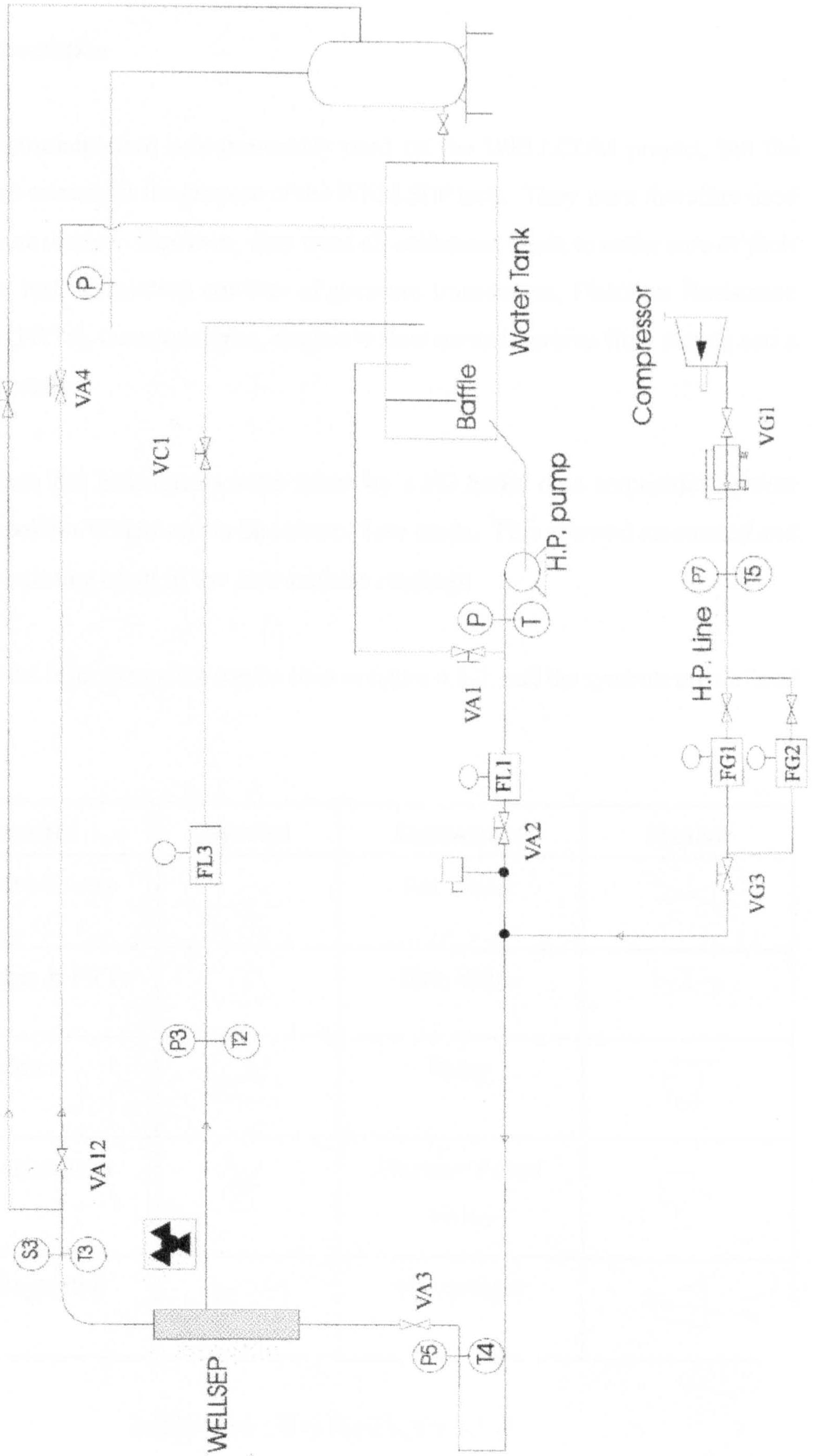

Figure 4.1-2 : Simplified Process Flow Diagram of the WELLSEP rig

4.2 Instrumentation

Most of the instrumentation was previously used on the WELLCOM project, but the specification was correct for the purpose of the WELLSEP tests. They were therefore used once again to save money. However, they were all calibrated again to make sure of their accuracy. The instrumentation consists of pressure transducers, Platinum Resistance Thermometers (PRTs), thermocouples, magnetic flow meters, turbine flow meters and a gamma densitometer.

All readings from the instruments were taken by a PC based data acquisition system (Labtech Notebook for Windows) via Strawberry Tree cards. This allowed automated and simultaneous recording of all of the instrument's readings.

The position of the instrumentation can be seen in figure 4.1-2, and the symbols are defined in table 4.2-a.

Instrument	Symbol	Instrument	Symbol
Pressure Transducers		Ball Valve	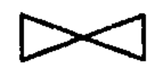
Thermocouples & PRTs		Gate Valve	
Flow Meters	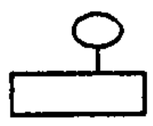	Pump	
Gamma densitometer		Pressure Relief Valve	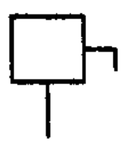
Pressure Regulator	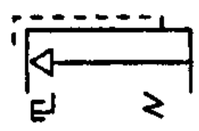	Compressor	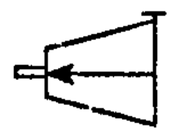

Table 4.2-a : Key for Figure 4.1-2

4.2.1 Pressure

Pressure is measured by a range of pressure transducers (Data Instruments 0-10 bar (gauge) and Schaevitz 0-15 bar (gauge) pressure transducers.

4.2.2 Flow Meters

Liquid flow rate was measured by a 3 inch magnetic flow meter downstream of the pump (before the gas injection point) and by a 2 inch magnetic flow meter on the tangential outlet of WELLSEP. The input gas flow rate was measured by two gas turbine meters positioned in parallel to cover a broader range of flow rates. Another turbine flow meter was also used on the outlet of the vertical separator, and all flow meters were calibrated externally by the manufacturers. Table 4.2-b illustrates the flow meters used, their accuracy, and location on the test rig.

Type	Range (m^3/h)	Position on Rig	Accuracy
Quadrina Gas Turbine QEG16B/EP1	1.5-15	Gas Input metering section	± 2 %
Quadrina Gas Turbine QEG50B/EP1	15-250	Gas Input metering section	± 2 %
Quadrina Gas Turbine QFG 75BS/EP1	16-180	Gas outlet of Vertical Separator	± 2 %
Altoflux Magnetic flow meter K380/A	3.5-70	Liquid Input	± 2 %
Magnetic Flow meter	3.5-70	Tangential Outlet of WELLSEP	± 2 %

Table 4.2-b : Flow Meter Range, Accuracy and Location on Test Rig

4.2.3 Temperature

Temperature measurements were taken at four locations around the rig, by either PRTs or thermocouples (2 Ch Type T). The PRTs are more accurate (as shown in table 4.2-c) but thermocouples were used because there were not enough PRTs available. These readings were taken to determine the gas temperature and permit the calculation of mass flow rates.

Instrument	Accuracy
PRT	± 1 °C
Thermocouple	± 2 °C

Table 4.2-c : Accuracy of Temperature Measurement Instruments

4.2.4 Gamma Densitometer

A gamma densitometer was used on the tangential outlet of WELLSEP to gauge the Gas Carry Under (GCU) in the separated liquid. The device was a GammaTrol Density Gauge (PRI 121/116) manufactured by ICI Tracerco. It was fitted with a PRI 116 detector and a Caesium 137 radioactive source, and mounted such that the radioactive beam was projected in a vertical direction.

A brief description of the principle of operation of the gamma densitometer will be described here, but further details can be found in the manufacturer's handbook (an extract of which is held in Appendix B). For full details on the design, operation, and calibration refer to the manufacturer's handbook.

4.2.4.1 Principle of operation

A narrow radiation beam is transmitted, from the Caesium 137 source, through a pipe section and received by a detector on the other side of the pipe. The beam is attenuated

(absorbed) by the pipe walls and the gas/liquid mixture in the pipe. As the walls will constantly attenuate the signal, any variation will be due to the gas/liquid ratio in the pipe. Calibration of the densitometer establishes a relationship between the gas/liquid ratio and the signal received by the detector; this allows the signal processor to compute density for a given attenuation.

The detector uses a scintillating crystal, which produces a minute pulse of light at a frequency proportional to the intensity of the radiation. This light is converted to a voltage pulse by a high voltage photomultiplier tube, which amplifies the voltage generated by the crystal.

The gamma densitometer can calculate density by several algorithms. Tracerco's recommended option was the logarithmic calculation which uses the following equation:

$$I = I_o \, e^{-ux(p - p_o)} \qquad 3.2.4.1a$$

which, once an allowance has been made for an offset to the natural background radiation (I_b), re-arranges to:

$$p = p_o - Ln\left(\frac{I - I_b}{I_o - I_b}\right)(K) \quad g/ml \qquad 3.2.4.1b$$

(See Appendix B for definition of variables)

To use the logarithmic calculation, three parameters must be known: a reference (known) density, the count rate at this density (I_o), and the calibration constant K.

4.2.4.2 Response time

The gamma densitometer has the option of either fixed or dynamic response times. As the conditions expected at the metering point are expected to change, a dynamic response time of 0.1s was selected. The response time affects the accuracy of the display on the signal processor. A longer response time would provide a more accurate reading under stable conditions but would not suit the conditions used in these tests.

4.2.4.3 Calibration

Calibration of the gamma densitometer is the process by which the unknown variables in equation 4.2.4.1b are obtained. The background count (I_b) is first obtained by shutting the source and recording a reading from the signal processor over a fixed time (the longer the better). This can be repeated several times and an average taken. The calibration constant K is computed in the following way:

Initially K and P_o are entered into the signal processor unit as 1 and 0.001 g/ml respectively. An Io reading (count rate) is then taken on a pipe containing only air. The pipe is then filled with water and the indicated density on the output display of the signal processor is recorded (P_{ind}). P_{ref} is the density of water (1.000 g/ml @ STP).

K is corrected by applying the following equation:

$$K = \frac{P_{ref} - P_o}{P_{ind} - P_o} \qquad 3.2.4.3$$

4.2.5 Data Acquisition

A data acquisition system was required to record the data automatically rather than manually as synchronised reading of all of the instrumentation would have been impossible by hand. Labtech Notebook for Windows was the software package used for all of the tests performed in this research project, and was operated through a 75MHz Pentium PC which was connected to the instrument signal box via two Strawberry Tree Cards. The sample rate was 10 Hz and information was recorded from the flow meters, PRTs, pressure transducers, thermocouples and the gamma densitometer over a period of 60 seconds per test. This allowed enough time for fluctuations in the readings to be observed without making the data files too large.

To save on time and money, the data acquisition system used for the WELLCOM project was used. However, not all of the channels were needed, and the numbering system may therefore not seem sequential. The numbers refer to the schematic shown in figure 4.1.1.

4.3 Health & Safety

A Hazard and Operability (HAZOP) examination was performed on the WELLCOM rig to highlight any potential hazards and these were taken into account in the design and construction of the rig, and for all modifications made to the rig afterwards. A Care of Substances Hazardous to Health (COSHH) assessment was not needed as the only fluids being used were water and air.

The main potential problem that arose from the HAZOP was the presence of pressure. The PVC-glas pipework has an operating pressure of up to 10 bar and was pressure tested during commissioning to 1.5 times the operating pressure (15 bar) as recommended by HSE (1989). The rig was also fitted with pressure relief valves set to open if the pressure became too high.

Both pumps are fitted with an electrical isolation switch and the compressor has an emergency stop button fitted.

4.4 Calibration

The flow meters were calibrated externally by Quadrina. Pressure transducers, thermocouples and Platinum Resistance Thermometers (PRTs) were calibrated internally by the instrumentation section of BHR Group. All calibration certificates are held in Appendix B.

4.5 Commissioning Procedure

The purpose of the commissioning procedure was to ensure that the rig was safe and that all of the instrumentation was working satisfactorily. This was achieved by the methods described in sections 4.5.1 to 4.5.2.3.

4.5.1 Pressure test

The pressure test was performed with water to prove the strength and integrity of the pipework. The exit valves V_{C1}, V_{A13} and V_{A11} were closed and the pump started. Valves V_{A1} and V_{A2} were adjusted until the operating pressure was reached and the rig was checked for leaks. At the same time the readings from the pressure transducers was checked. Normally the pressure test is completed with a hand pump gradually increasing the pressure, but as the rig had been used before it was carried out in the stated method.

Finally the pressure was increased until the pressure release valve (PRV) opened. If this was not correct, it was adjusted until it opened at the correct pressure.

4.5.2 Instrumentation Check

All of the instrumentation was checked to confirm that the readings were accurate. Flow meters were checked against each other, pressure transducers were checked against a fixed static head and compared and the gamma densitometer was compared to various static Gas Void Fractions (GVFs).

4.5.2.1 Liquid Flow Meters

Only liquid was allowed to flow through the rig with the valves V_{A13} and V_{A11} (axial outlet) closed, so that the liquid flowed through the two liquid flow meters (F_{L1} and F_{L3}). The readings from two flow meters was checked so that they both gave the same reading (F_{L3} may be less due to losses and an increase in static head - leading to a reduction in velocity head (this may influence the reading as the meter calculates flow rate using velocity)).

The meters were also checked against the vertical separator. This was done by measuring the time for the water level to rise a certain amount in the vertical separator. As the diameter of the separator was known, the volume could be calculated and a volumetric flow rate determined.

4.5.2.2 Gas Flow Meters

With valves V_{C1} and V_{A13} closed and V_{A11} open, gas was injected into the rig so that it passed through the inlet gas flow meters (F_{G1} and F_{G2}) and the gas flow meter on the outlet of the vertical separator (F_{G3}). The pressure and temperature readings were taken at the metering points so that the mass flow rate could be calculated and the two mass flow rates were checked to read the same.

4.5.2.3 Gamma Densitometer

With various gas/liquid ratios in a controlled section under the gamma densitometer readings were taken and compared with visual observations.

4.6 Design of WELLSEP Components

WELLSEP is essentially made up of six components shown schematically in figure 4.6-1 : helix (1), helix housing (2), settling chamber (3), involute (4), vortex finder (5), and the expansion section (6). There is also a square to circular conversion section to connect the tangential, liquid removal line to the circular section pipework.

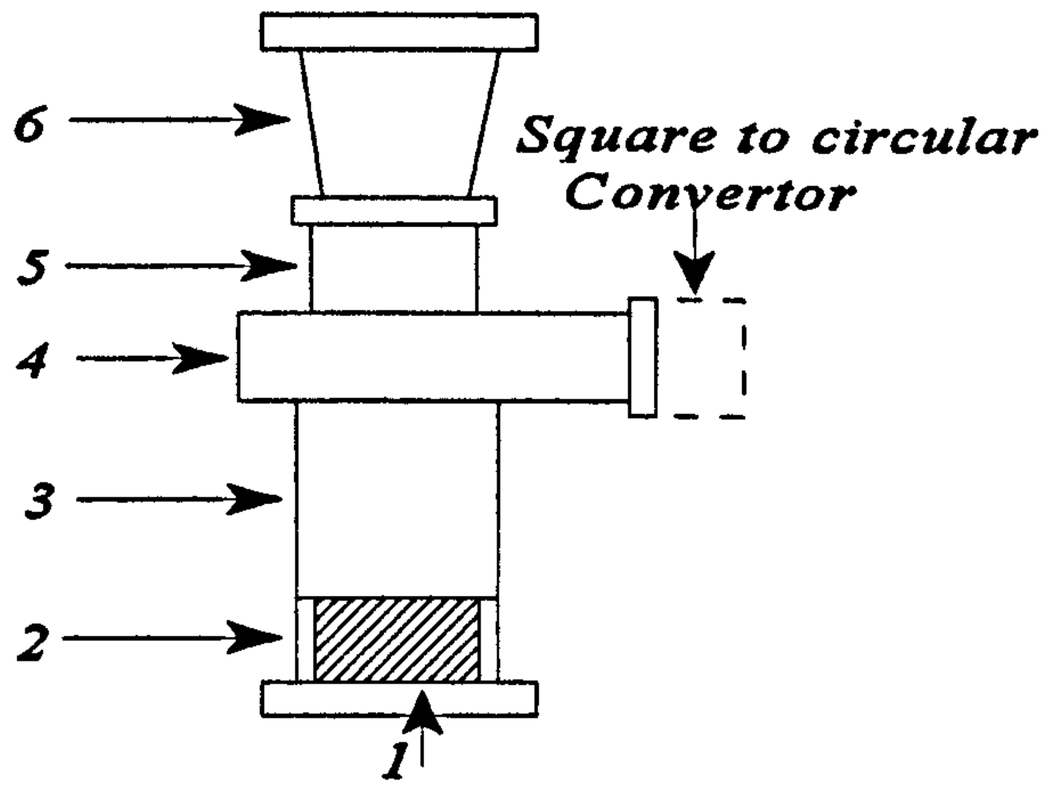

Figure 4.6-1 : Schematic of WELLSEP components

The helix is machined from aluminium, as are the involute, helix housing and expansion section. The settling chamber and vortex finder are made from perspex to allow visual observations within WELLSEP.

4.7 Experimental Work

The tests were divided into two sections both of which had their own specific objectives, as outlined in chapter 3. Firstly, a number of different geometric configurations were tested over a range of flow conditions. This led to the selection of one design which was tested over a more thorough range of flow conditions than before. The second round of

tests had the specific intention of relating pressure drop to separation efficiency and flow split, as well as investigating other affects caused by the fluids.

4.7.1 Objective of Geometry Tests

The objective of these tests was to determine the affect of varying the settling chamber length, the vortex finder diameter and two helices on WELLSEP's separation performance. This was done by testing different geometric configurations, at the points shown in the test matrix in figure 3.2-1, to improve the design of the original. These tests should lead to the selection of a particular geometric design of WELLSEP for a particular flow condition.

4.7.2 Geometry Tests

The geometric variations described in section 3.1.1.3, were tested initially over a wide range of gas and liquid flow rates as described in section 3.2.1. This was to enable a particular design to be characterised over these ranges. The intention was to see if a particular design performed better under particular conditions. The test plan is indicated in fig 3.2-1 where the shaded areas are the points intended to be tested.

To achieve the required flow conditions, firstly the compressor was started and allowed to charge up the accumulator until a pressure of around 9.5 bar (gauge) was achieved. At this point the compressor automatically cut out, but started itself again once the pressure fell during a test. The pump was then started against a closed valve. Valves (V_{A1} V_{A2}) were then adjusted so that a pressure of 4 bar (gauge) was observed on the gauge downstream of the pump, and the correct liquid flow rate was observed on the display channel of the magnetic flow meter (on the data acquisition system). Once the correct liquid flow rate was achieved, the gas was gradually introduced into the liquid by adjusting the valve (V_{G3}). Both gas and liquid flow rates were subsequently adjusted, using the same valves, if they changed slightly by the presence of the other phase. When the correct flow rates were accomplished the valves downstream of WELLSEP (V_{C1} and V_{A4}) were adjusted so that

no gas was visible in the tangential outlet of WELLSEP (if possible). The data acquisition system was set to record and started once all of the conditions were correct. For each test run, the rig was left for one minute to record the data from the instrumentation.

This procedure was repeated for all of the test points in the test matrix and for all of the combination of geometries.

4.7.3 Measurement of efficiency

Chapter one described the problems with determining the efficiency of separators. The matter is complicated further by the presence of multiphase flow. It is difficult to meter this type of flow unless expensive multiphase flow meters are used, and even then their accuracies are not of the same order of accuracy as single phase flow meters.

Therefore, another way of comparing the performance of the different geometric configurations is required. The chosen method was to test each configuration at the designated test points on the test matrix. The valves downstream of WELLSEP were then adjusted so that only liquid was flowing through the tangential outlet line. This means that if the input flow rates of the gas and liquid, and the liquid flow rate through the tangential line are known, the flow rates through the axial line can be calculated. The separation performance is measured by comparing the flow rate of liquid through the tangential line (Q_{L3}), as a percentage of the input liquid flow rate (Q_{L1}) or:

$$Liquid\ Extraction = \frac{Q_{L3}}{Q_{L1}}\ x\ 100\% \qquad 4.7.3$$

Where no gas is visible in both Q_{L1} and Q_{L3}.

Calling this term the separation efficiency may cause confusion and therefore it will be

referred to as liquid extraction. A higher liquid extraction is therefore achieved if more liquid (free from gas) can be separated from the gas/liquid input mixture. It is important that the liquid through the tangential exit is free from gas - otherwise the readings cannot be compared.

4.7.4 Retrospective Analysis of Test Rig and Test Procedures

The geometry tests highlighted some unforseen problems which needed to be resolved for both the geometry and fluid tests. One important modification was to the support of the pipework. This was needed because of the high "sudden"forces which were generated by the slug flow regime.

Another major modification to the test procedure was with the comparison of the GVFs. The problem was that the input liquid and gas flow rates were volumetric. This did not cause any problem with the liquid flow rates but as the pressure changed throughout the rig, different volumetric gas flow rates were obtained. This meant that some of the geometric tests could not be compared as they had different gas flow rates. A different method was therefore used for the fluid tests, which is described in full in section 4.7.5.

The test matrix also had to be modified as the maximum gas and liquid flow rates could not be achieved together. This was because of the holdup affect of one phase on the other. Instead of the proposed achievable conditions, something more like the conditions shown in figure 4.7-1 were actually obtained, where the shaded areas indicate the gas and liquid flow rates achievable

Ql (l/s)														
13														
12														
11														
10														
9														
8														
7														
6														
5														
4														
3														
2														
1														
	0.5													31
														Qg(l/

Figure 4.7-1 : Actual Achievable Test Conditions on the Rig

Bearing the achievable conditions in mind the following operational recommendations were made for the fluid tests.

The tests should not be planned to be at a particular gas flow rate; instead they should be performed at a given GVF which allows for the difference in pressure at the separator.

Therefore for each liquid extraction rate (or flow split) and the suggested fixed configuration of WELLSEP, test the points shown in table 4.7-a. The ones crossed out are not expected to be obtainable, but all will be attempted.

Q_L (l/s)	GVF	GVF	GVF	GVF	GVF
13	~~50~~	~~60~~	~~70~~	~~80~~	~~90~~
11	50	~~60~~	~~70~~	~~80~~	~~90~~
9	50	60	70	~~80~~	~~90~~
7	50	60	70	80	90
5	50	60	70	80	90
3	50	60	70	80	90
1	50	60	70	80	90

Table 4.7-a : Proposed Matrix for Fluid Tests

4.7.5 Objectives of Fluid tests

The fluid tests had more than one objective. They were:

- To determine the affect of GVFs on the separation efficiency and pressure drop.
- To investigate the affect of the liquid flow rate (and hence the liquid velocity).
- To examine the relationship between separation efficiency (or liquid extraction) and pressure drop (or Euler number).
- Ultimately to produce some design guidelines which will aid in the selection of the correct size and geometric configuration of WELLSEP.

It was also decided to test for conditions where some gas was allowed to be carried under into the tangential exit line of WELLSEP. This was because certain applications exist where this situation is acceptable. One example is on the WELLCOM system, where up to 15% of gas is permitted in the motive line of the jet pump, before significant affect is noticed in its performance.

One geometric design was selected, based upon which one gave the best gas-free liquid

extraction rate. This one design should be tested over the proposed conditions shown in table 4.7-a (if all are possible).

The selected design was as below:

Settling chamber length = 3 x diameter = 3 x 75mm = 225mm
Vortex finder diameter = 0.4 x diameter = 0.4 x 75mm = 30mm
4 start helix.

An explanation for why these were chosen will be detailed in the following sections.

4.7.6 Fluid Tests

The compressor and pump were started and the same procedure as in the geometry tests was followed until the correct liquid flow rate was achieved. At each liquid flow rate the gas flow was adjusted until the GVF displayed on the data acquisition was correct (the GVF displayed on the computer allowed for the difference in pressure and temperature at the metering section and at WELLSEP).

Valve V_{A12} was closed to direct the flow through the vertical separator. This was so that it could be used to calculate the liquid flow rate (as described in section 4.1), as the magnetic flowmeter may not give the correct reading with too high a gas content.

The valves downstream of WELLSEP (V_{C1} and V_{A11}) were adjusted so that there was no gas visible in the tangential exit of WELLSEP. A test run was the recorded. Valve V_{C1} was then opened until some gas was present in the tangential exit and another test was recorded. This was repeated allowing more gas each time to be carried under, until about 15% gas by volume was seen. The whole process was repeated for each GVF and each liquid flow rate that could be achieved in table 4.7-a.

4.8 Summary of Chapter

A full description of the test rig has been given in chapter four, along with a review of the instrumentation used. The accuracy and measurement principles of the instrumentation have also been described, together with an illustration on a Process Flow Diagram (PFD) of the metering points.

In order to reduce costs, a previous test rig was modified for the purpose of the tests performed in this research project. Commissioning of the rig disclosed certain limitations of the test rig and modifications had to be made which have been discussed in section 4.7.4. The ultimate testing procedure of the geometry and fluid tests has been described in 4.7.2 and 4.7.6 respectively.

CHAPTER FIVE

5 RESULTS

Chapter five displays the results obtained from both the geometry and fluid tests. The affect of changing the settling chamber length, vortex finder diameter, and helix design upon liquid extraction is reported in the geometry test results. This led to the selection of one configuration, which was expected to have the highest liquid extraction, for use in the fluid tests. In the fluid tests, the influence of GVF, liquid flow rate/velocity and liquid extraction on Gas Carry Under (GCU) and pressure drop are reported.

Certain patterns and observations are highlighted in the fluid tests for discussion and modelling in chapter six.

5.1 Foreword on Test Data

Each test run was recorded for one minute to take a representative sample of readings and allow for the fluctuations which occurred due to the two phase flow. A typical example of the Euler number & GCU fluctuations (represented by the gamma plot) are portrayed in figures 5.1-1 and 5.1-2 respectively, which show the fluctuations in test 397. The data recorded from the test runs is summarised in table 5.1, where the average values of the data required in this chapter are displayed.

Boyles law was used to calculate the gas flow rate, and hence the GVF, upstream of WELLSEP, using equation 5.1.1. This was to allow for the difference in pressure and temperature between the metering point and upstream of WELLSEP.

$$Q_g' = \frac{P_i\, Q_{g\,i}}{T_i} \; x \; \frac{T'}{P'} \qquad 5.1.1$$

Where

Q_g = Volumetric gas flow rate

P = Pressure

T = Temperature in degrees Kelvin

And i and ' refer to the input conditions and conditions just upstream of WELLSEP respectively.

Figure 5.1-a illustrates the location of the flow rates referred to in this section of the thesis. The suffices L and G refer to Liquid and Gas flow rates respectively.

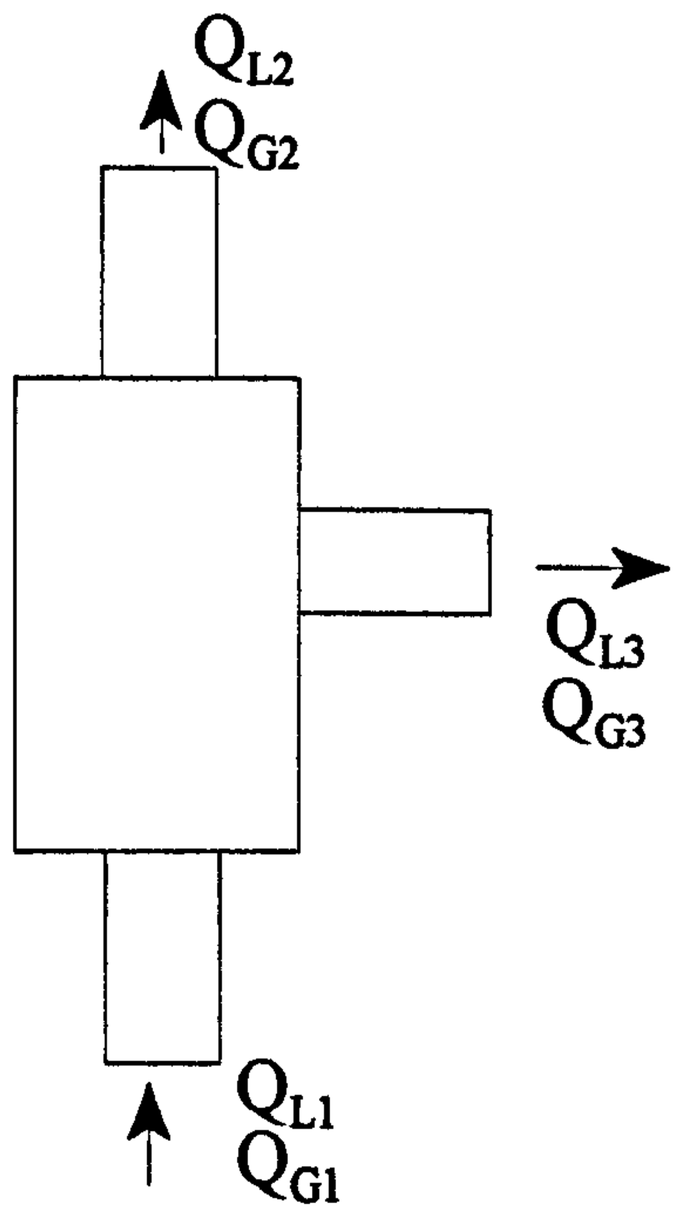

Figure 5.1-a : Measurement locations

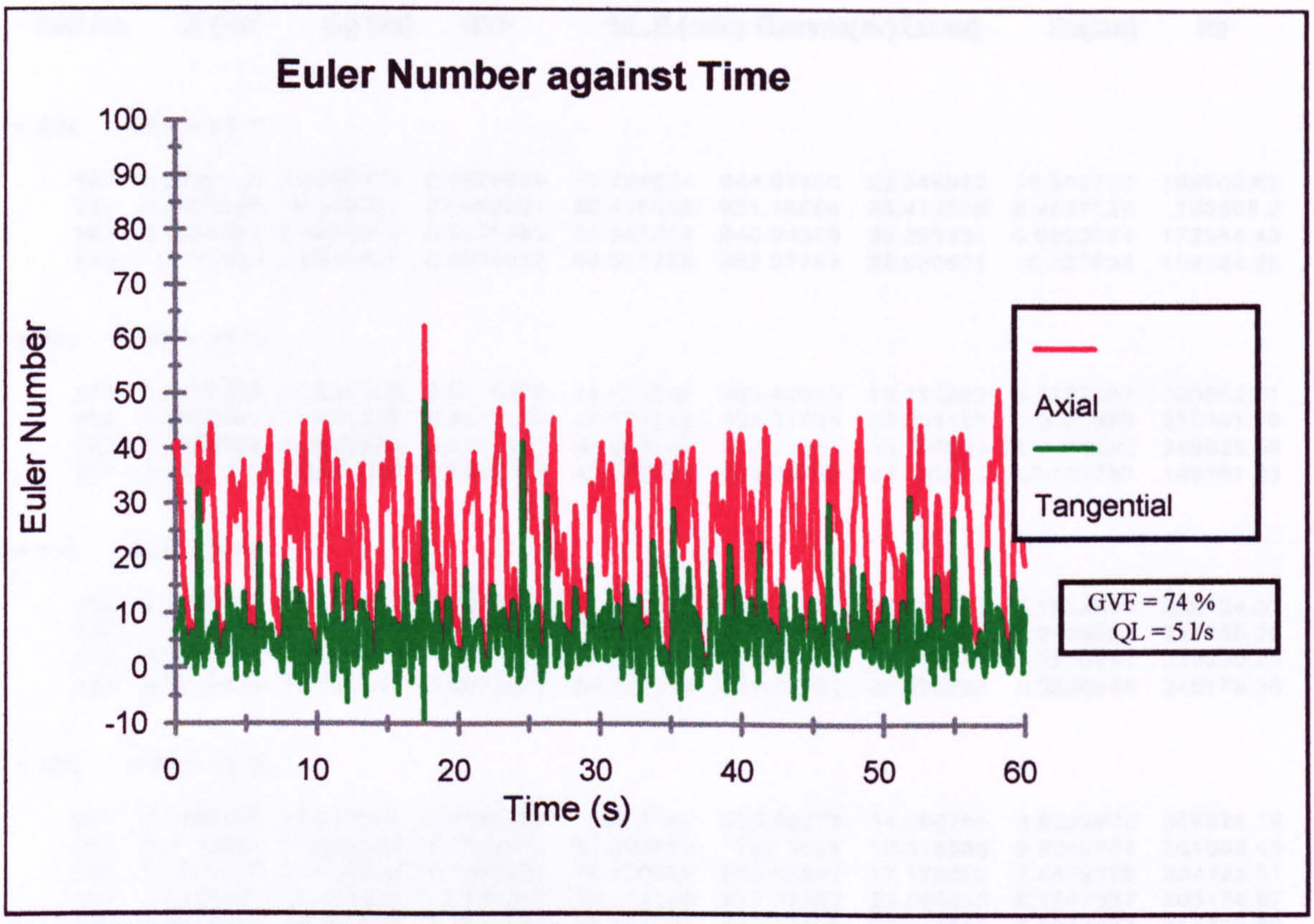

Figure 5.1-1 : Graph Illustrating Euler Number Fluctuations over a One Minute Test

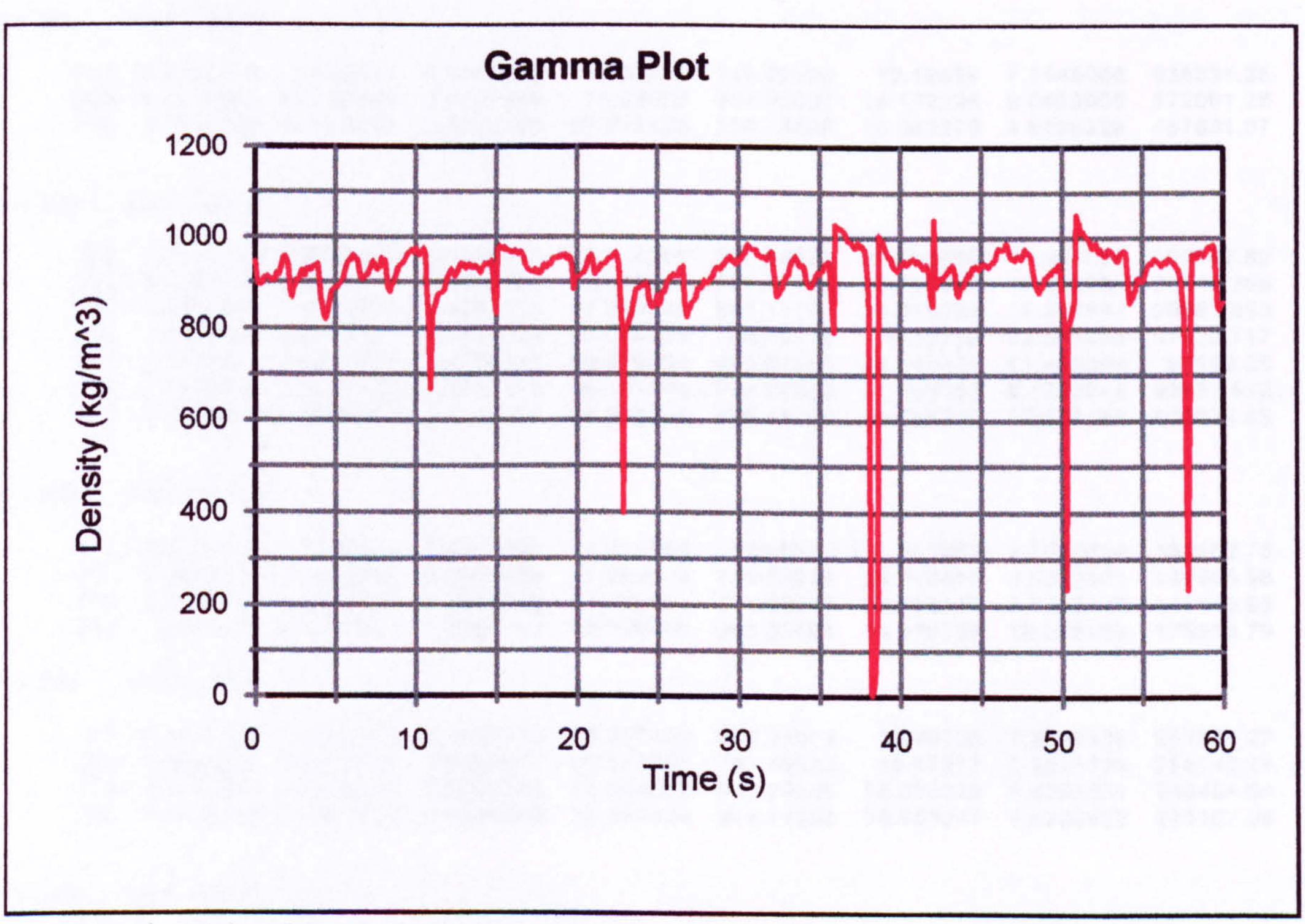

Figure 5.1-2 : Graph Illustrating GCU Fluctuations over a One Minute Test

Test No.	Ql (l/s)	Qg (l/s)	GVF	%L.E.(calc)	Gamma(av)	Eu(ax)	Eu(tan)	Re
Ql = 9 l/s	**GVF = 50%**							
341	9.215873	10.919704	0.542309	89.604621	864.00968	20.474649	14.648541	321087.52
342	8.687025	9.5255255	0.5230199	90.211381	859.36962	20.189293	15.021487	290666.11
343	8.7234521	9.4542158	0.5201006	88.807714	865.82683	20.171478	14.5234	290408.52
344	8.7300178	9.3840175	0.5180523	86.753953	867.35427	20.76332	14.545831	289106.35
345	8.7182707	9.3382777	0.5171685	85.823454	875.73504	20.693968	14.070417	288178.89
346	8.6948762	9.1523861	0.5128174	84.98712	881.64348	21.432859	13.884322	285179.23
347	8.6510933	9.0615955	0.5115878	82.904035	903.91538	21.954209	13.191341	282773.8
348	8.611206	8.748703	0.5039602	79.658707	915.06403	22.940448	12.03285	277279.71
349	8.5402231	8.3007392	0.4928898	73.465244	933.57256	25.463388	11.489001	268892.84
350	8.4635622	7.7855452	0.4791368	67.645003	947.45241	27.667464	10.602324	259756.45
305	8.8315243	6.7508293	0.4332355	33.713717	970.68647	32.366752	8.8681995	250158.43
Ql = 9 l/s	**GVF = 60%**							
351	8.9431105	14.514471	0.6187539	86.861059	851.70867	19.573042	13.009375	372315.66
353	8.9248431	14.144225	0.6131251	84.076609	868.61826	19.985845	12.20749	366404.28
354	8.8767915	13.732111	0.6073763	82.072039	898.29046	20.617407	11.156981	359054.24
355	8.8023057	13.011745	0.5964846	76.270369	920.91569	22.08691	10.011406	346623.96
356	8.707401	11.972526	0.5789443	69.327794	941.89469	25.150138	9.408851	328974.11
306	8.6777263	11.004819	0.5591157	44.224072	973.9799	33.752386	6.4634069	313712.16
Ql = 9 l/s	**GVF = 70%**							
357	8.9624671	18.072058	0.6684807	89.20163	850.7212	18.343774	11.927008	427114.9
358	8.9234822	17.578742	0.6632931	85.465703	880.7578	18.791556	11.030918	418869.49
359	8.8422468	16.539033	0.6516233	81.906184	902.73353	20.303934	10.163727	401730.63
307	8.30057	15.9865	0.6582309	56.69141	968.05051	35.529462	3.8495226	384958.22
Ql = 9l/s	**GVF = 80 %**							
360	8.4070027	29.378514	0.7775073	85.870915	866.40459	16.044629	8.0488369	586619.92
361	8.440021	26.081957	0.7555175	81.833912	913.79512	17.817174	7.0335321	539113.35
Ql = 7l/s	**GVF = 50 %**							
401	7.0203882	8.3759218	0.5440214	76.963264	907.99575	21.90251	11.845145	245173.39
402	7.0306389	8.6629827	0.5520066	80.438693	889.52054	20.754352	12.703474	249776.3
403	7.0322777	8.6953648	0.5528715	82.451615	861.2759	20.798972	13.96881	252417.48
404	7.0260795	9.0441471	0.562789	85.068362	854.80077	20.166576	14.625137	255705.55
Ql = 7l/s	**GVF = 60 %**							
406	6.9838669	12.289856	0.6376483	87.590751	822.51832	17.651278	13.317337	305098.53
407	6.9531647	12.17495	0.636495	85.636345	842.18296	17.675862	12.67334	302612.41
408	6.9493689	11.887166	0.6310697	83.910746	863.02889	18.470753	12.17891	298175.83
409	6.9606797	11.554858	0.6240628	81.045522	874.78165	19.327575	11.329317	293299.07
410	6.925429	10.905595	0.6116079	74.761024	914.37748	20.996716	10.295412	282610.87
411	6.840311	10.234152	0.5993835	68.366674	933.34251	23.385305	8.7090165	270931.5
302	6.9546514	9.9846285	0.5894364	36.463085	966.77744	28.381672	7.9249179	269052.97
Ql = 7l/s	**GVF = 70 %**							
333	6.9970502	15.185161	0.6845648	78.497279	882.76889	18.889495	9.7722196	349142.69
334	6.9687111	14.58137	0.6766272	74.888823	906.36628	19.799586	8.8331601	339518.42
335	6.8736101	13.487401	0.6624131	65.335263	938.88181	22.627006	7.55289	321262.07
303	6.9968681	15.297282	0.6861568	41.615807	958.65219	28.223279	5.337158	351204.54
Ql = 7l/s	**GVF = 80 %**							
336	6.9057374	25.602368	0.7875687	89.827833	704.98538	14.027494	10.503048	503188.28
337	6.8764737	25.050674	0.7846199	86.967072	796.93795	14.718142	9.5209595	494451.05
338	6.8271567	23.605249	0.7756616	82.793434	856.96078	15.782969	8.3634357	471952.19
339	6.7384945	21.713501	0.7631627	75.65437	898.21633	17.878491	7.5019896	442626.48
304	6.9028384	22.27186	0.7633964	44.501625	968.63994	26.944757	4.7748779	455227.29

Test No.	Ql (l/s)	Qg (l/s)	GVF	%L.E.(calc)	Gamma(av)	Eu(ax)	Eu(tan)	Re
Ql = 5l/s GVF = 50 %								
384	5.2782178	6.6599079	0.5578688	71.794024	844.91498	22.348982	10.856732	189700.62
385	5.2405356	6.309925	0.5462921	65.416538	921.16666	25.412556	8.4837128	183668.2
386	5.0258564	5.8455214	0.5376983	51.547014	940.94338	33.321931	8.0922054	172984.43
295	5.023423	4.9640534	0.4970278	50.817788	952.57767	39.953601	10.337953	159284.25
Ql = 5l/s GVF = 60 %								
387	5.9195326	12.094204	0.6713879	74.974502	883.42045	19.712829	9.2737907	283652.71
388	5.8005551	11.351662	0.6618189	68.024818	906.61725	22.231497	8.0022495	270381.39
389	5.7936662	9.9295924	0.6315226	48.245141	949.73252	29.207818	6.3574292	248628.55
297	4.8841225	7.0551026	0.590918	49.402288	955.94023	34.455912	10.122767	189567.33
Ql = 5l/s GVF = 70 %								
390	4.9303148	13.139685	0.7271547	72.2427	828.58105	18.201754	8.1814835	282124.37
391	4.88321	11.804123	0.7073703	61.138374	908.75503	22.773448	5.9544682	261985.25
392	4.7540884	9.8153736	0.673695	31.228006	957.06914	35.386857	3.2950443	229230.28
298	4.8712839	10.731167	0.6877873	54.907926	961.61702	32.270233	6.9828844	245179.36
Ql = 5l/s GVF = 80 %								
394	5.1392156	18.074029	0.7786085	85.2469	696.94378	14.890785	9.9392923	358624.19
395	5.2183967	17.508834	0.7703901	81.303892	752.3011	15.315356	8.9048784	351968.43
396	5.1744409	16.34832	0.7595828	73.828229	836.85387	17.178003	7.4679978	334226.01
397	5.1460351	14.421903	0.737017	60.714108	917.57983	22.265613	6.1247357	305174.97
299	4.8219775	15.387082	0.7613953	65.197744	969.49459	34.144815	6.0913433	314325.86
Ql = 5l/s GVF = 90 %								
398	5.0176864	38.32141	0.8842226	86.62239	742.02194	12.19529	7.3646066	638031.35
399	4.9174411	33.549599	0.8721648	76.54039	884.95007	14.172226	6.0459905	572061.28
400	4.7647298	27.544991	0.8525295	57.716135	929.43599	18.949273	4.5135329	487891.07
Ql = 3l/s GVF = 50 %								
363	3.3146842	2.9625078	0.4719479	78.116255	750.82871	27.802896	17.597296	100147.82
364	3.2957038	2.9691875	0.4739408	73.902538	781.82968	27.712967	16.209974	99944.369
365	3.2281957	2.9595675	0.4782936	71.399647	845.11171	28.875279	13.976583	98687.838
366	3.192497	2.9172201	0.4774722	67.599373	858.2416	30.12722	12.651338	97430.717
367	3.1072894	2.8617647	0.4794335	58.679059	885.62564	33.546071	11.483009	95192.05
368	3.0977443	2.7727418	0.4723189	46.169676	934.90308	37.563363	9.1762841	93657.812
292	3.0695542	3.8067401	0.5536034	69.520459	949.49769	53.085357	17.306198	109214.63
Ql = 3l/s GVF = 70 %								
374	2.9324341	6.7494811	0.6971225	64.373669	726.6516	21.312652	9.7080439	151462.75
375	2.8988028	6.5464067	0.6930928	57.264564	748.55828	24.549418	8.6502451	147885.98
376	2.8237323	6.1900357	0.6867312	37.295097	868.59075	29.053149	7.1722122	141665.95
294	3.190876	8.0278641	0.7155763	78.590708	953.32784	44.576707	10.569905	175318.79
Ql = 3l/s GVF = 80 %								
377	2.9970396	14.709402	0.8307373	76.327409	666.39274	13.49205	7.5716339	267684.27
378	2.9654121	14.070062	0.8259272	69.517157	751.49533	15.67977	7.3823598	258143.14
379	2.9040093	13.302752	0.8208149	56.944552	831.39206	18.936622	6.4951801	246454.04
380	2.8147097	11.921701	0.8089963	33.550534	944.14052	26.653947	4.8300462	225167.39
Ql = 3l/s GVF = 90 %								
381	3.5113403	19.85446	0.8497231	70.639541	823.78758	12.964959	4.9130167	350887.33
382	3.437579	18.244025	0.8414518	53.882651	879.95735	17.560364	4.9711362	327132.07
383	2.7644527	15.762209	0.8507852	-0.6052335	937.46443	37.52305	5.376421	272882.85

Table 5.1 : Summary of Test Results

The average of the data points for each channel was calculated in order to assist in the observance of any trends or patterns. The standard deviations of the data points were also calculated, to depict the spread of results registered, and a typical spread is shown by the error bars in figure 5.1-3.

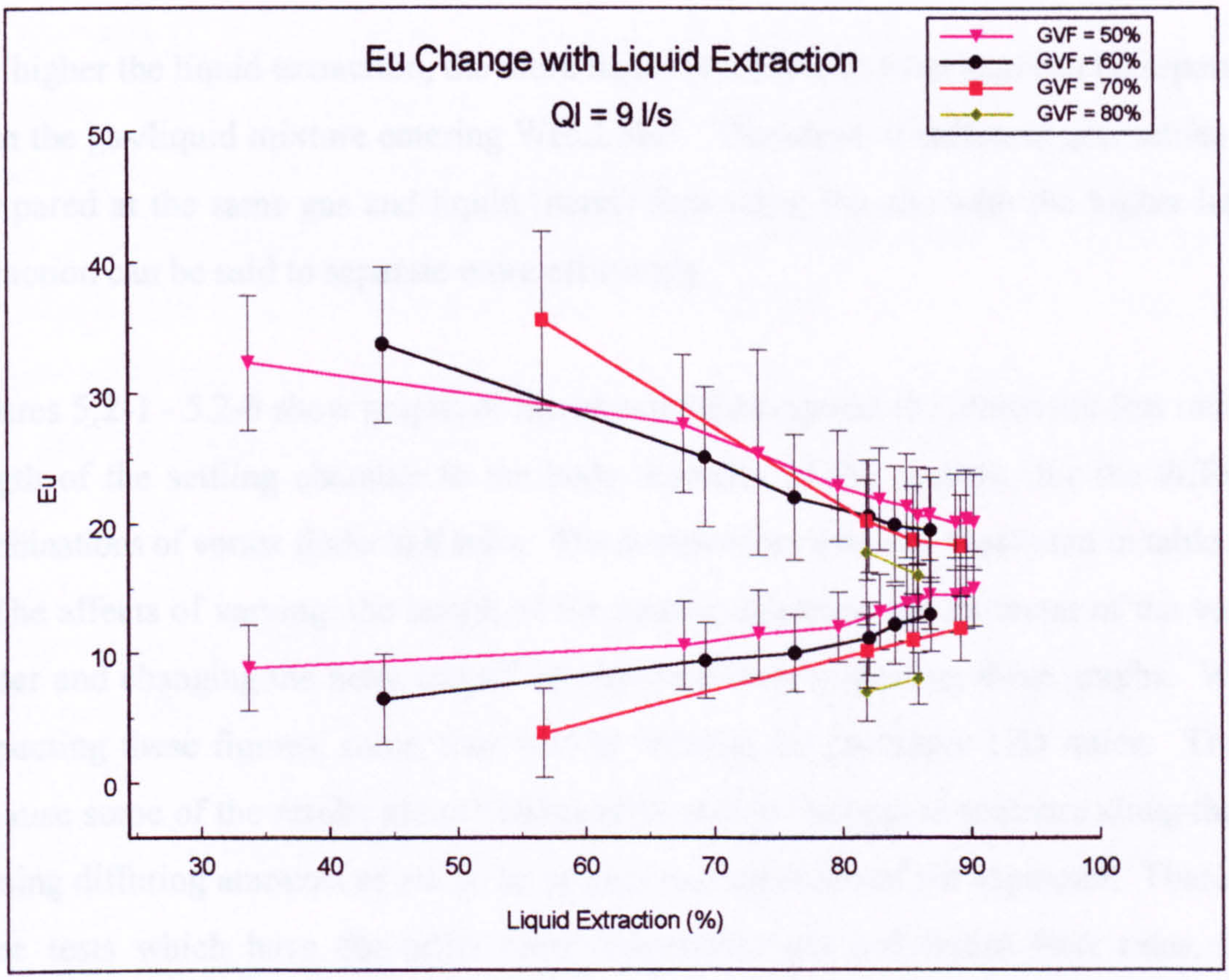

Figure 5.1-3 : Graph Showing the Sample Standard Deviation of the Data Points

5.2 Geometry Tests

To compare the various geometric configurations, conditions where the gas and liquid flow rates were the same (or very close) were selected. The gas flow rate was calculated using equation 5.1.1 and the average value was used.

The Liquid extraction (percentage of liquid flowing through the tangential outlet of WELLSEP (Q_{L3}) compared to that entering it (Q_{L1})) was used to gauge the performance of

the geometric variations and is defined by equation 4.7.3 as:

$$Liquid\ Extraction = \frac{Q_{L3}}{Q_{L1}} x\ 100\%$$

The higher the liquid extraction, the more liquid (visibly free from gas) can be separated from the gas/liquid mixture entering WELLSEP. Therefore, if different geometries are compared at the same gas and liquid (mass) flow rates, the one with the higher liquid extraction can be said to separate more efficiently.

Figures 5.2-1 - 5.2-6 show graphs of liquid extraction against the dimensionless ratio of length of the settling chamber to the body diameter of the cyclone, for the different combinations of vortex finder and helix. The components used are illustrated in table 5.4-a. The affects of varying: the length of the settling chamber, the diameter of the vortex finder and changing the helix can all be observed from inspecting these graphs. When inspecting these figures, some tests will be missing for particular L/D ratios. This is because some of the results are not comparable due to changes in pressure along the rig causing differing amounts of gas to be present just upstream of the separator. Therefore some tests which have the same input volumetric gas and liquid flow rates, have completely different volumetric ratios of gas to liquid at WELLSEP. Flow rates stated in these graphs refer to the volumetric flow rate at WELLSEP.

5.2.1 Affect of Settling Chamber Length

To investigate the affect of the settling chamber length on efficiency, figures 5.2-1 - 5.2-6 should be inspected. Plots of L/D against liquid extraction (Q_{L3}/Q_{L1}) are shown, where L/D is the ratio of the settling chamber length to the diameter of the cyclone.

The test performed with a gas flow rate (Q_g) of 2 l/s and a liquid flow rate (Q_L) of 12 or 13 l/s shows a similar pattern in all of the graphs. An increase in L/D from 1.2 to 3 raises

the gas-free liquid extraction in all tests. However once the L/D ratio is increased further to 5, the liquid extraction either falls, or increases slightly. The maximum liquid extraction at this flow rate is 81% with the 4 start helix, L/D = 3, and a vortex finder diameter of 30mm.

The test with Q_g = 2 l/s and Q = 7 l/s shows a similar pattern to the one described previously. There is an increase in the gas-free liquid extraction with an increase in L/D from 1.2 to 3. Thereafter a marginal increase, decrease or no change in liquid extraction is seen, as the L/D is increased to 5, with all of the different designs. The maximum gas-free liquid extraction is achieved with the two start helix, L/D = 3 and a vortex finder diameter of 30mm, where there is a liquid extraction of 61%. It is worth noting here that the 4 start helix with the same geometry produced a maximum liquid extraction of 60% (only 1% less).

Unfortunately, the problems of pressure and volume discussed earlier have prevented comparison of the other flow rates for all of the geometric designs - particularly that with the L/D=3. However, the trend of an increased L/D ratio leading to an increase in WELLSEP's separation performance can still be seen in all but one of the conditions.

In summary, the following can be suggested. Up to a point, an increase in the length of the settling chamber results in an increase in the separation efficiency. Beyond this point any further increase does not offer any substantial increase in efficiency and in some cases, slightly decreases it. Therefore the recommended L/D ratio for the fluid tests is 3.

5.2.2 Vortex Finder Affect

The influence of the vortex finder can also be seen by comparing figures 5.2-1 - 5.2-6. The results of the test with a gas flow rate (Q_g) of 2 l/s and a liquid flow rate (Q_L) of 12 or 13 l/s in figures 5.2-1 - 5.2-3 shows the affect of increasing the vortex finder diameter from 30mm to 45mm and then to 60mm respectively. Generally, an increase in the vortex

finder diameter is shown to decrease the gas-free liquid extraction rate. This is true for all of the L/D ratios except for the L/D = 1.2. The test of a 2 l/s gas flow rate and a 7 l/s liquid flow rate confirms these results. Figures 5.2-4 - 5.2-6 also show a similar trend with the two start helix. The best performance in all of these tests was achieved with the smallest vortex finder diameter of 30mm.

Therefore, a change in the diameter of the vortex finder also contributes to the liquid extraction. Decreasing the vortex finder diameter causes an increase in the liquid extraction. This would only be pragmatic down to a lower limit, because when the diameter equals zero, there would only be one exit!

5.2.3 Helix Design

Comparing figures 5.2-1 and 5.2-4, the two start helix seems to perform almost as well as the four start at higher liquid flow rates (in terms of liquid extraction), but unfortunately the same is not true at lower ones. This means that a separator using a two start helix would not have the same turndown ratio, and hence not be as versatile. The turndown ratio is the ratio between the maximum and minimum flow rate which will provide a minimum separation efficiency.

5.2.4 Selection of Design for Fluid Tests

The results of the geometry tests suggested that the smaller the diameter of the vortex finder, the higher the liquid extraction. A vortex finder diameter of 30mm was therefore selected for the fluid tests. This has a Dx/D ratio of 0.4 which is a more convenient way of expressing the chosen diameter for scaling purposes.

Increasing the L/D ratio to 3 also led to a higher liquid extraction rate. Increasing the L/D further had either little or no affect and as WELLSEP was required to be compact the L/D of 3 was selected for the fluid tests.

The four start helix was chosen over the two start for the fluid test, as it was expected to increase the turndown ratio.

Figures 5.2-1 - 5.2-6 show the results of tests performed on different designs of WELLSEP. Table 5.2-a clarifies which of the figures refers to which design of WELLSEP.

FIGURE NUMBER	VORTEX FINDER DIAMETER	STARTS ON HELIX
5.2-1	30mm	4
5.2-2	45mm	4
5.2-3	60mm	4
5.2-4	30mm	2
5.2-5	45mm	2
5.2-6	60mm	2

Table 5.2-a : Key for Figures 5.2-1 to 5.2-6

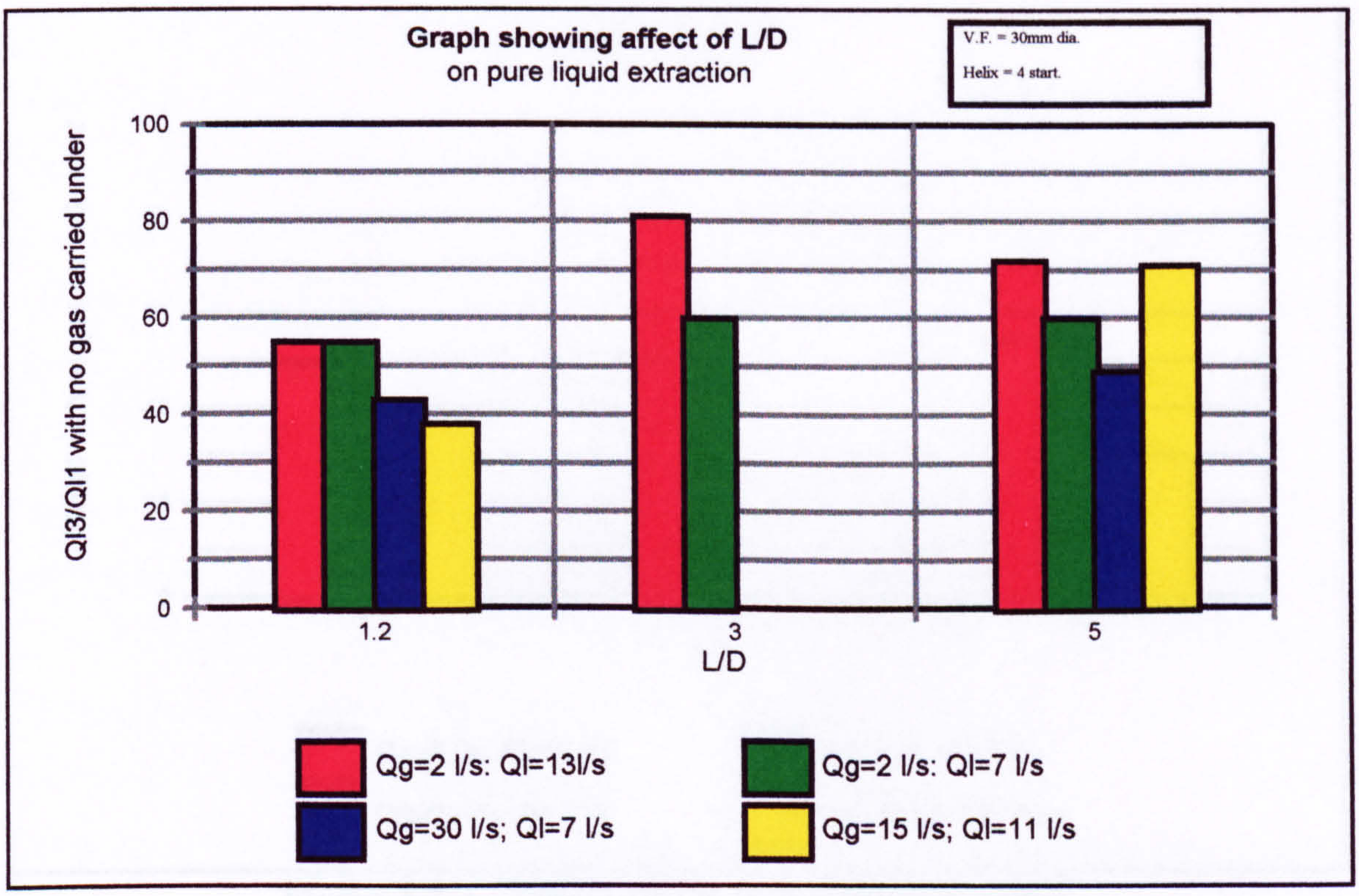

Figure 5.2-1 : Affect of L/D on Liquid Extraction

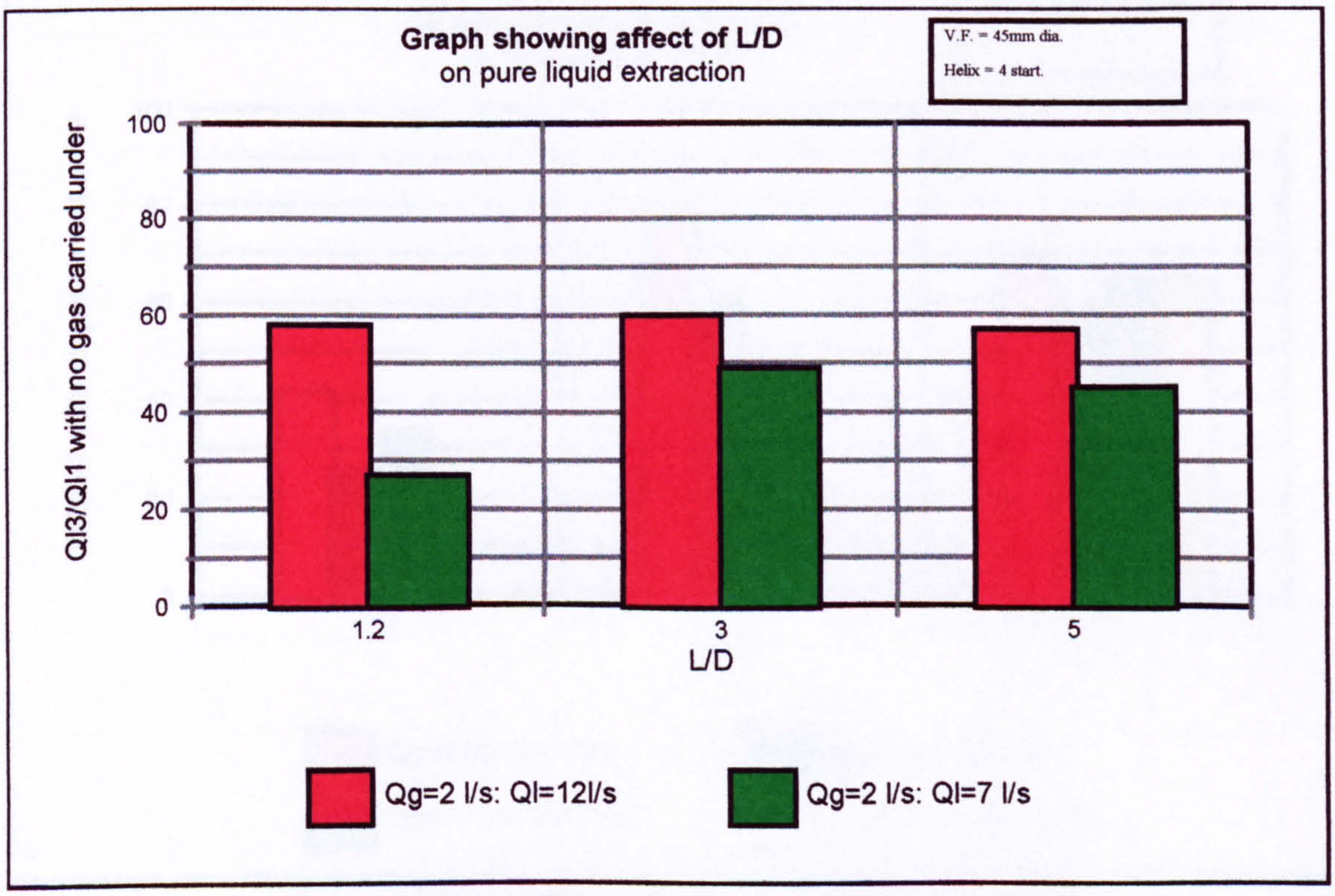

Figure 5.2-2 : Affect of L/D on Liquid Extraction

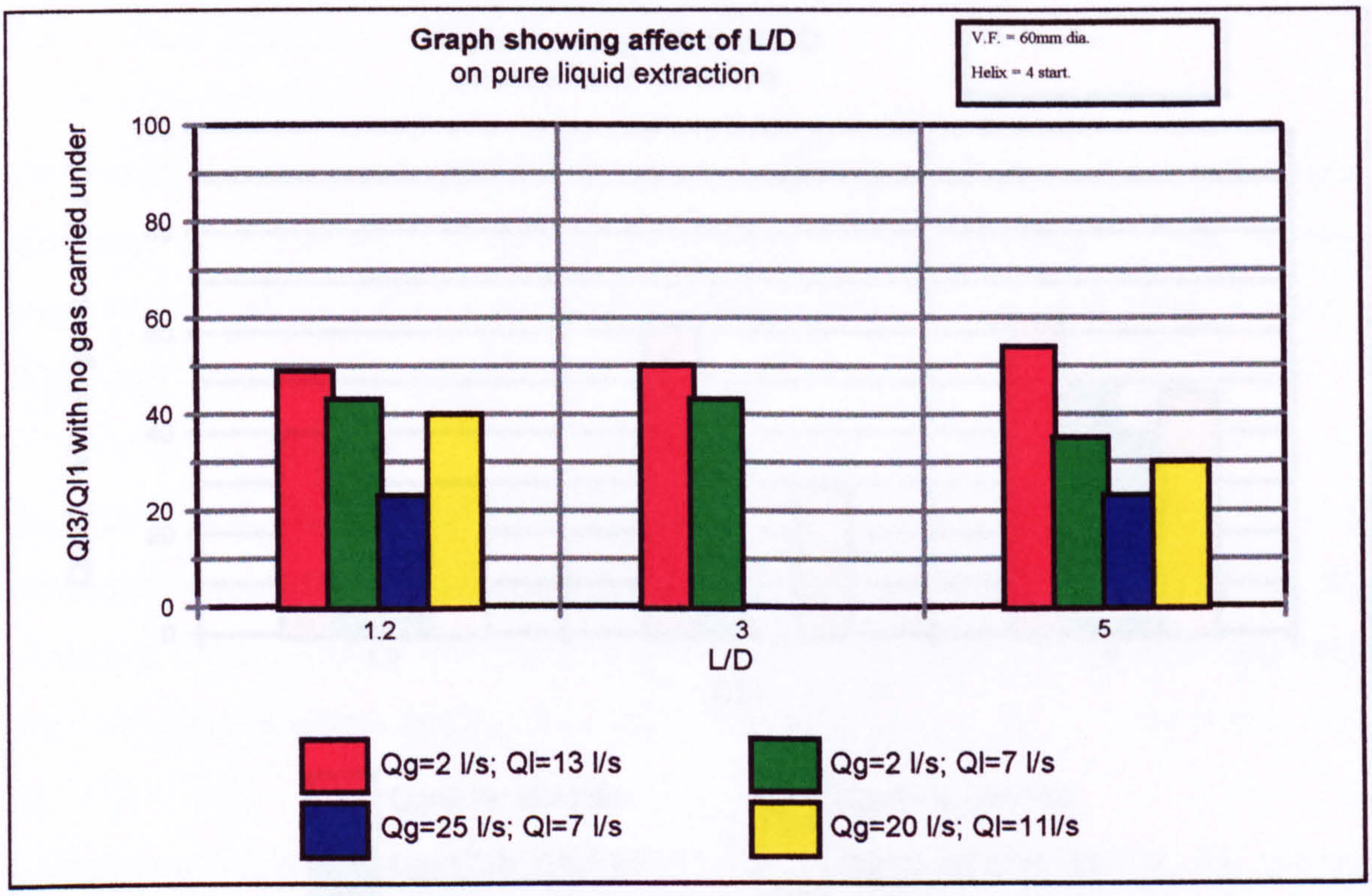

Figure 5.2-3 : Affect of L/D on Liquid Extraction

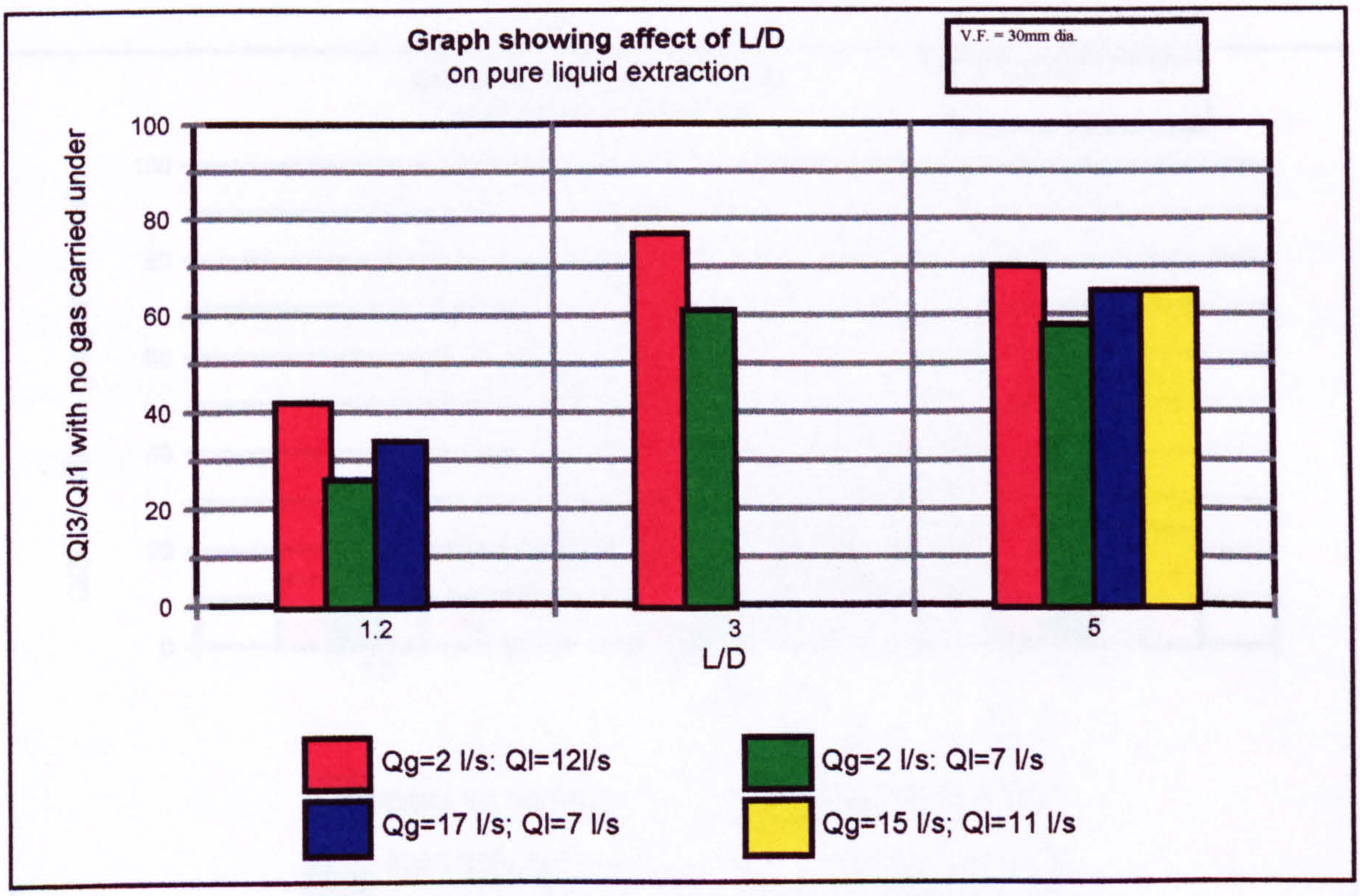

Figure 5.2-4 : Affect of L/D on Liquid Extraction

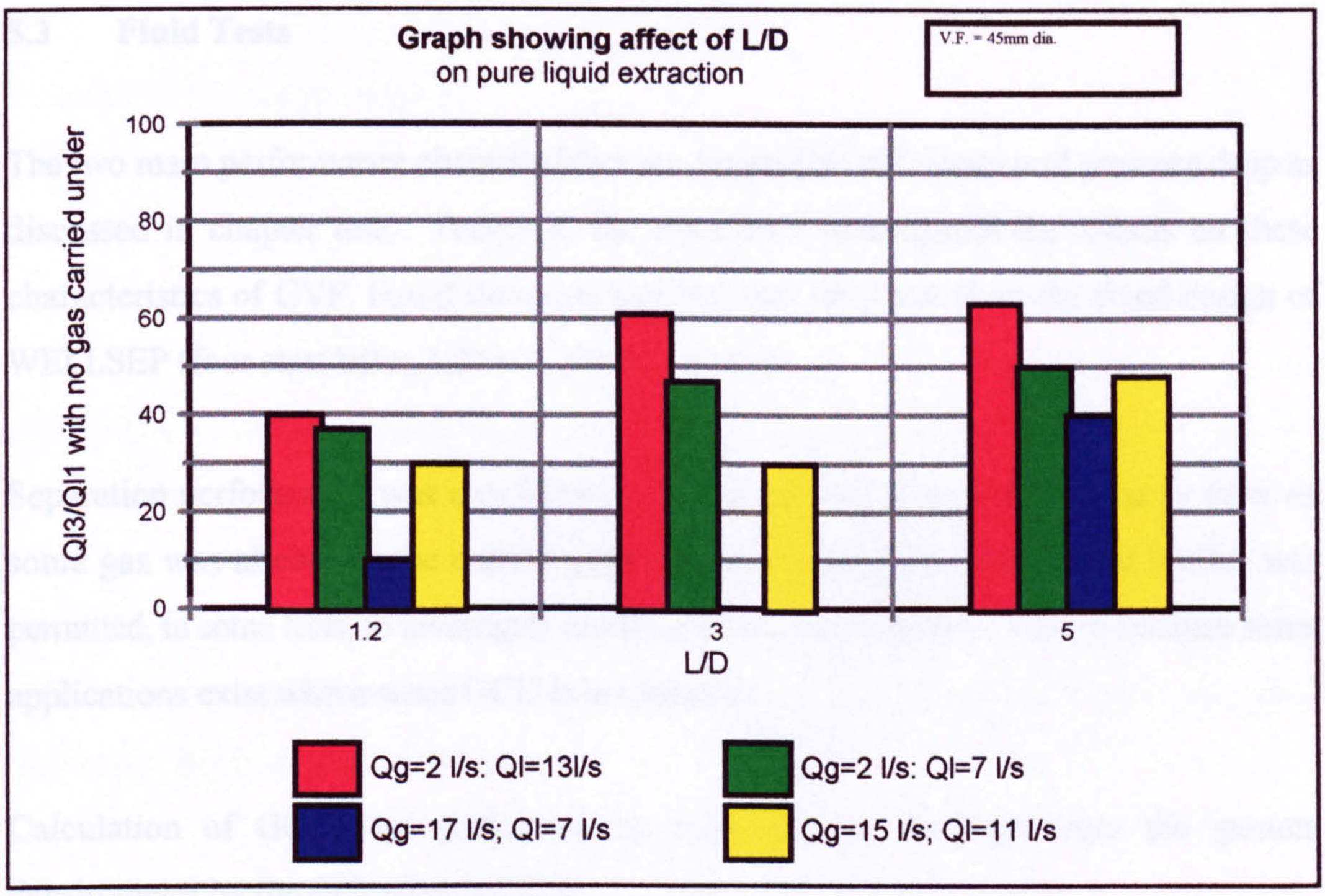

Figure 5.2-5 : Affect of L/D on Liquid Extraction

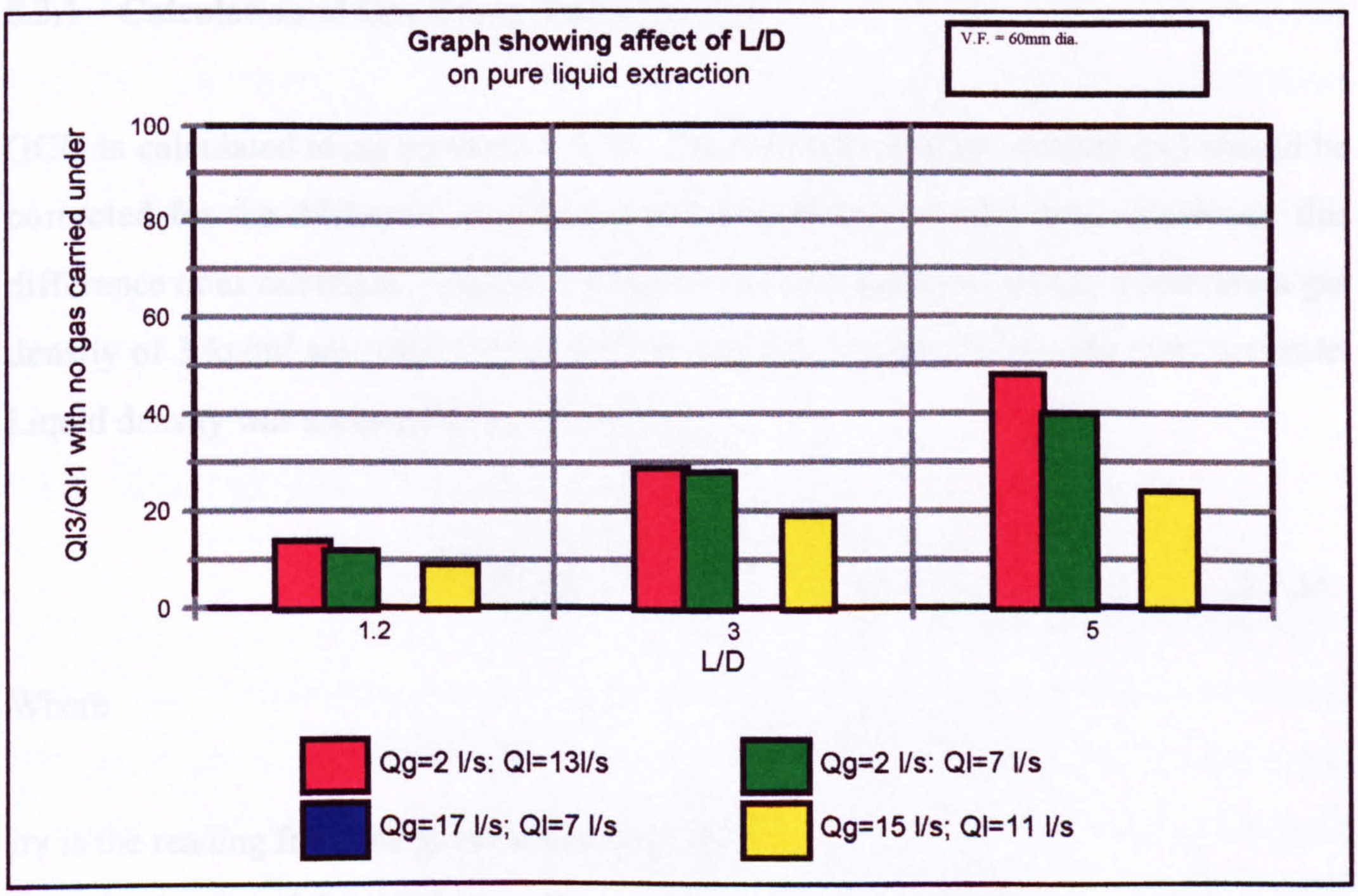

Figure 5.2-6 : Affect of L/D on Liquid Extraction

5.3 Fluid Tests

The two main performance characteristics are separation efficiency and pressure drop as discussed in chapter one. Therefore the fluid tests investigated the affects on these characteristics of GVF, liquid flow rate and pressure drop tested on the fixed design of WELLSEP (four start helix, L/D = 3, Dx/D = 30mm).

Separation performance was measured in a different way than in the geometry tests, as some gas was allowed to be carried under in some tests. Gas Carry Under (GCU) was permitted, in some tests, to investigate its affect on liquid extraction. This is because some applications exist where some GCU is acceptable.

Calculation of GCU was performed by analysing the readings from the gamma densitometer by the following method.

5.3.1 Calculation of Gas Carry Under (GCU)

GCU is calculated using equation 5.3.1b. Theoretically, the gas density (ρ_g) should be corrected for the difference in pressure and temperature of each test. However, this difference does not cause a dramatic affect in the calculation of GCU. Therefore a gas density of 3 kg/m^3 was used as this method was not expected to be extremely accurate. Liquid density was assumed to be 1000kg/m^3.

$$\rho_\gamma = (GCU\ \rho_g) + [\ (1-GCU)\ \rho_L\ ] \qquad 5.3.1a$$

Where

$\rho\gamma$ is the reading from the gamma densitometer.

ρ_g is the density of the gas.

ρ_L is the density of the liquid.

This can be rearranged to give

$$GCU = \frac{\rho_L - \rho_\gamma}{\rho_L - \rho_e} \qquad 5.3.1b$$

It should be noted that this method of measuring two phase flow is not extremely accurate and without calibration against another method, its accuracy cannot be quantified. However, without the budget for expensive multiphase or two phase flow meters, this method was adopted. The readings obtained in this manner also gave a good agreement with experimental observations; a pipe full of water and an empty pipe both gave good agreement when calculated this way.

5.3.2 Separation Efficiency - GCU

The problems with the term "efficiency" used to describe the performance of a cyclone have been discussed in chapter one. The method used to determine the separation efficiency of WELLSEP was to measure the GCU at particular liquid extractions. This should enable the designer to select the amount of liquid extraction required for the purpose and know what GCU will be expected. Therefore, the affect of the fluid variables on the GCU will be investigated.

5.3.3 Affect of Liquid Extraction on GCU

Figures 5.3-1 - 5.3-4 illustrate the influence of liquid extraction on GCU. As more liquid is extracted through the tangential outlet of WELLSEP, more gas is carried under with it. With the exception of the 3 l/s liquid flow rate, the trend is the same no matter what liquid flow rate, and GCU varies exponentially with liquid extraction. In the case of 3 l/s liquid flow rate, WELLSEP was not functioning properly due to a lack of motive force in the liquid.

5.3.4 Affect of GVF on GCU

Graphs 5.3-1 - 5.3-4 show plots of liquid extraction against GCU for the four liquid flow rates of 9, 7, 5, and 3 l/s tested. Each graph displays the results for the GVFs tested at these flow rates.

Figures 5.3-1 and 5.3-2 show the test points for all of the GVFs falling about a common curve. The same is true in figure 5.3-3 but there is more of a spread. However, the data points in figure 5.3-4 are very scattered and the trend, previously seen for the higher flow rates in figures 5.3-1 - 5.3-3, starts to break down at a liquid flow rate of 3l/s.

This observation indicates that the GVF has little significance upon the GCU at flow rates of 7 l/s and above. For design scaling purposes, this flow rate can be expressed as a superficial liquid velocity of 1.58 m/s.

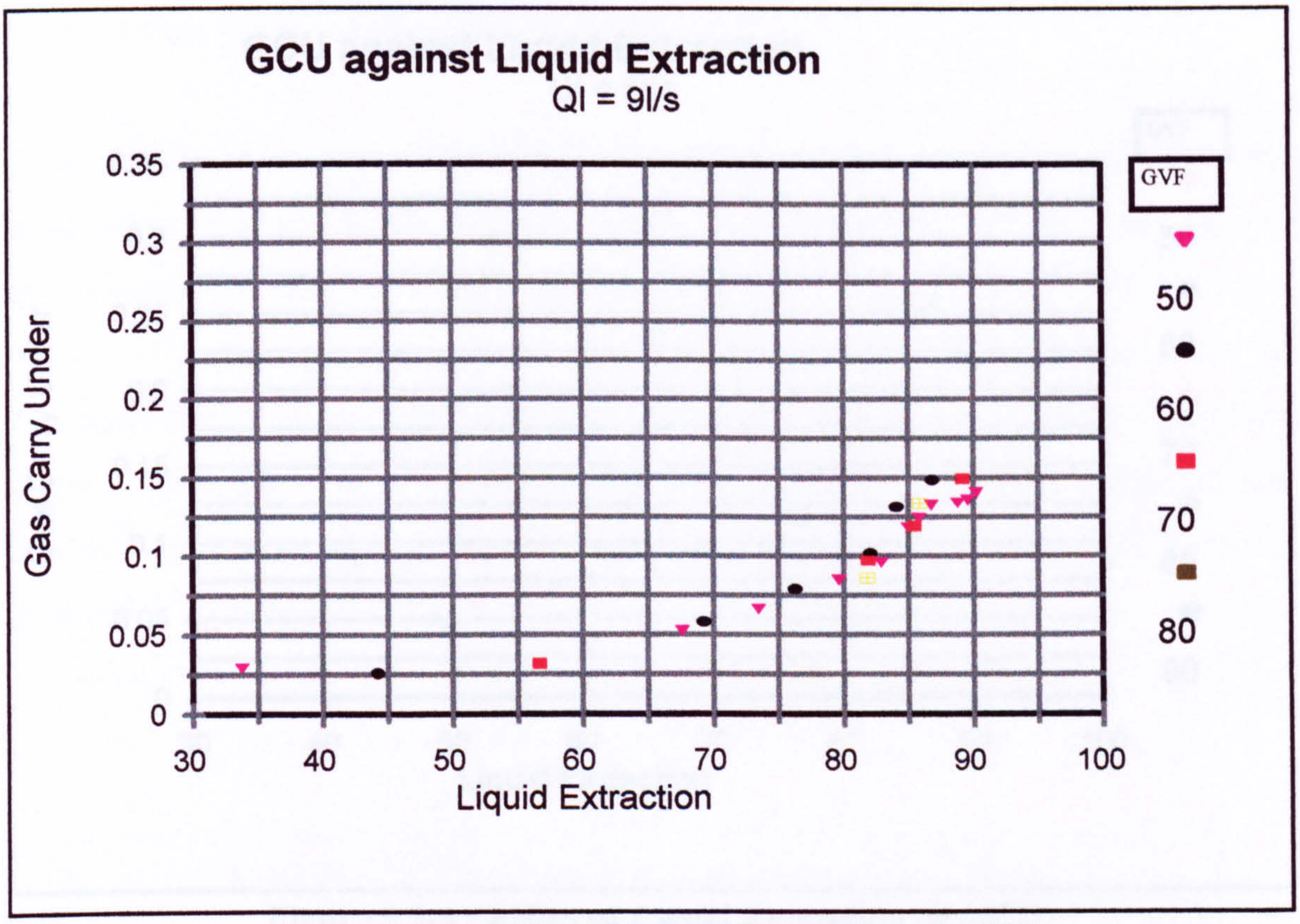

Figure 5.3-1 : Affect of Liquid Extraction on GCU

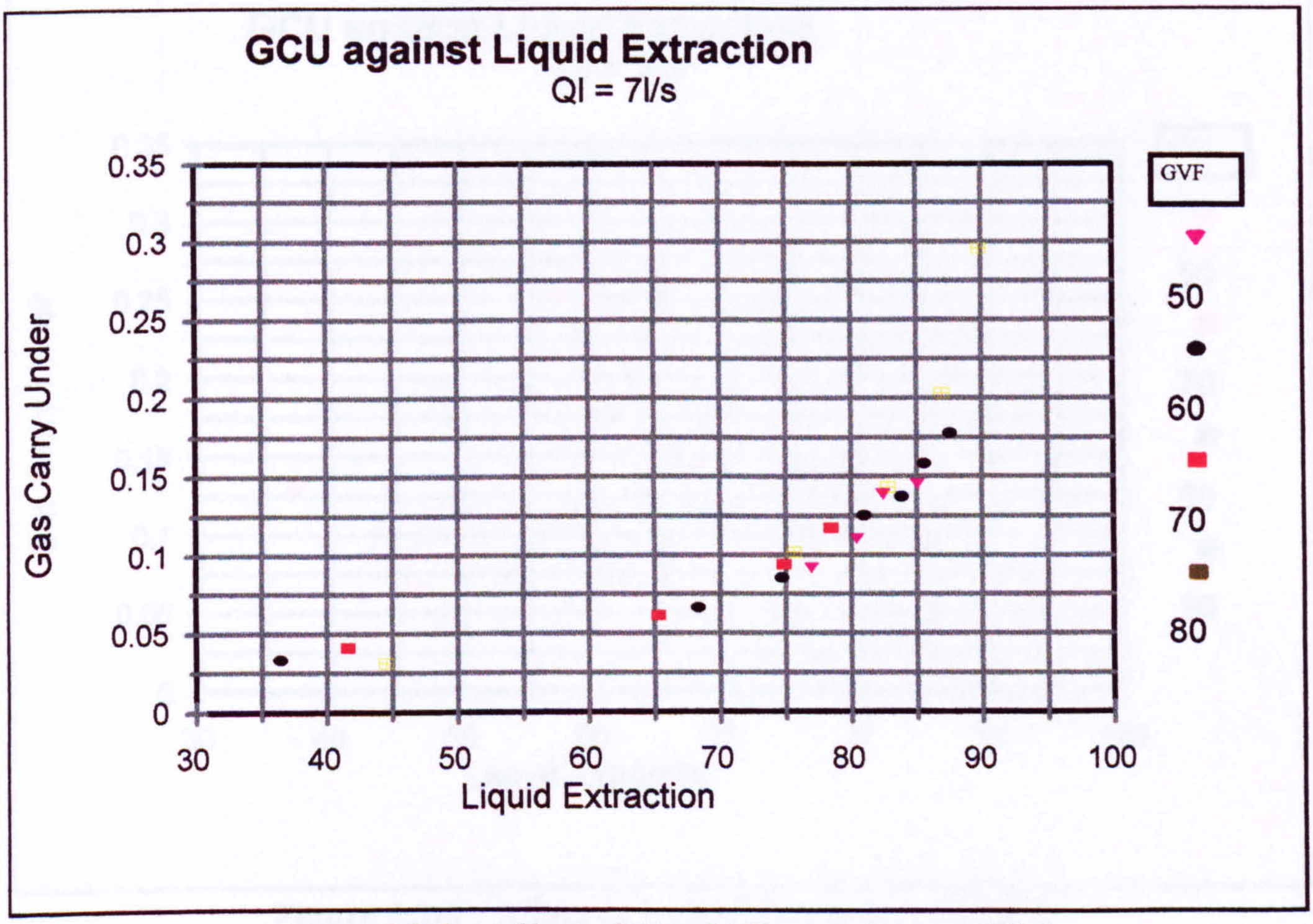

Figure 5.3-2 : Affect of Liquid Extraction on GCU

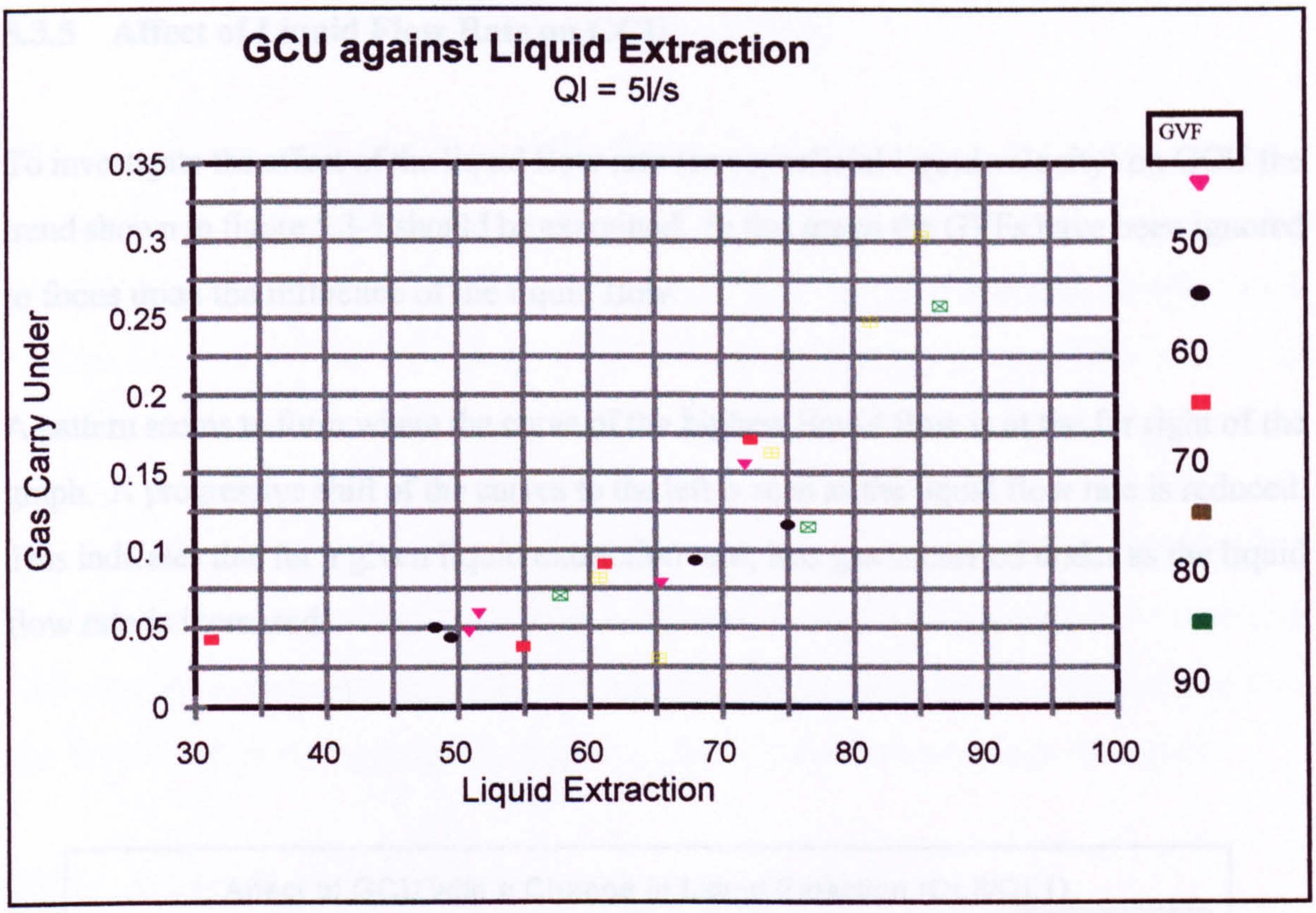

Figure 5.3-3 : Affect of Liquid Extraction on GCU

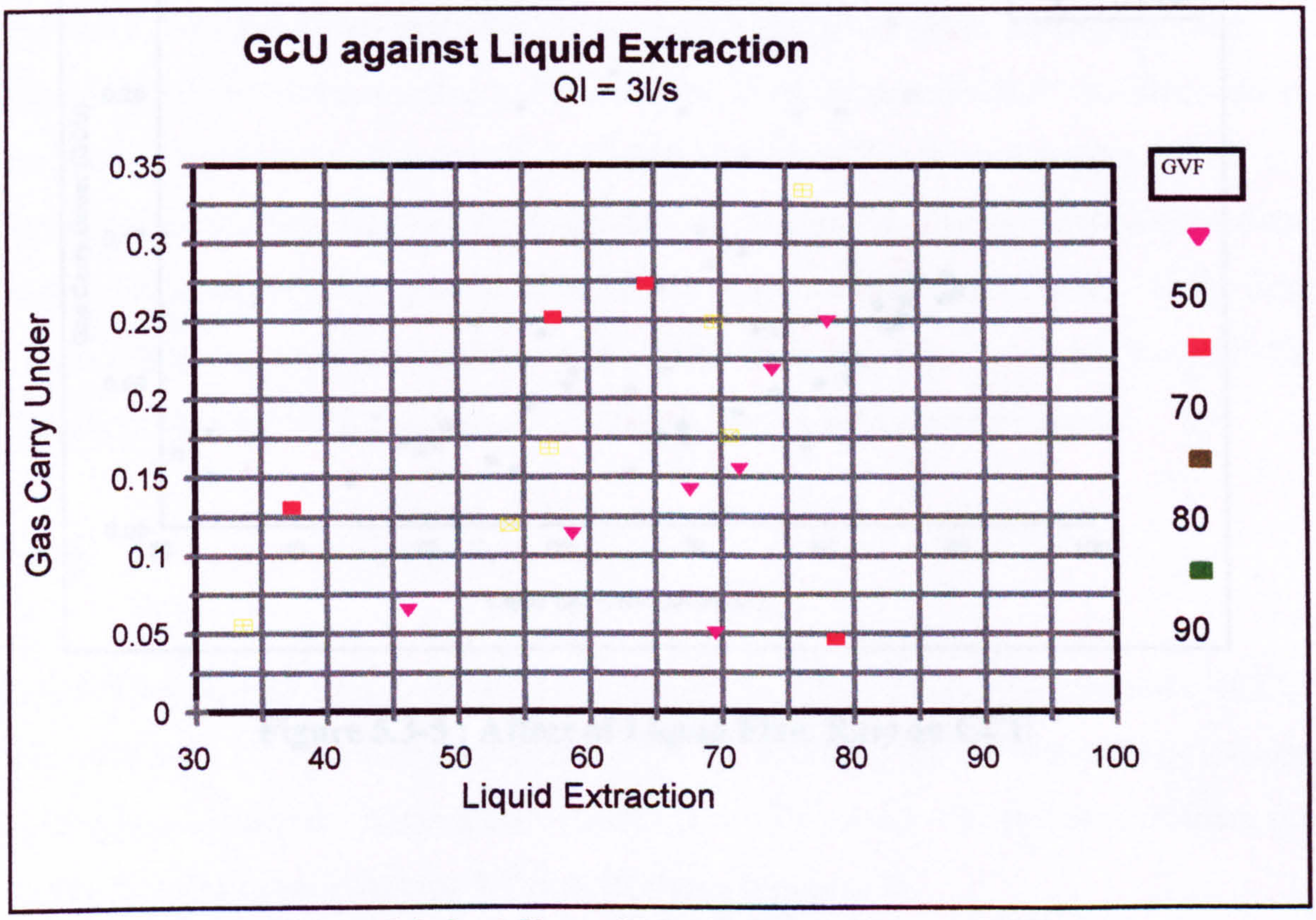

Figure 5.3-4 : Affect of Liquid Extraction on GCU

5.3.5 Affect of Liquid Flow Rate on GCU

To investigate the affect of the liquid flow rate (or superficial liquid velocity) on GCU the trend shown in figure 5.3-5 should be examined. In this graph the GVFs have been ignored to focus upon the influence of the liquid flow.

A pattern seems to form where the curve of the highest liquid flow is at the far right of the graph. A progressive shift of the curves to the left is seen as the liquid flow rate is reduced. This indicates that for a given liquid extraction rate, less gas is carried under as the liquid flow rate is increased.

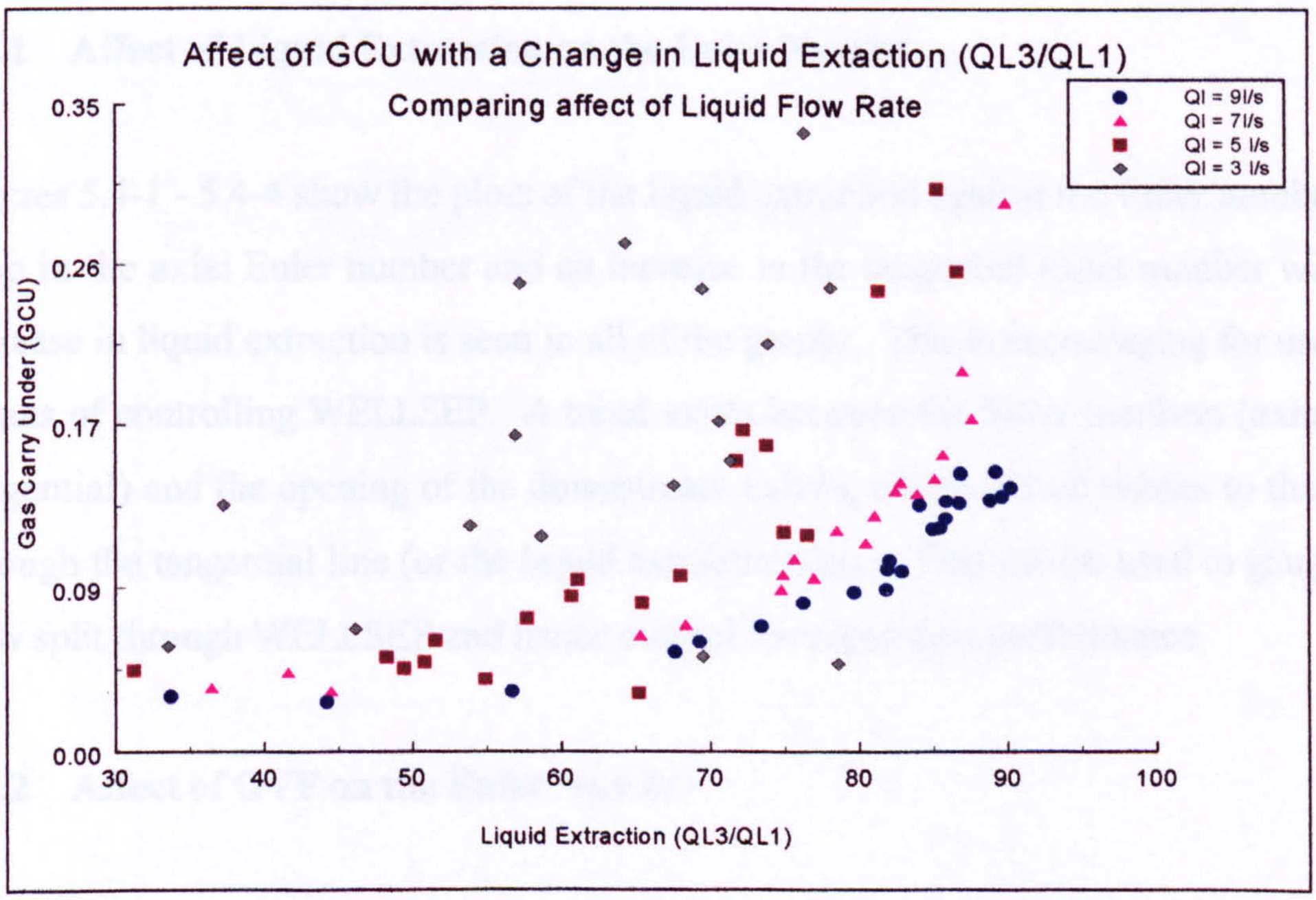

Figure 5.3-5 : Affect of Liquid Flow Rate on GCU

5.4 Euler Number (Dimensionless Pressure Drop)

The second performance characteristic is the Euler number which is related to the flow split and pressure drop across the separator. The relationship between the Euler number and GCU is also important as it can be used in both the design and operation of WELLSEP. Figures 5.4-1 - 5.4-4 show the plots of the liquid extraction against the Euler number for both the axial and tangential lines. Note that the axial line is the one which is "straight through" or on the same axis as the input line (where Q_{L2} is measured) and the tangential line is the one at a tangent to the input (where Q_{L3} is measured). There is a different pressure drop across both lines and hence there is a different Euler number for each line. Lines sloping from the top left to the bottom right of the graph for the axial line and from the bottom left to top right for the tangential line can be drawn through the results.

5.4.1 Affect of Liquid Extraction on the Euler Number

Figures 5.4-1 - 5.4-4 show the plots of the liquid extraction against the Euler number. A drop in the axial Euler number and an increase in the tangential Euler number with an increase in liquid extraction is seen in all of the graphs. This is encouraging for use as a means of controlling WELLSEP. A trend exists between the Euler numbers (axial and tangential) and the opening of the downstream valves, which in turn relates to the flow through the tangential line (or the liquid extraction rate). This can be used to gauge the flow split through WELLSEP and hence control the separation performance.

5.4.2 Affect of GVF on the Euler Number

The GVF does seem to have an affect on the Euler number, even though it did not on GCU. Figures 5.4-1 - 5.4-4 show that an increase in GVF shifts the lines downwards (ie causing a reduction in the Euler number at the intercept on the y axis). This means that there is a lower pressure drop across the WELLSEP with a higher GVF.

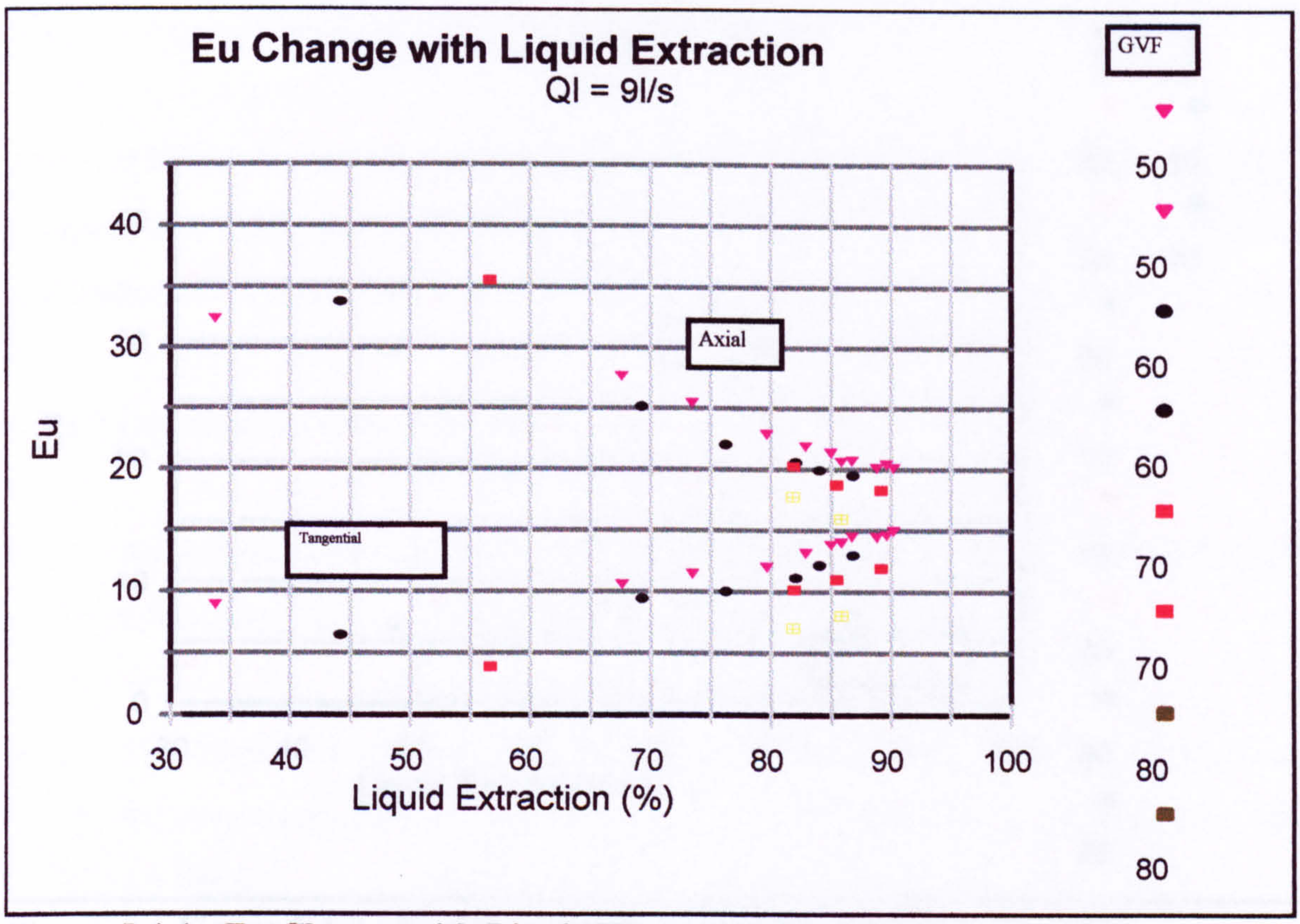

Figure 5.4-1 : Eu Change with Liquid Extraction for Q_L = 9l/s

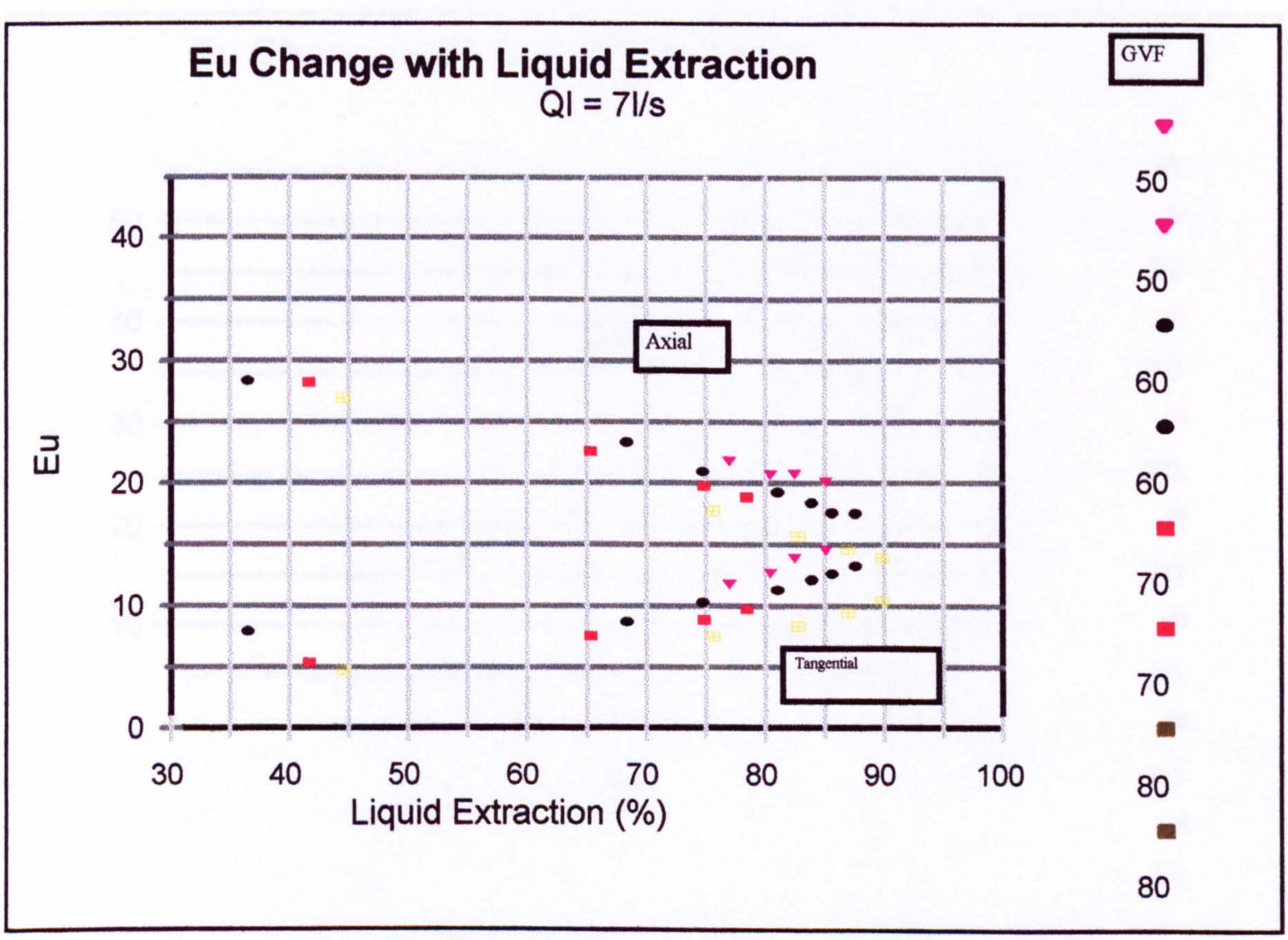

Figure 5.4-2 : Eu Change with Liquid Extraction for Q_L = 7l/s

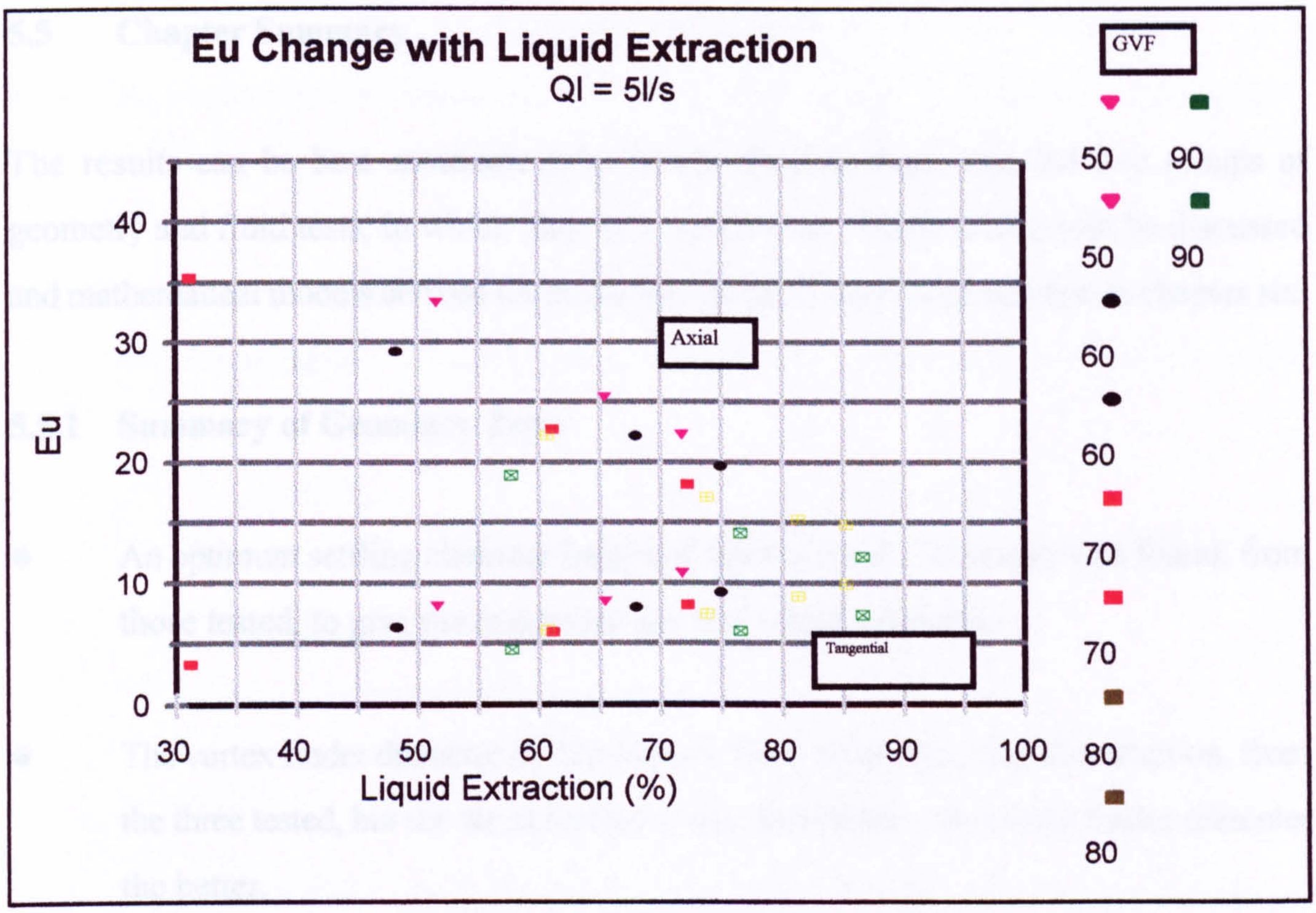

Figure 5.4-3 : Eu Change with Liquid Extraction for Q_L = 5l/s

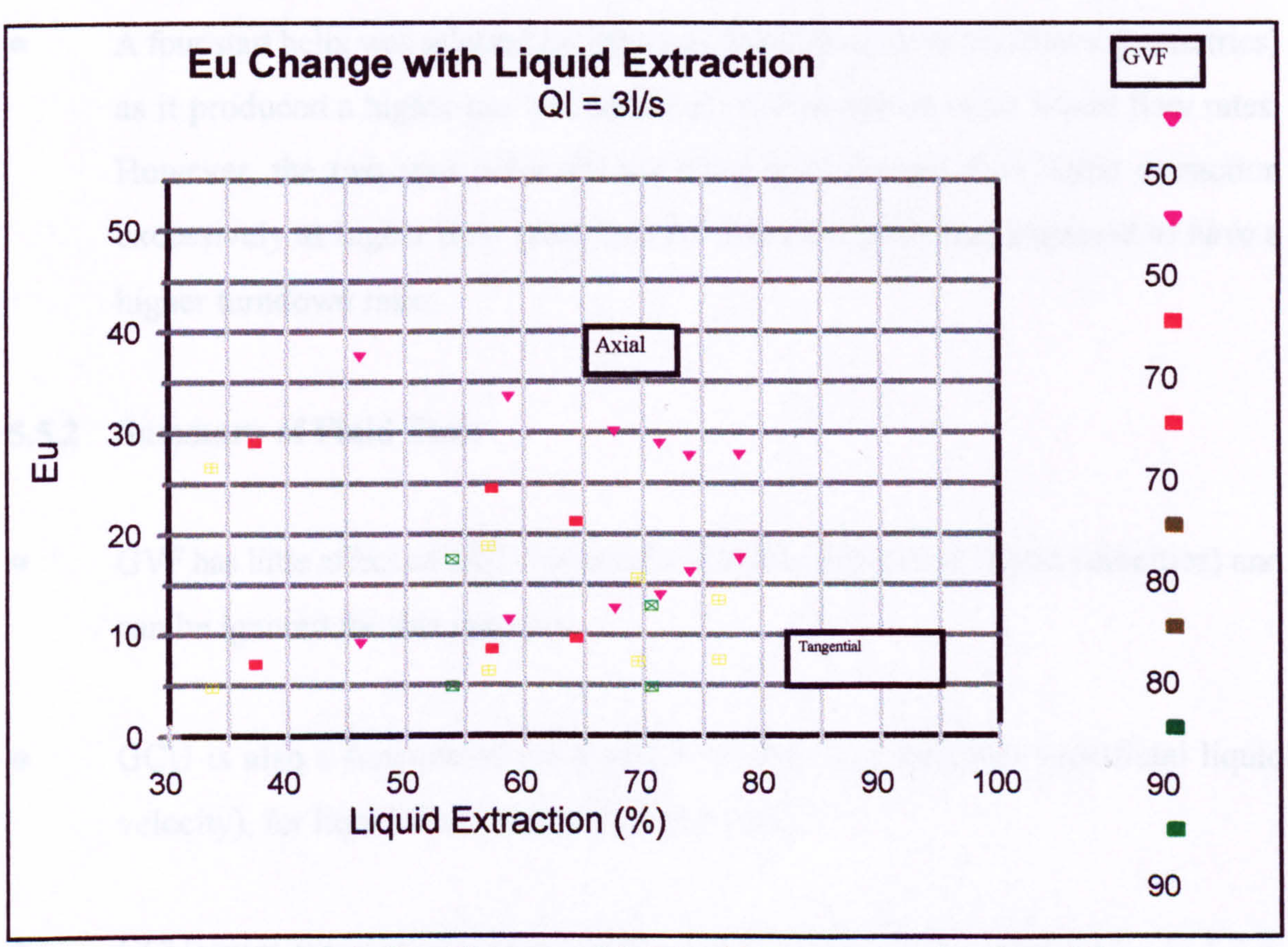

Figure 5.4-4 : Eu Change with Liquid Extraction for Q_L = 3l/s

5.5 Chapter Summary

The results can be best summarised by firstly dividing them into the two groups of geometry and fluid tests, in which they were performed. These results will be discussed and mathematical models derived for prediction of GCU and Euler number in chapter six.

5.5.1 Summary of Geometry Tests

- An optimum settling chamber length of three times the diameter was found, from those tested, to give the maximum gas free liquid extraction.

- The vortex finder diameter of 30mm gave the best gas free liquid extraction, from the three tested, but the trend indicated that the smaller the vortex finder diameter the better.

- A four start helix was selected for the fluid tests (along with the above geometries) as it produced a higher gas free liquid extraction rate at lower liquid flow rates. However, the two start helix did not deteriorate the gas free liquid extraction excessively at higher flow rates, but the four start helix was expected to have a higher turndown ratio.

5.5.2 Summary of Fluid Tests

- GVF has little affect on GCU (especially at higher superficial liquid velocities) and can be ignored for this purpose.

- GCU is also a function of the liquid flow rate (and therefore superficial liquid velocity), for liquid flow rates of 5, 7 and 9 l/s.

- GCU varies exponentially with liquid extraction as shown in figures 5.3-1 to 5.3-3.

- An increase in GVF leads to a decrease in Euler number, as shown in figures 5.4-1 to 5.4-4.

- An increase in liquid extraction causes a decrease in the axial Euler number and an increase in tangential Euler number, which is also illustrated in figures 5.4-1 to 5.4-4.

CHAPTER SIX

6 DISCUSSION AND MODELLING OF THE RESULTS

The results given in chapter five are reviewed in this chapter and the phenomena observed are discussed; suggestions are made as to why they occur. Mathematical models are suggested which describe the influence of the fluid parameters. These models can be used in the design of WELLSEP and an example of this has been given. This chapter ultimately summarises the advantages and commercial implications of this work and emphasises its contribution to knowledge.

6.1 Geometry tests

The geometry tests produced findings related to the settling chamber, vortex finder diameter, and the helix, and investigated their influence upon liquid extraction. This work led to the selection of one design for use in the fluid tests.

6.1.1 Settling Chamber Length

The results showed that up to a point, an increase in the length of the settling chamber resulted in an increase in the liquid extraction. Beyond this point any further increase did not offer any substantial increase in liquid extraction and in some cases, slightly decreased it.

This corresponds with the results with Stenhouse and Trow (1985) who also found that there was an optimum length of cyclone, above and below which separation efficiency would deteriorate. Daniels (1957) also reported that an increase in length led to an increase in separation efficiency, but both researcher's work was based upon solid particle removal from a gas stream. Daniels attributed the increased separation efficiency, brought about by an increase in length of cyclone, to Stokes Law of Sedimentation. Stokes Law predicts that a smaller particle would take longer to reach the wall of the cyclone, and therefore a longer cyclone will allow the smaller particles to reach the cyclone wall and

hence be separated.

Previous gas cleaning research by Daniels and Alden (1959) has highlighted the problem of particle bounce which is where solid particles bounce off the wall of the cyclone and become re-entrained into the gas flow. Therefore if the length of the cyclone is too long, larger particles can become re-entrained and the separation efficiency can be reduced. This may account for the findings of Stenhouse and Trow (1985), but gas/liquid separation should not have the problem of particle bounce. Instead, the liquid droplets would coalesce at the cyclone wall, for low concentrations of liquid, and have no affect for high liquid loadings. Therefore once an optimum length has been reached where the smaller particles have reached the cyclone wall, no change should occur in separation efficiency. Daniels also found that wetting the wall of a cyclone can prevent re-entrainment of particles which would otherwise bounce off the wall.

The theories of equilibrium orbit and residence time would both have predicted that an increase in length would lead to an increased separation efficiency.

Observation also assisted in determining why the length of the settling chamber affected the performance of WELLSEP. If the settling chamber was inspected just downstream of the helix, then a pattern of bubbles in the shape of a Christmas tree (broadly dissipated at the tip of the helix reducing to a smaller diameter further downstream) and from then on, the gas formed a core in the centre. It stands to reason that if the settling chamber is not long enough then the liquid may be removed before the bubbles have formed a more settled core in the centre of the chamber. This would lead to an increase in GCU. Conversely, once the bubbles have formed the core in the centre, then there would be no need to increase the settling chamber length further.

6.1.2 Vortex Finder

The test results indicate that a reduction in vortex finder diameter causes an increase in the

gas free liquid extraction rate. This occurred with every settling chamber length and both helices. Obviously, the vortex finder diameter can only be reduced down to certain point if there is still to be an axial exit.

It is difficult to explain why this phenomenon occurs. In fact the opposite may have been expected due to the reduced flow area on the axial outlet forcing the flow through the tangential outlet of WELLSEP. Therefore, it may well have been expected that more gas would be carried under. Nonetheless, this result cannot be ignored (even if not explained) and should be noted for geometric designs of WELLSEP.

One would have expected that higher GVFs would lead to a larger diameter of gas core forming in the settling chamber and therefore a larger vortex finder diameter would be more suitable to allow the gas to flow through the axial outlet; the same logic may well have been expected for a smaller vortex finder diameter. However, although a higher GVF does produce a larger gas core diameter (and conversely a lower GVF yields a smaller diameter of gas core) the smaller vortex finder diameter provides a gas free liquid extraction which is as good as or better than the larger diameters for all GVFs.

One possible explanation could be due to local pressure differences (eg. In figure 6.1-1, $p1 > p2 > p3$ and $p4 > p3$. If this is the case then an increase in velocity would be expected in the central gas core region. If a smaller vortex finder creates a lower local pressure and causes an increase in velocity then separation efficiency could be increased.

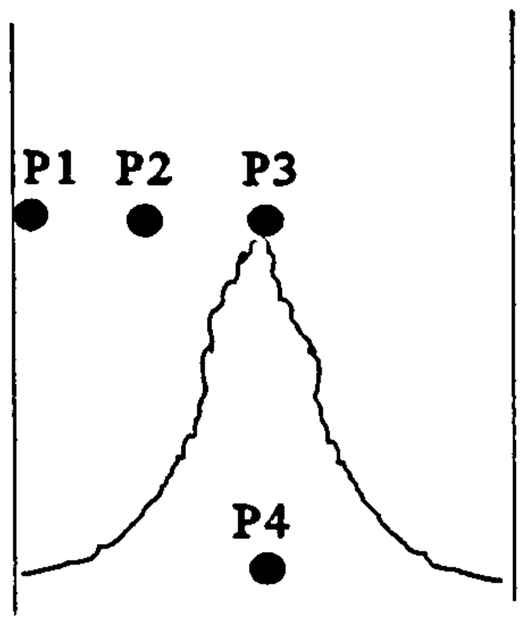

Figure 6.1-1 : Pressure Variation in the Settling chamber

This phenomenon is interesting and more information from test data is required for a justified argument to be made. Pressure measurements should be taken at various locations within the settling chamber. This could be done using a Pitot tube or LDA techniques (the latter being non-intrusive and therefore preferable). This is a suggestion for further work.

6.1.3 Helix Design

The results showed that there was very little affect on separation efficiency between the two and four start helices at higher liquid flow rates. However at lower liquid flow rates, the two start was not as effective. Therefore, the two start helix can generate the required centrifugal force at higher flow rates, but it is not sufficient when the flow rate is lower. This can be explained by the fact that the four start helix obscures more of the flow path than the two start helix which causes an increase in velocity due to the reduced area. At the lower liquid velocities this becomes more relevant as found in the fluid tests where the performance of WELLSEP deteriorated with low superficial liquid velocities.

6.2 Fluid tests

The results of the fluid tests produced many findings relating to both the pressure drop and separation efficiency. Influences of factors such as GVF, liquid velocity/flow rate, and liquid extraction on both separation efficiency and pressure drop are also discussed and models for pressure drop and separation efficiency are derived in the following sections.

6.2.1 Liquid Extraction on Gas Carry Under (GCU)

GCU varies exponentially with liquid extraction as can be seen in figures 5.3-1 - 5.3-4. This means that as more liquid is removed from the tangential outlet of WELLSEP, the amount of GCU increases. It also means that GCU is much more sensitive at higher liquid extractions - or a small change in liquid extraction at a higher liquid extraction rate can change the amount of GCU much more than at a lower liquid extraction.

This sort of relationship is what would be expected. If more liquid is allowed to pass through the tangential line (ie the liquid extraction is increased) then the valve on the tangential line has been opened more which would encourage both liquid and gas to flow through the exit. A change in pressure is brought about by opening the valve on the tangential line. The back pressure on the line is lowered and a higher flow rate is permitted through. The tangential Euler number, however, increases as a higher flow rate leads to higher frictional losses. Therefore a balance has to be sought between the amount of liquid which is wished to be removed and the amount of GCU present.

6.2.2 Effect of Gas Void Fraction (GVF) on Gas Carry Under (GCU)

The GVF seems to have very little significance on the graphs of liquid extraction against GCU (figures 5.3-1 - 5.3-4), at liquid flow rates of 9 and 7 l/s (or superficial liquid velocities of 2.04 and 1.58 m/s). The data points for all of the different GVF's fall very close to one curve. At 5 l/s (v_{SL} = 1.13 m/s), however, the data points no longer fall as

close to the one curve but are more scattered about it. However, it is difficult to see any particular relationship between the data points for the different GVF's. At 3 l/s (v_{SL} = 0.68 m/s), the scatter about the curve has become much larger, and the performance of WELLSEP is poor. The use of WELLSEP at such low superficial liquid velocities is not recommended. WELLSEP should therefore be designed to operate with a turndown which provides a superficial liquid velocity above 1.13 m/s.

Visual observation of WELLSEP's performance also provided some additional assistance in describing what was happening. At the higher liquid flow rates, WELLSEP seemed to cope much better with separation. Any fluctuations in the flow, such as those caused by slug flow upstream, caused a fluctuation in the diameter of the gas core in the settling chamber. However, at the lower liquid flow rates, the liquid flow could momentarily appear to stop flowing through WELLSEP. In other words a large bubble of gas with very little liquid would churn through and it was not possible to achieve a liquid flow free from gas in the tangential exit of WELLSEP.

One possible explanation for this is that the liquid phase (being denser and hence having more momentum) is the principal contributor towards the centrifugal force required for good separation. As long as the superficial liquid velocity is high enough , the superficial gas velocity will not influence the separation performance.

6.2.3 Liquid Flow Rate Effect on GCU

Figure 5.3-5 shows a graph of GCU against liquid extraction for each liquid flow rate tested. The results show that a trend exists between the liquid flow rate and the amount of GCU at a particular liquid extraction, illustrated by the progressive shift of the curves to the left. This indicates that GCU is a function of liquid flow rate as well as liquid extraction as described by equation 6.2.3.1.

$$GCU = f(Q_L, L.E.) \qquad 6.2.3.1$$

The trend indicates that a higher liquid flow rate will result in a lower GCU, and a lower liquid flow rate will result in a higher GCU, at a particular liquid extraction.

If curves are drawn through the data points in figure 5.3-5, it can be seen that GCU varies exponentially to the power of about 4.3 times the liquid extraction (expressed as a decimal, e.g. 70% = 0.7) for all of the curves.

Or

$$GCU \propto f(Q_L) e^{(4.3 \times L.E.)} \qquad 6.2.3.2$$

The function of the liquid flow rate $f(Q_L)$ can be found by plotting the function against liquid flow rate as seen in figure 6.2-1, which shows that the higher the liquid flow rate and hence superficial liquid velocity, the lower the GCU will be (as GCU is proportional to $f(Q_L)$). The GCU will decrease exponentially with an increase in liquid velocity.

Therefore the function can be found empirically as:

$$f(Q_L) = 0.087\ e^{(-0.74\ Q_L + 0.041 Q_L^2)} \qquad 6.2.3.3$$

Combining equation 6.2.3.2 with equation 6.2.3.3 gives:

$$GCU = 0.087\ e^{(4.3\ L.E.\ -0.74 Q_L + 0.041 Q_L^2)} \qquad 6.2.3.4$$

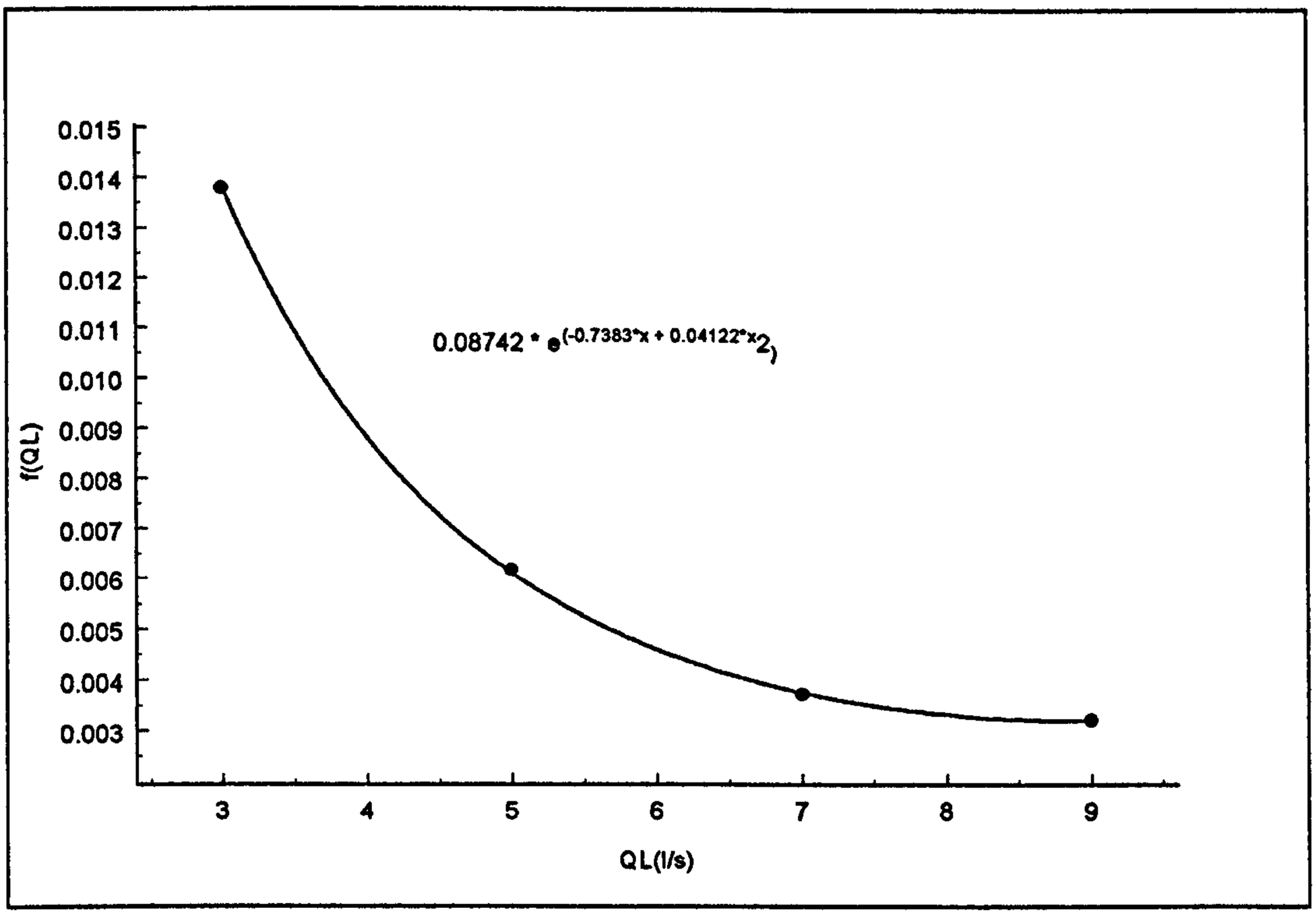

Figure 6.2-1 : Graph to Determine the Function of Liquid Velocity

For scaling purposes it would be better to describe the liquid flow rate as a superficial liquid velocity and design the diameter of WELLSEP to provide that velocity. Therefore, using the law of conservation of mass (Q = vA) equation 6.2.3.4 can be re-written as:

$$GCU = 0.087\ e^{(0.8\ v_{SL}^2\ -\ 3.27\ v_{SL}\ +\ 4.3\ L.E.)} \qquad 6.2.3.5$$

6.2.3.1 Accuracy of the GCU Prediction Model

Figures 6.2-2 - 6.2-5 compare the GCU prediction model (equation 6.2.3.5) to the actual test data for all of the superficial liquid velocities tested. The model predicts the GCU very well for superficial liquid velocities of 1.13 m/s and above. Below this threshold the model breaks down but so does the performance of WELLSEP. Therefore, it would not be advisable to use WELLSEP below a superficial liquid velocity of 1.13 m/s, and the model

can be confidently used within this boundary.

It should also be remembered that both the predicted values and test data correspond to average readings taken over a sample period of one minute. The instantaneous readings would fluctuate around this value and may produce cases where more and less gas is carried under.

The model also becomes less accurate at the extremes of liquid extraction. This can be seen in figure 6.2-3 for liquid extractions above 85% and to a lesser extent at the lower liquid extraction rates (around 40%).

If it is essential that no more than the predicted GCU is actually carried under, then a factor of safety is recommended at the designer's discretion. However, due to the nature of two phase flow, fluctuating flow is unavoidable unless the flow is pre-conditioned.

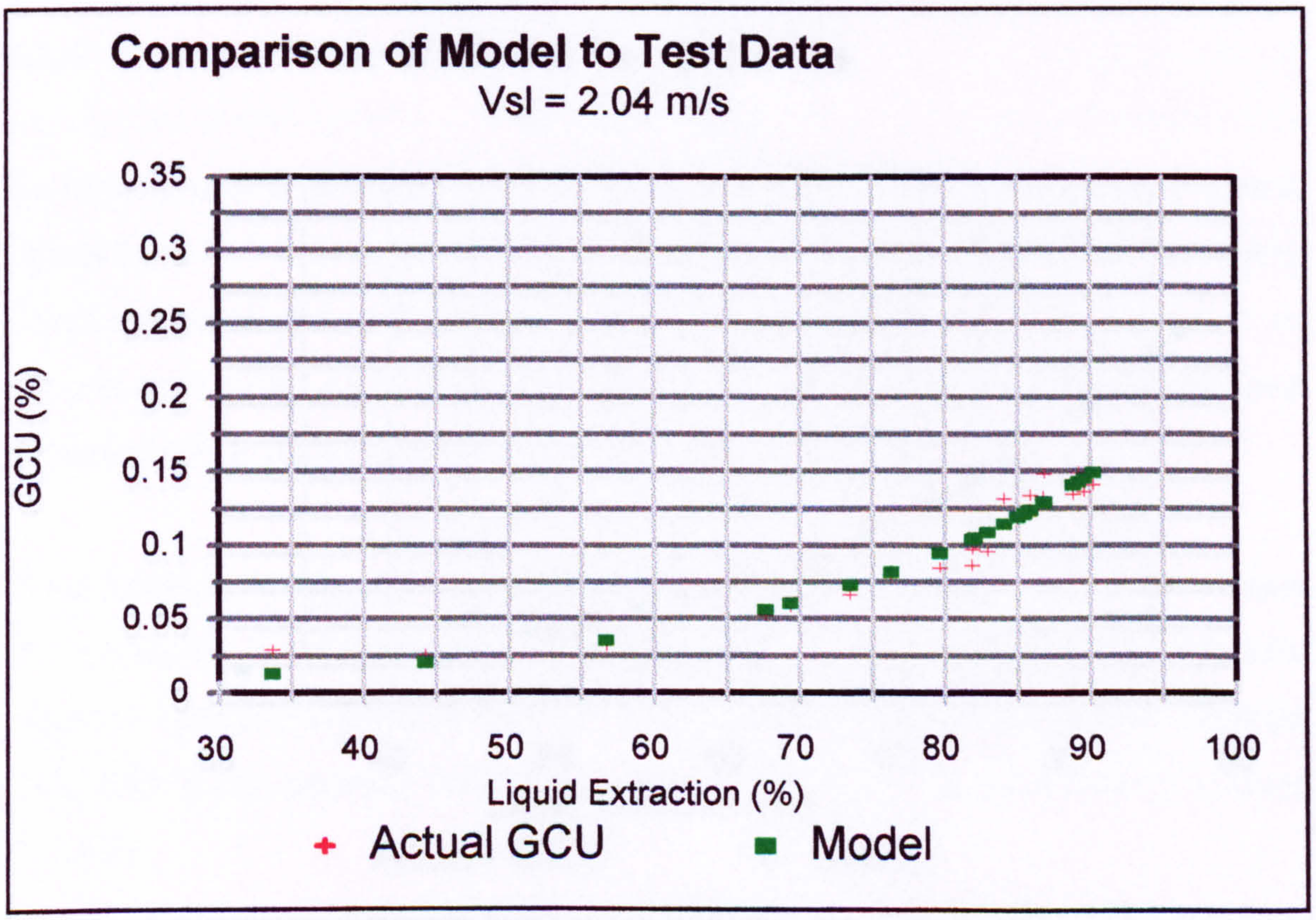

Figure 6.2-2 : Comparison of GCU Model to Data

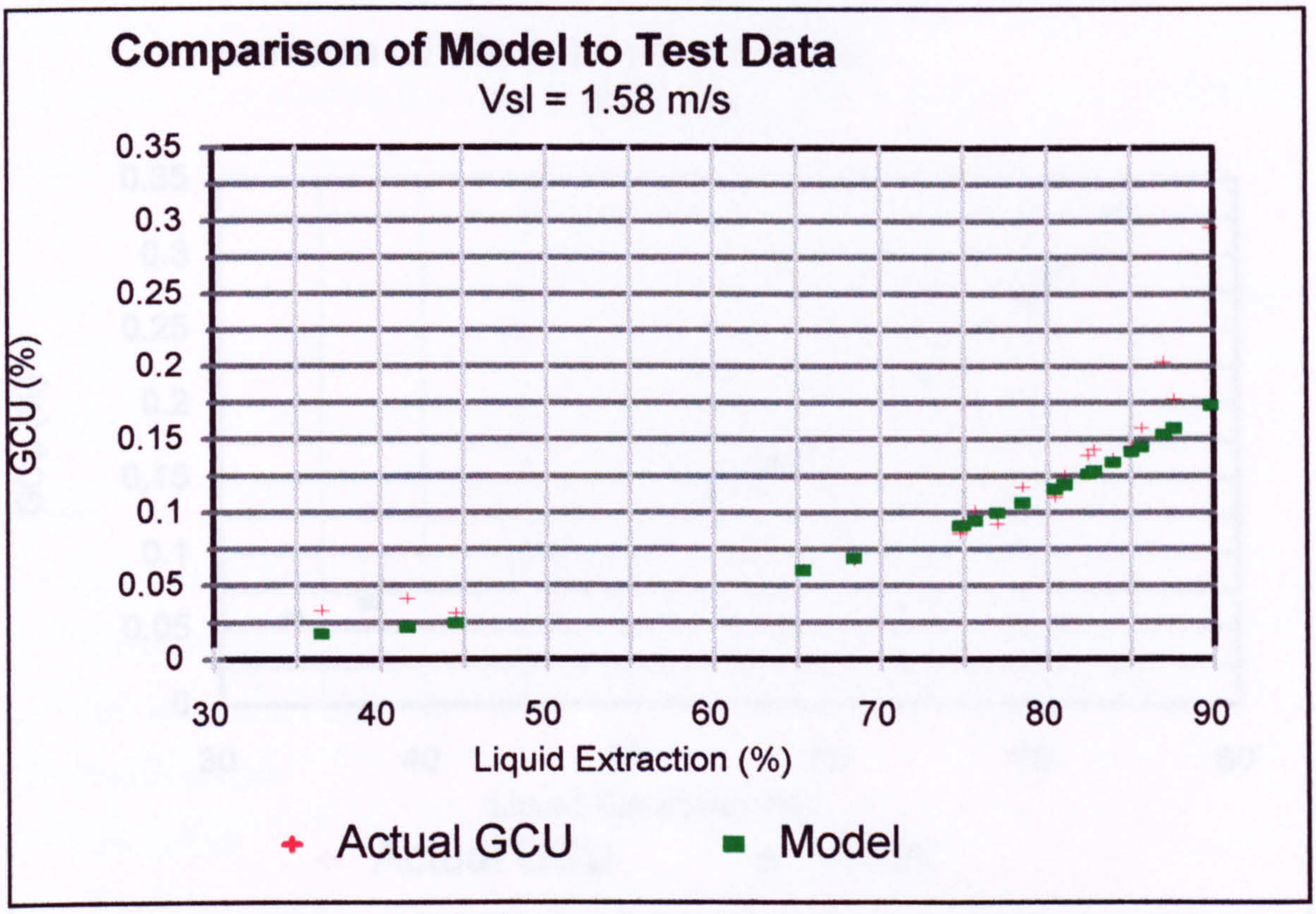

Figure 6.2-3 : Comparison of GCU Model to Data

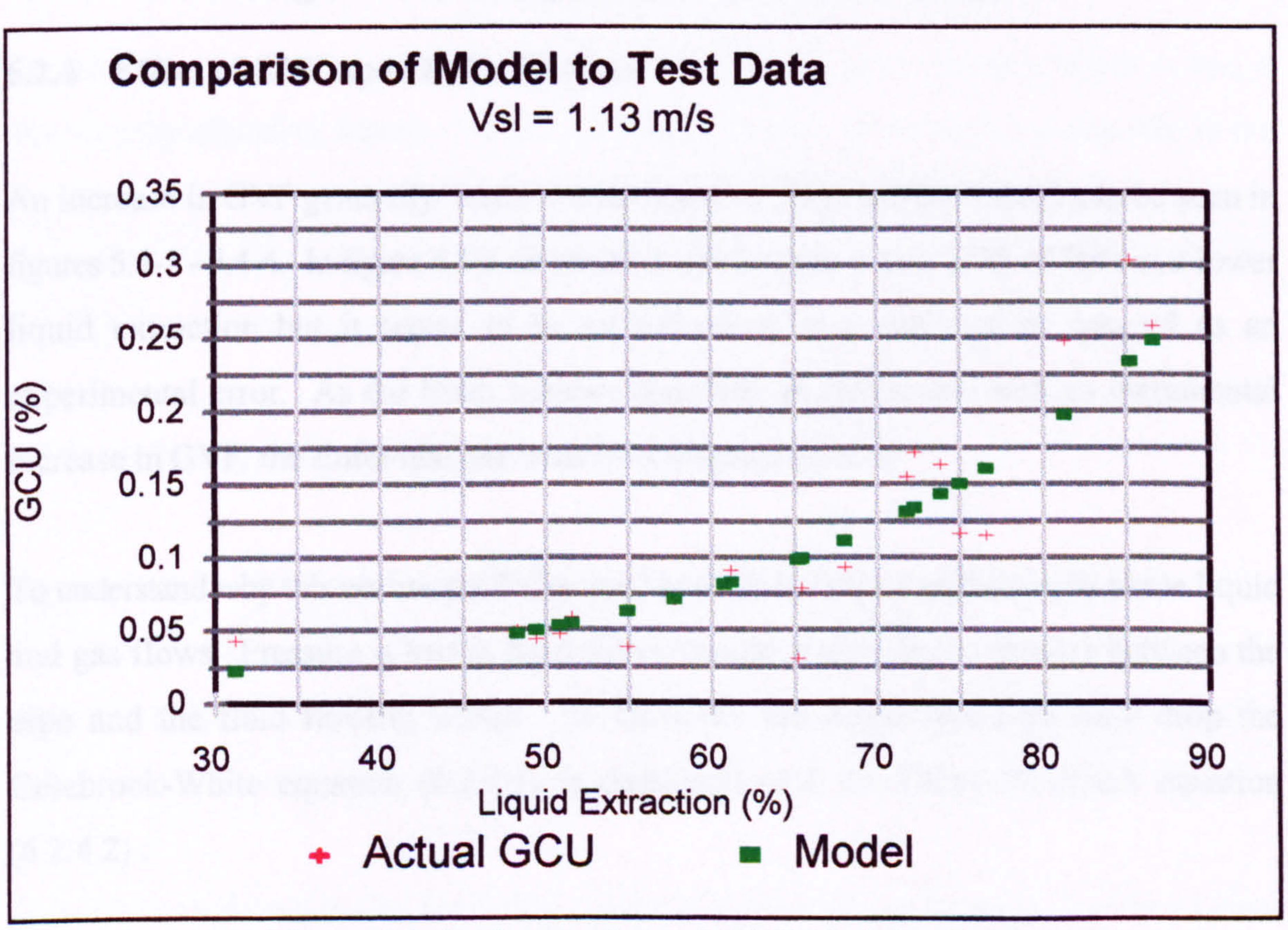

Figure 6.2-4 : Comparison of GCU Model to Data

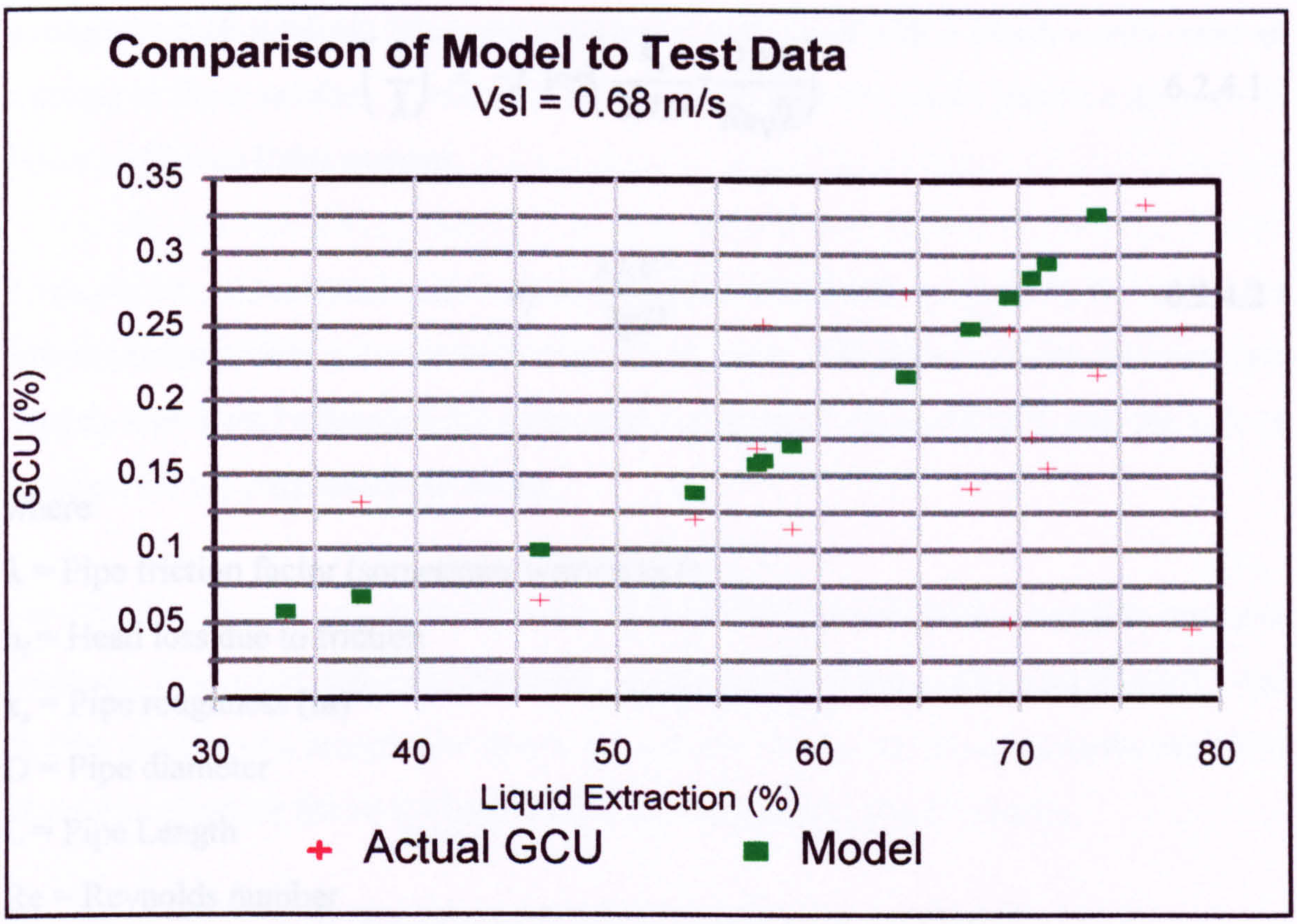

Figure 6.2-5 : Comparison of GCU Model to Data

6.2.4 Effect of GVF upon Euler Number

An increase in GVF generally leads to a decrease in Euler number which can be seen in figures 5.4-1 - 5.4-4. In figure 5.4-1 an anomaly can be seen with a GVF of 70% at a lower liquid extraction but it seems to be an individual case and can be ignored as an experimental error. As the Euler number decreases progressively with an incremental increase in GVF, the Euler number must be a function of GVF.

To understand why this occurs, the Euler number must be inspected for single phase liquid and gas flows. Pressure is lost as fluid flows through a pipe due to friction between the pipe and the fluid flowing within. To calculate the single phase pressure drop the Colebrook-White equation (6.2.4.1) is combined with the Darcy-Weisbach equation (6.2.4.2) :

$$\left(\frac{1}{\lambda}\right) = -2\log\left(\frac{k_s}{3.7D}+\frac{2.51}{Re\sqrt{\lambda}}\right) \qquad 6.2.4.1$$

$$h_f = \frac{\lambda L V^2}{2gD} \qquad 6.2.4.2$$

where

λ = Pipe friction factor (sometimes written as f)

h_f = Head loss due to friction

k_s = Pipe roughness (m)

D = Pipe diameter

L = Pipe Length

Re = Reynolds number

Therefore the pressure loss is directly proportional to Reynolds Number which in turn is directly proportional to density. For gas the density is much lower and consequently so are the losses and the converse is true for liquid. Therefore if the GVF increases with a two phase flow then less losses would be expected (which is common in the case of partially full pipes), as is shown to be the case in these results.

6.2.5 Influence of Liquid Extraction on Euler Number

Figures 5.4-1 - 5.4-4 show graphs of Euler number against liquid extraction and as discussed in section 5.4.1 a pattern exists for which a model can be suggested. Generally there is a drop in the axial Euler number and an increase in the tangential Euler number with an increase in liquid extraction.

This can be explained by the fact that an increase in liquid extraction means that more flow exits through the tangential exit and less through the axial exit. As more flow passes

through at a higher velocity, there are more losses associated with it which would cause an increase in Euler number. Contrarily, a decrease in velocity would lead to a decrease in losses and hence Euler number.

To produce a mathematical model of this affect, an assumption must firstly be made as to how the Euler number varies with the liquid extraction. The Euler number seems to vary linearly with liquid extraction for a particular superficial liquid velocity, and this will be assumed for the purpose of the model.

For all GVFs the lines which can be drawn through the data points have virtually the same gradient. This would imply that the liquid extraction has the same affect for all GVF's and that the gradient of a straight line drawn through the data points would describe the affect of liquid extraction for all GVFs at a particular superficial liquid velocity.

Therefore, the equation for a straight line can be used:

$$y = mx + c \qquad 6.2.4.1$$

Where m is the gradient and c is the intercept on the y axis. The equation can thus be written as:

$$Eu = mLE + c \qquad 6.2.4.2$$

where c is a function of GVF, and L.E. is the liquid extraction rate.

However, the gradients for the axial and tangential Euler numbers are different and they must therefore be investigated separately.

6.2.5.1 Tangential Euler Number

Upon inspection of figures 5.4-1 to 5.4-4, the tangential Euler number is shown to increase with an increase in liquid extraction. The gradient is approximately 25 for all of the tests (assuming that the liquid extraction is expressed as a decimal, e.g. 70% = 0.7) with the liquid flow rate of 9 l/s, and therefore equation 6.2.4.2 can be rewritten for the tangential line as:

$$Eu_{tangential} = 25L.E. + f(GVF) \qquad 6.2.4.3$$

For the axial line the gradient is about -34 and equation 6.2.4.2 becomes:

$$Eu_{axial} = -34L.E. + f(GVF) \qquad 6.2.4.4$$

The function of GVF for the tangential line can be found by plotting the function against GVF as shown in figure 6.2-6. A trend can be seen for all of the liquid flow rates where an increase in GVF leads to a decrease in the function. All flow rates have a gradient which is very similar and one can therefore be approximated for all cases. Some pattern may well also exist between the function and liquid flow rate but there is not enough information to suggest anything from these results. This is because it would be unfair to use the lower flow rates as WELLSEP is not functioning properly.

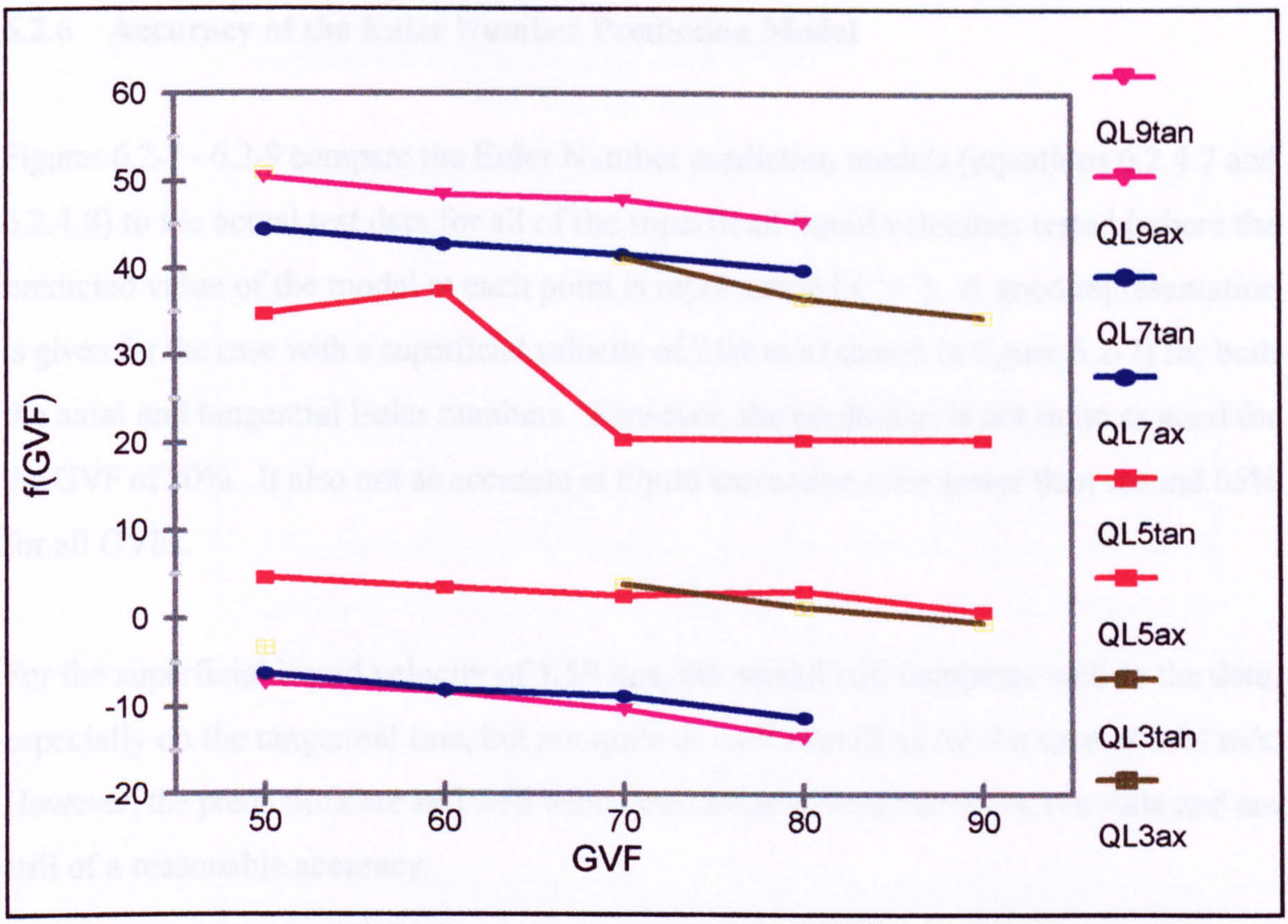

Figure 6.2-6 : Graph to Determine the Function of GVF

Therefore the function of GVF, f (GVF), for tangential line can be expressed as:

$$f(GVF) = 35 - 21GVF \qquad 6.2.4.5$$

assuming that GVF is expressed as a decimal, and for the axial line

$$f(GVF) = 61 - 21GVF \qquad 6.2.4.6$$

Combining equations 6.2.4.3 and 6.2.4.4 with 6.2.4.5 and 6.2.4.6 respectively gives the following equations for the axial and tangential lines:

$$Eu_{axial} = -34L.E. - 21GVF + 61 \qquad 6.2.4.7$$

$$Eu_{tangential} = 25L.E. - 21GVF + 3.5 \qquad 6.2.4.8$$

6.2.6 Accuracy of the Euler Number Prediction Model

Figures 6.2-7 - 6.2-9 compare the Euler Number prediction models (equations 6.2.4.7 and 6.2.4.8) to the actual test data for all of the superficial liquid velocities tested (where the predicted value of the model at each point is represented by '+'). A good representation is given for the case with a superficial velocity of 2.04 m/s (shown in figure 6.2-7) for both the axial and tangential Euler numbers. However, the prediction is not quite as good for the GVF of 70%. It also not as accurate at liquid extraction rates lower than around 65% for all GVFs.

For the superficial liquid velocity of 1.58 m/s, the model still compares well to the data, especially on the tangential line, but not quite as well overall as for the case of 2.04 m/s. However, the predictions are still well within the standard deviation of the test data and are still of a reasonable accuracy.

Although for the case of the superficial liquid velocity, the prediction is within the standard deviation, the model is not as good and it is not recommended that WELLSEP should be used at a lower superficial liquid velocity.

As with the GCU prediction model, it should also be remembered that both the predicted values and test data correspond to average readings taken over a sample period of one minute. The instantaneous readings would fluctuate around this value and may produce cases where a higher and lower Euler number is experienced.

When using the Euler number to set up WELLSEP on site, it should be remembered that an over-prediction of the tangential Euler number will lead to a higher liquid extraction and hence more GCU. Once the tangential Euler number has been predicted by the model, a reduction should be made (at the discretion of the designer) to force a lower liquid extraction and hence a lower GCU.

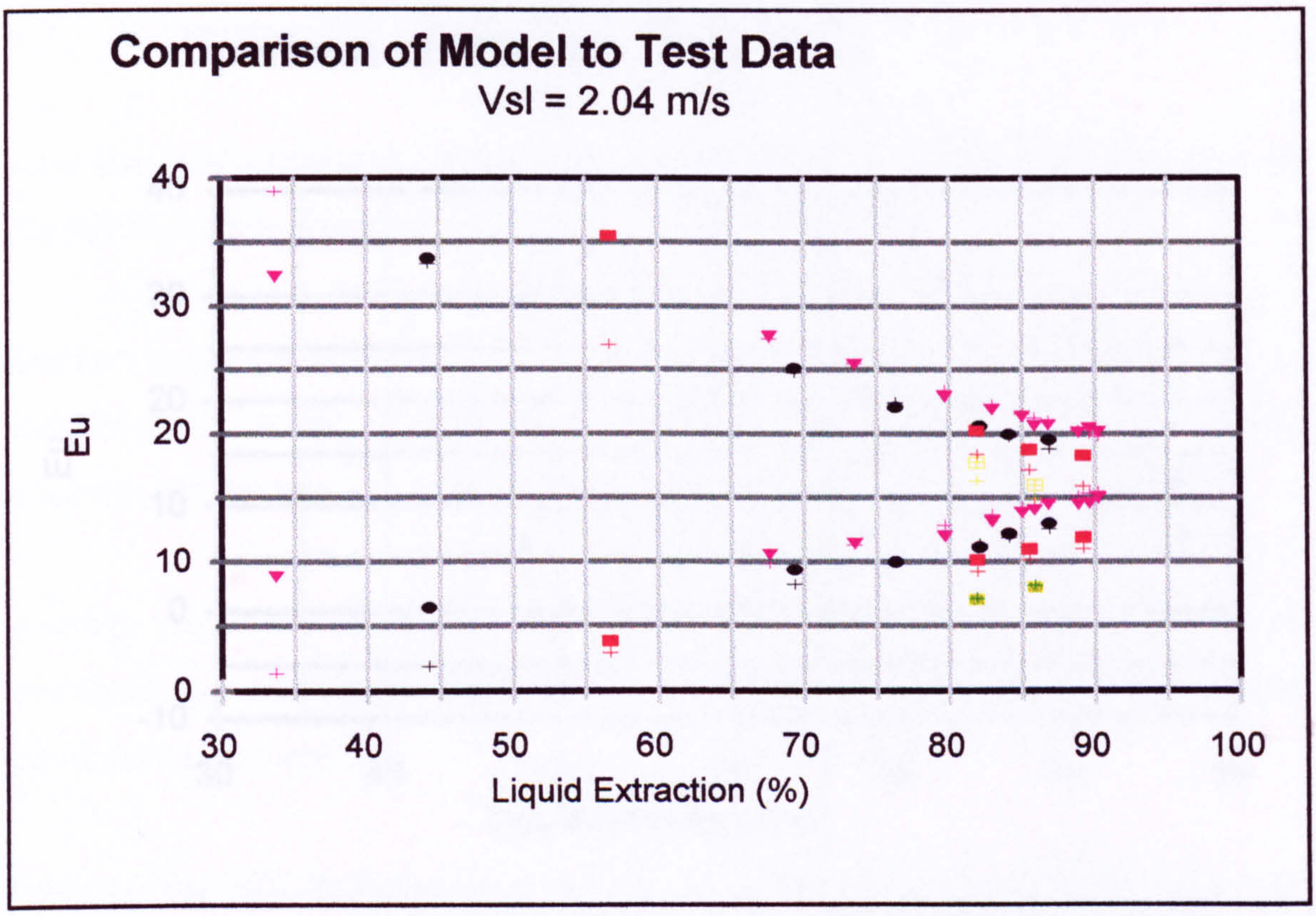

Figure 6.2-7 : Comparison of Euler Number Prediction Model to Test Data

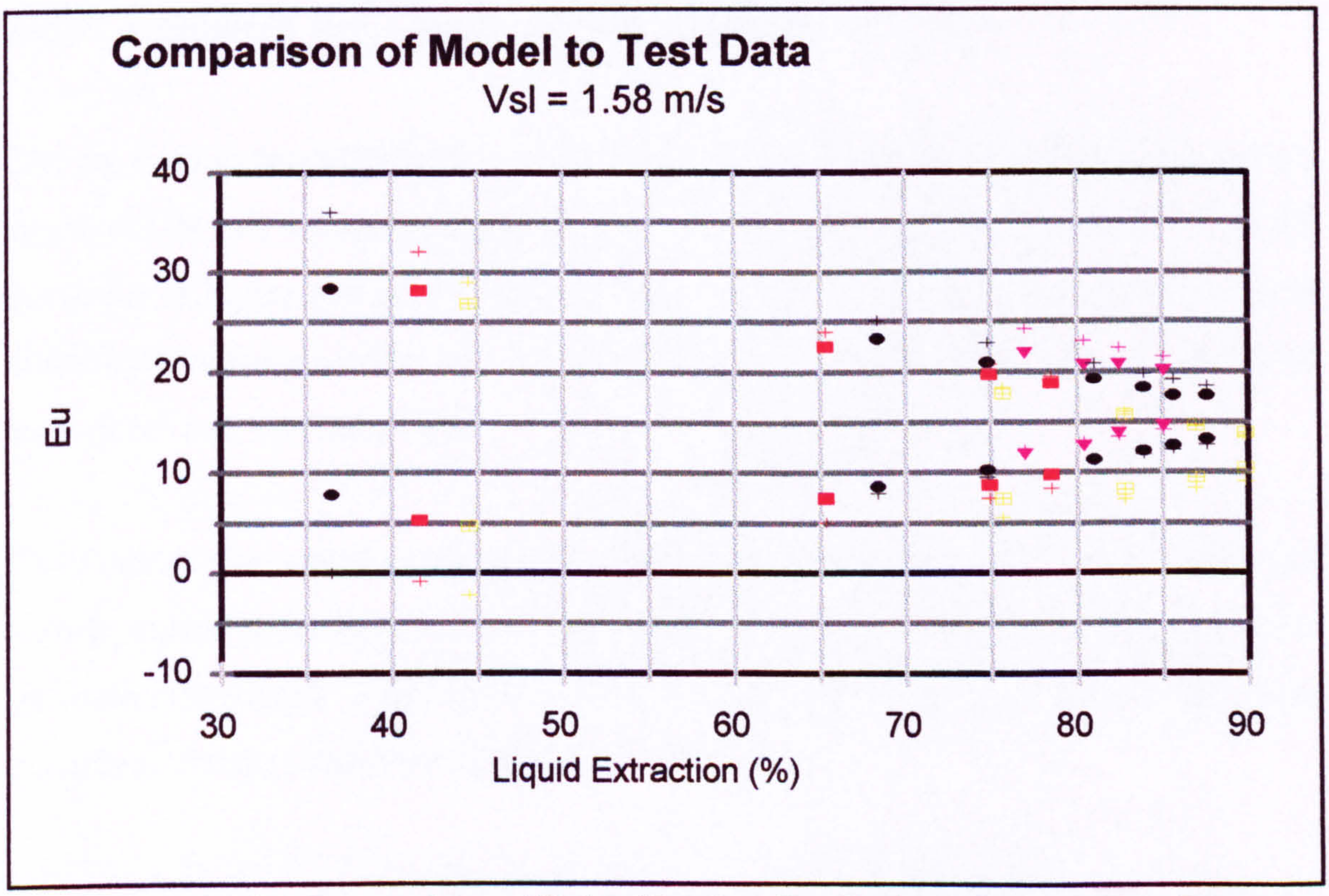

Figure 6.2-8 : Comparison of Euler Number Prediction Model to Test Data

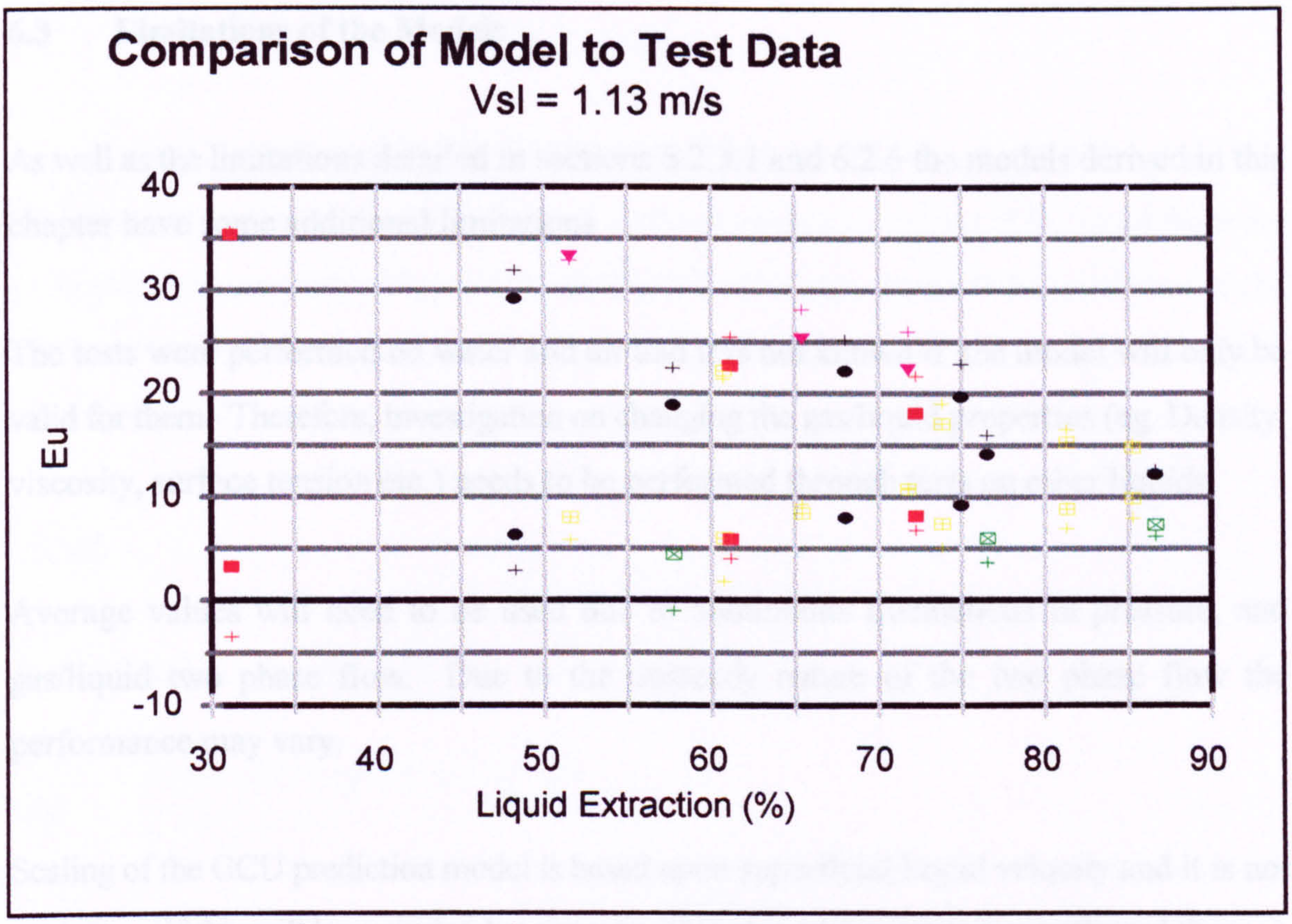

Figure 6.2-9 : Comparison of Euler Number Prediction Model to Test Data

6.3 Limitations of the Models

As well as the limitations detailed in sections 6.2.3.1 and 6.2.6 the models derived in this chapter have some additional limitations.

The tests were performed on water and air and it is not known if the model will only be valid for them. Therefore, investigation on changing the gas/liquid properties (eg. Density, viscosity, surface tension etc.) needs to be performed through tests on other liquids.

Average values will need to be used due to continuous fluctuations in pressure, and gas/liquid two phase flow. Due to the unsteady nature of the two phase flow the performance may vary.

Scaling of the GCU prediction model is based upon superficial liquid velocity and it is not yet known if this will be completely accurate. This should therefore be confirmed through further experiments with a smaller and larger diameter WELLSEP.

The rig used to test WELLSEP was only capable of an upper superficial liquid velocity limit of 2.04 m/s with some of the gas flows. It is therefore unknown how WELLSEP performs at higher superficial liquid velocities, yet this work has shown that a higher superficial velocity leads to an increased separation efficiency. However a maximum throughput may be experienced.

The Euler number model is also in need of refinement. The influence of superficial liquid velocity should be investigated further and the effect of the different geometries and swirl generators introduced. If this can be done then it will be a step closer to producing a more generic model for axial flow cyclones.

6.4 Design Example

A well head is producing 10 000 bbl/day of oil which has a density of 800 kg/ m^3 and 85000 scf/day of gas. If a company required a separator to extract 70% liquid from the gas/liquid mixture with no more than 20% GCU, what size would WELLSEP have to be and how would the downstream valves have to be adjusted (to provide what pressure drop) to achieve this?

Liquid

10 000 bbl/day = 0.0184 m^3/s

Gas

85 000 scf/day = 0.0279 m^3/s

Therefore

$$GVF = \frac{0.0279}{(0.0279+0.0184)} = 0.6 = 60\%$$

If GCU, and Liquid extraction are known, then the required superficial liquid velocity can be found from equation 6.2.3.5.

$$GCU = 0.087\ e^{(0.8\ v_{SL}^2\ -\ 3.27\ v_{SL}\ +\ 4.3\ L.E.)} \qquad 6.2.3.5$$

Substitute the values into equation 6.2.3.5 and take the natural log

$$\ln (0.2) = \ln (0.087) + 0.8\ v_{SL}^2\ -3.27\ v_{SL} + (4.3\ x\ 0.7)$$

which gives

$$-1.61 = -2.44 + 0.8\ v_{SL}^2\ -3.27\ v_{SL} + 3.01$$

$$-2.18 = (0.8\ v_{SL}^2\ -3.27\ v_{SL})$$

$$0 = 0.8\ v_{SL}^2\ -3.27\ v_{SL}\ +2.18$$

which is a quadratic equation solved by:

$$x = \frac{-b \pm \sqrt{(b^2\ -4ac)}}{2a}$$

Therefore

$$v_{SL} = \frac{53}{16} \quad or \quad \frac{13}{16}$$

which gives superficial velocities of 3.3 or 0.8 m/s.

0.8 m/s would be too low so the value of 3.3 m/s should be used.

Using the equation of conservation of mass:

$$Q_L = v_{SL}\ A$$

The required area would be

$$A=\left(\frac{0.0184}{3.3}\right) = 5.5\ x\ 10^{-3}\ m^2 = \frac{\pi D^2}{4}$$

Therefore

$$D = 0.0843\ m = 84\ mm$$

But to make certain that the GCU doesn't become too high a slightly smaller size would be recommended - say 80 mm.

The settling chamber length should be such that L/D = 3. L = 80 x 3 = 240mm
and the vortex finder diameter should be such that $_{\text{Vortex finder}}$ /D = 0.4. Therefore 32mm.

Therefore an 80mm diameter with a settling chamber length of 240mm and a vortex finder diameter of 32mm should be used.

The valves downstream of WELLSEP can be adjusted so that an Euler number which is satisfied by equations 6.2.4.7 and 6.2.4.8 is achieved.

$$Eu_{axial} = -34L.E. - 21GVF + 61 \qquad 6.2.4.7$$

$Eu_{axial} = 24.6$

$$Eu_{tangential} = 25L.E. - 21GVF + 3.5 \qquad 6.2.4.8$$

$Eu_{tangential} = 8.4$

The Euler number is used due to its dimensionless form but it would be easier to adjust the valves downstream if a pressure drop was given (as it could be directly read from a ΔP

Cell).

Therefore the axial pressure drop will be:

$$\Delta P = Eu \cdot \frac{1}{2} \rho_m \cdot v_m^2$$

$$\rho_m = (0.6 \cdot 1) + (0.4 \cdot 800) = 320 \ kg/m^3$$

$$v_m = \left(\frac{(18.4 + 27.9) \ x \ 10^{-3}}{5.5 \ x \ 10^{-3}} \right) = 8.42 \ m/s$$

$$= 24.6 \cdot \frac{320}{2} \cdot 8.42^2$$

$$= 2.79 \ x \ 10^5 \ Pa$$

$$\Delta P_{axial} = 2.79 \ bara$$

Similarly the tangential pressure drop will be:

$$\Delta P_{tangential} = 0.953 \ bara$$

6.5 Concluding Remarks

Separation performed in a cyclone has a number of distinct advantages over conventional gravity separators which has made them increasingly more popular for use in offshore oil and gas process systems. Some of these advantages, which were tabulated in table 1.2, can lead to considerable cost savings. Their small size and hence lighter weight makes them

ideally suited for platforms where supporting infrastructure is of a high premium. It also means that they can be more easily retrofitted (if required as the reserves in the reservoir deplete), in small spaces on platforms. No moving parts makes them reliable which is an extra advantage of particular importance especially to subsea use.

Subsea separation has been tried a number of times before with conventional gravity separators but problems with reliability, maintenance, repair and level control were experienced. Any of these factors which are not as vital to a topside process system are made all the more important when used subsea due to the high costs incurred in installation, downtime and retrieval. Where a faulty piece of equipment can be easily inspected and repaired on a manned platform, subsea systems require expensive vessels to deploy them subsea which can cost hundreds of thousands of dollars per day.

The likelihood of achieving total separation of both gas and liquid phase (ie. Removing all gas from the liquid and vice versa) is extremely low if it is to be performed in one stage through a single cyclone. If both phases are required totally free from each other then a subsequent process stage would be required; this could be another cyclone or another separator.

Many possible future uses of cyclones in the oil and gas industry can be identified along with those already mentioned and those already used. Some of these are listed below:

- Removing carbon dioxide and/or water which together form carbonic acid and can corrode pipelines and other equipment. When pipelines are designed to carry potentially corrosive substances they either have to have an extra sacrificial thickness in the pipe, be made from more expensive materials which do not corrode so easily (eg. Duplex), be lined, or have corrosion inhibitors injected. All of these add costs to the extraction of oil or gas.

- Downhole separation (actually in the well) to remove water from the produced

fluids. This could not only save the transportation of a non-essential product which could result in the need for larger pipes and added disposal and treatment costs but could also be re-injected back into the reservoir to maintain pressure. Water injection is common practice for pressure maintenance but currently requires the cleaning of water that may carry particulates which could block the reservoir and also requires an additional injection Christmas tree which costs of the order of £1M.

- Water removal can also prevent the formation of hydrates in the pipeline which can block flow or require the addition of inhibiting chemicals to prevent their formation.

- Liquid removal from gas lines which can otherwise drop out of the flow and build up a sufficient head to block the flow from the well.

Potential problems with subsea and downhole separation also include the fact that conditions at the wellhead will not be the same as those further along the transporting pipeline and ultimately at the termination point (offshore platform or onshore process plant). Therefore liquid can 'drop out' from the gas or gas can 'flash' from the liquid due to the different pressure and temperature along the pipeline.

The high costs associated with installation and retrieval make the need for IMR (Inspection, Maintenance and Repair) to be kept minimal.

Slug flow, which has been mentioned in chapter two, can develop upstream of a cyclone and cause unsteady flowing conditions. This can have a detrimental effect upon the performance of a cyclone.

The accomplishments of the work undertaken in this thesis mean that WELLSEP, which previously had no reliable design criteria, can now be more confidently designed for

commercial applications. A pressure drop model and separation efficiency prediction model have both been derived using dimensionless numbers to enable their use on different scale models (geometrically similar) of the design.

CHAPTER SEVEN

7 CONCLUSIONS & FURTHER WORK

Chapter seven highlights the information discovered as a result of this research work, and suggests possible avenues for future work which will be advantageous to the development of WELLSEP and other cyclone separators. The novelty and contribution to knowledge derived from this work are also emphasised.

7.1 Conclusions

The work reported in this thesis set out to achieve the following objectives:

i. To develop a design basis which will permit the design of WELLSEP for a particular duty.

ii. To investigate the affect of geometric changes on WELLSEP and use the information to select an improved geometry for improved separation.

iii. To develop a pressure drop model for WELLSEP.

All of these objectives have been achieved by this work which means that a commercial unit can now be designed with better confidence in its performance.

The research work produced a number of conclusions relating to both the geometry and the fluid parameters to which WELLSEP was subjected. As has been consistent throughout this thesis, the conclusions will therefore be divided into these categories in sections 7.1.1 and 7.1.2 respectively.

7.1.1 Conclusions of Geometry Tests

- An optimum settling chamber length of three times the diameter was found (from those tested) to give the maximum gas free liquid extraction. This was attributed to smaller gas bubbles requiring longer to reach the central core (by Stokes Law). Beyond this length, only a very small benefit may be noticed.

- The vortex finder diameter of 30mm gave the optimum gas free liquid extraction (from those tested), but the trend indicated that the smaller the vortex finder diameter the better. Obviously this is only practical to a limit or there will be only one exit from the cyclone.

- A four start helix was selected for the fluid tests (along with the above geometries) as it produced a higher gas free liquid extraction rate at lower liquid flow rates. However, the two start helix did not deteriorate the gas free liquid extraction excessively at higher flow rates, but the four start helix was expected to have a higher turndown ratio. This was explained by the fact that the four start helix obscures more of the flow path than the two start helix which causes an increase in velocity due to the reduced area. At the lower liquid velocities this was found to be more relevant as found in the fluid tests where the performance of WELLSEP deteriorated with low superficial liquid velocities.

7.1.2 Conclusions of Fluid Tests

- GVF has little affect on GCU (especially at higher superficial liquid velocities) and can be ignored for GCU prediction.

- GCU is also a function of superficial liquid velocity.

- GCU varies exponentially with liquid extraction.

- The above findings have been combined and the following semi-empirical model produced to predict GCU:

$$GCU = 0.087\ e^{(0.8\ v_{SL}^2\ -\ 3.27\ v_{SL}\ +\ 4.3\ L.E.)}$$

[where v_{SL} is in m/s, and Liquid Extraction (L.E.) is expressed as a decimal eg. 70% = 0.7)]

- An increase in GVF led to a decrease in Euler number.

- An increase in liquid extraction caused a decrease in the axial Euler number and an increase in tangential Euler number.

- The Euler number may also be a function of superficial liquid velocity, but insufficient data was obtained to quantify this. Consequently the influence of superficial liquid velocity was not included in the following Euler number models, which combines the other findings related to the Euler number:

$$Eu_{axial} = -34L.E. - 21GVF + 61$$

$$Eu_{tangential} = 25L.E. - 21GVF + 3.5$$

7.2 Further Work

The limitations of the models developed in this thesis and discussed in section 6.3 indicate some of the possible further work. These are summarised below:

i. Effect of different fluids (eg Oil and hydrocarbon gas)

The work carried out here has only investigated air and water as the gas/liquid mixture to be separated. For the models derived in chapter six to be applicable to oil and hydrocarbon gas, density, viscosity and surface tension variations need to be investigated and the effect on separation efficiency and pressure drop determined.

ii. Scaling Tests

Studies of different sizes of WELLSEP, but with the same geometric proportions should be undertaken to confirm that the dimensionless parameters used in conventional cyclone design are applicable. This is particularly necessary due to the presence of two phase flow.

iii. Higher liquid flow rates

The upper limit on the permissible flow rate through WELLSEP was not obtained as the capability of the test rig could not achieve it. For this to be determined a pump which can produce a higher flow rate should be used. Alternatively a smaller scale model would produce higher superficial velocities.

iv. Refine Euler number prediction model

As discussed in section 6.2.5.1, the Euler number may well be a function of the liquid flow rate. The further tests with different liquid flow rates, suggested previously, could also provide data to incorporate this relationship.

v Geometry optimisation

A number of other geometries of swirl generator have been tested by people such as Swanborn and his optimum design could be tested. Other geometric variations such as

angled settling chamber, protruding vortex finder are other possibilities. If each component is tested individually and modelled accurately, all of the data can be collected and an overall model developed which accounts for each component.

vi Demisting applications (models for solid/gas separation may apply)

WELLSEP has been used in this project for degassing applications but preliminary tests have indicated that it is also suitable for demisting. Work in this area would also be of benefit as the use of cyclones in this area has long been established. Comparison to the models already developed for solid/gas separation would also be of interest.

vii Flow pre-conditioner/slug catcher

It was apparent during the testing of WELLSEP that the performance was severely affected by pulsating flow such as slug flow regimes. A means of preventing the occurrence of slug flow will also be of use to all cyclones and other types of separator which are expected to encounter this flow regime.

7.3 Concluding Remarks

The cyclone separator, WELLSEP, previously had no design methodology and although it was known to achieve desirable separation, there was no way of designing it to give a known level of separation efficiency for a specific flow rate and GVF. This work has provided such a design guideline which can also assist in determining the correct aperture of the downstream valves by pressure drop prediction.

Future designs can be sized accurately by scaling of the dimensionless numbers as described in this thesis. WELLSEP can be designed for a particular separation efficiency under particular flow conditions. A multicyclone arrangement can be used if a larger throughput is required but a space reduction can still be offered over conventional gravity

separators.

Future applications of WELLSEP are on offshore oil & gas platforms where space is at a premium. WELLSEP also has no moving parts which reduces the risk of failure (ie. Increases reliability) and therefore also makes it more attractive for subsea and downhole separation.

8. REFERENCES

Alden, J., (1959). "Design of Industrial Exhaust Systems". 3rd ed. New York : Industrial Press.

Alexander, R.McK., (1949). "Fundamentals of Cyclone Design and Operation". Proc. Austral. Inst. Mining Metall. Processes, Vol. 152, pp. 203-228.

Arato, E., Barnes, N. (1992). "Application of a Novel In-Line Free-Vortex Separator in a Two Phase Pumping System". 4th International Conference on Hydrocyclones, Southampton, 23-25 September 1992, pp.377-396.

Bandyopadhyay, P.R., Pacifico, G.C., Gad-el-Hak, M (1994). "Sensitivity of a Gas Core vortex in a Cyclone type Gas-Liquid Separator". Proc. Of the ASME Fluids Engineering Division Summer Meeting. Part 14 of 18.

Barth, W., (1932). Rauch and Staub., Vol. 22, pp. 93.

Bloor, M.I.G., Ingham, D.B., Laverack, S.D. (1980). "An analysis of boundary layer effects in a hydrocyclone". Proc. Int. Conf. On Hydrocylones, Cambridge, 1-3 October 1980 Paper 5, pp.49-62. BHRA Fluid Engineering, Cranfield.

Bloor, M.I.G and Ingham, D.B. (1975). "Turbulent spin in a cyclone". Trans. I. Chem. E., 53, 1.

Bradley, D, (1965). "The Hydrocyclone". 1st ed : Pergammon Press.

Brill, J.P. and Beggs, H.D. (1984). "Two phase flow in pipes". Course notes, University of Tulsa.

Caplan, K.S., (1977). "Air Pollution", Vol. IV, Academic Press, New York.

Casal, J., Martinez-Benet, J.M. (1983). "A Better Way to Calculate Cyclone Pressure Drop". Chem Engng., Vol.90, No. 2, pp.99-100.

Criner, H.E. (1950). "The Vortex Thickener". Int. Conf. On Coal Preparation, Paris.

Daniels, T.C., (1957). "Investigation of a Vortex Air Cleaner". The Engineer, 203, pp.358-362.

Dickson, P. (1997). "Investigating Gas/Liquid Separation Within A Novel Compact Inline Separator". ImechE. Seminar "Up and Coming in Fluid Machinery".

Driessen, M.G. (1951). "Review of Industrial Mining", Special Issue No.4, pp.449-461. St. Etienne.

Fahlstrom, P.H. (1960). Discussion on pages 632 to 643, Proc. Int. Minimum. Processing Congress, Inst. Mining and Metallurgy.

First, M.W., (1949). "Cyclone Dust Collector Design". ASME. Paper No. 49-A-127, pp. 26.

Gordon, I.C., (1986). "A Review of Separation Equipment", MPE Report No. 003, Vol. 1: Literature Review.

HSE (1989). "SAFETY OF PRESSURE SYSTEMS - Pressure Systems and Transportable gas C***** regulations". ISBN 011885514X

Jackson, R., (1963). "Uniflow Cyclones". The British Coal Utilisation Research Association Monthly Bulletin, Vol. 27, No. 8, pp. 329-351.

Lissman, M.A., (1930). "An Analysis of Mechanical Methods of Dust Collection". Chem. And Metall., Engng., Vol. 37, No. 10, pp. 630-634.

Loxham, Michael. (1976). "The flow pattern in the exit pipe of a cyclone". Ph.D Thesis Delft University of Technology.

Lynch, A.J. and Rao, T.C. (1975). "Modelling and scale-up of hydrocyclone classifiers".11th International Mineral Processing Congress, Cagliari, Paper 9, Instituto di Arte Mineraria, pp.9-25.

Lynch, A.J., Rao, T.C., Prisbrey, K.A. (1974). Int J. of Mineral Processing., 1, pp.173- 181

Lynch, A.J. and Rao, T.C. (1968). Indian J. Technol., Vol. 6, pp.106-114

Marti, S., Erdal, F.M., Shoham, O., Shirazi, S., Kouba, G.E. (1996). "Analysis of gas carry-under in gas-liquid cylindrical cyclones". Hydrocyclones '96.

Massingberd-Mundy P.D.G., Snooks K.B., Gulliver J.G. (1992). "Development of a Cyclonic Degassing Separator for use in a Roadside Fuel Dispenser". 4th International Conference on HYDROCYCLONES, Southampton, UK : 23-25 September 1992, pp. 229-241.

Muschelknautz, E., (1970). "Design of Cyclone Separators in Engineering Practice". Staub-Reinhalt Luft, Vol. 30, No.5, pp. 1-12.

Nebrensky, J.R., Morgan, G.E., Oswald, B.J. (1980). "Cyclones for gas/oil separation". Int. Conf. On Hydrocylones, paper 12, pp. 167-178. BHRA, Cranfield.

Nieuwstadt, F.T.M., Dirkzwager, Maarten (1995). "A Fluid Mechanics model for an Axial Cyclone Separator". Ind. Eng. Chem. Res., Vol. 34, pp. 3399-3404

Ogawa, A. (1987). "Particle and Multiphase Procaesses". Ed. Ariman, T., Nejat

Veziroglu, T., Hemisphere Publishing Corp., Washington, pp. 129-146.

Parker, J., Jain, R., Calvert, S., Drehmel, D., Abbot, J. (1981). "Particle Collection in Cyclones at High Temperature and High Pressure". Environ. Sci. Technol., Vol. 15, pp.451

Phillips, H.W., Deakin, A.W., (1991). "Separation Process Intensification - Gas Liquid Cyclones". CALTEC Report No. CR3191.

Plekhov,I.M., Ershov,A.I. (1971). "Investigations of a Direct Flow Centrifugal Separator".Translation from Khim. Neft., Vol 8, pp. 682-684.

Plitt, L.R. (1976). "A mathematical model of the hydrocyclone classifier". CIM Bulletin, December, pp.114-122.

Rietema, K (1961). "The Mechanism of the Separation of Finely Dispersed Solids in Cyclones".Cyclones in Industry, Elsevier Publishing Company

Schubert and Neesse (1980). "A hydrocyclone separation model in consideration of the turbulent multi-phase flow". Proc. Int. Conf. On Hydrocylones, Cambridge, 1-3 October 1980, Paper 3, pp.23-36. BHRA Fluid Engineering, Cranfield.

Seillan, M., (1929). "Note on Dust Removing Centrifuges" (in French). Chaleur et Ind., Vol. 10, pp.233-238.

Shepperd, C.B., Lapple, C.E., (1939). "Flow Pattern and Pressure Drop in Cyclone Dust Collectors". Ind. Engng. Chem., Vol 31, No. 8, pp.972-984.

Shepperd, C.B., Lapple, C.E., (1940). "Flow Pattern and Pressure Drop in Cyclone Dust Collectors - Cyclone without Inlet Vane". Ind. Engng. Chem., Vol 32, No. 9, pp.1246-1248.

Smith, J.L., (1961). ASME Paper No. 61-WA-189.

Stairmand, C.J., (1949). "Pressure Drop in Cyclone Separators". Engineering, pp. 409-412

Stenhouse, J.I.T., Trow,M (1985). "Particle Separation Efficiency of Uniflow Cyclones". Proc. Meet. Filt. Soc. On Gas Cyclones, London

Stenhouse, J.I.T., Trow, M., (1979). "The Behaviour of Uniflow Cyclones". 2nd World Filtration Congress, London, pp.151-156.

Stern, A.C., (1937). "The Separation and Emission of Cinders and Flyash". Trans. ASME, Vol. 39, pp. 289-296.

Strauss, W., (1966). "Industrial gas cleaning". Pergammon Press.

Svarovsky, L., (1984). "Hydrocyclones". Holt, Reinhart and Winston.

Svarovsky, L., (1996). "A critical review of hydrocylone models". Hydrocyclones '96, pp. 17-30.

Swanborn, R.A., (1988). "A New Approach to the Design of Separators for the Oil Industry". Ph.D. Thesis Delft University.

Taitel, Y. and Duckler, A.E., (1976). "A model for predicting flow regime transitions in horizontal and near horizontal gas-liquid flow". AIChE J., 22, pp.47-55.

Umney, L.E.R., (1948). "Theory and Design of an Improved Centrifugal Air Cleaner". National Gas Turbine Establishment Report No. RR 33.

Van Dongen, J.R.J., Ter Linden, A.J. (1958). "The Application of Gas/Liquid Cyclones in Oil Refining". Trans. ASME, Vol. 80, pp. 245-251.

Yoshioka, N., Hotta, Y. (1955). "Liquid cyclone as a hydraulic classifier". Chemical Engineering Japan. Vol 19 (12), pp. 632-640.

APPENDIX A

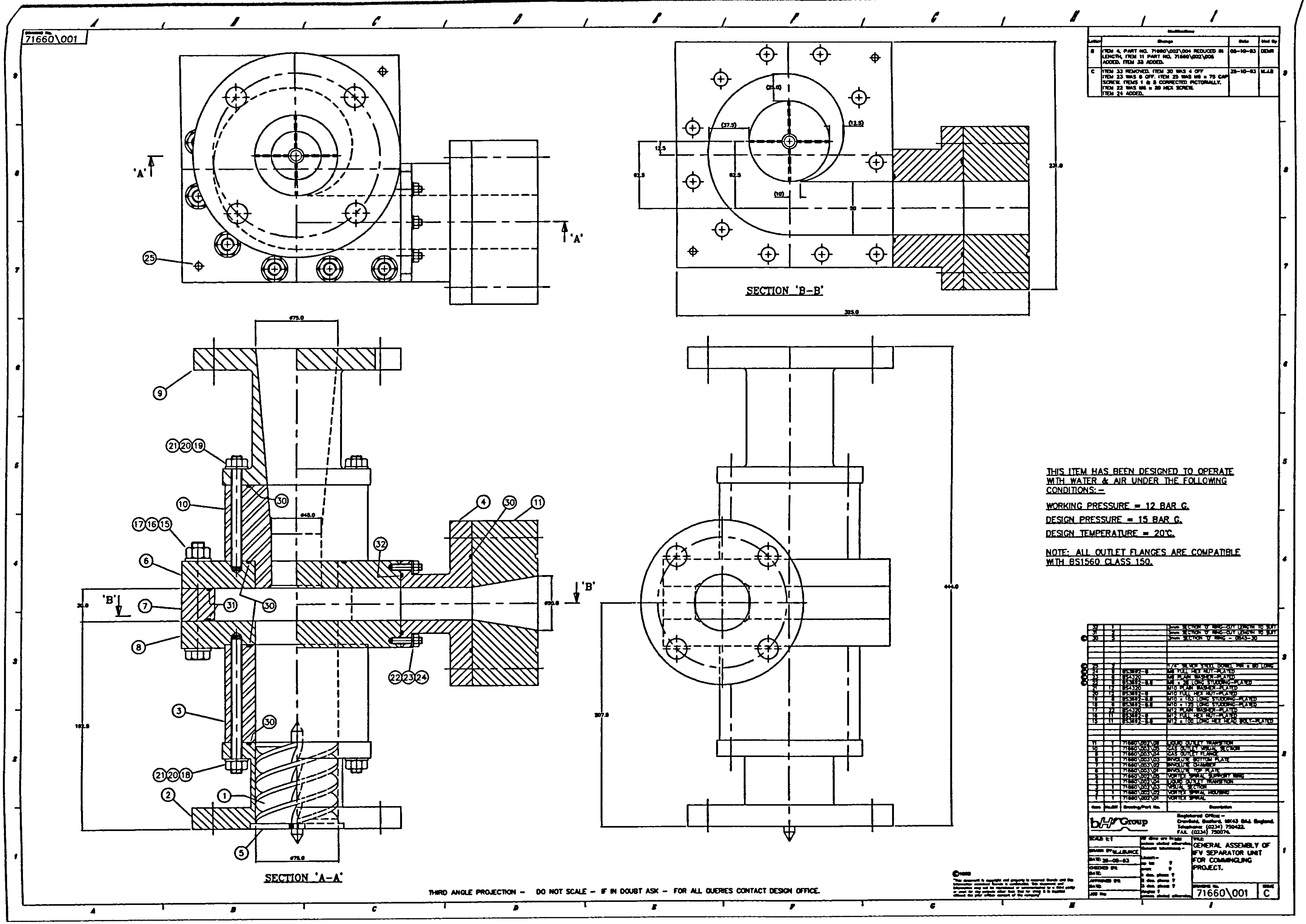
71660\001
ITEM 4, PART NO. 71660\002\004 REDUCED IN LENGTH, ITEM 11 PART NO. 71660\002\006 ADDED. ITEM 33 ADDED.
ITEM 33 REMOVED. ITEM 30 WAS 4 OFF ITEM 23 WAS 6 OFF. ITEM 25 WAS M6 x 75 CAP SCREW. ITEMS 1 & 8 CORRECTED PICTORIALLY. ITEM 22 WAS M6 x 20 HEX SCREW. ITEM 24 ADDED.
25-10-93
SECTION 'B-B'
SECTION 'A-A'
'A'
'B'
THIS ITEM HAS BEEN DESIGNED TO OPERATE WITH WATER & AIR UNDER THE FOLLOWING CONDITIONS:-
WORKING PRESSURE = 12 BAR G.
DESIGN PRESSURE = 15 BAR G.
DESIGN TEMPERATURE = 20°C.
NOTE:- ALL OUTLET FLANGES ARE COMPATIBLE WITH BS1560 CLASS 150.
M10 PLAIN WASHER-PLATED
M10 FULL HEX NUT-PLATED
M12 PLAIN WASHER-PLATED
M12 FULL HEX NUT-PLATED
LIQUID OUTLET TRANSITION
GAS OUTLET VISUAL SECTION
GAS OUTLET FLANGE
INVOLUTE BOTTOM PLATE
INVOLUTE CHAMBER
INVOLUTE TOP PLATE
VORTEX SPIRAL SUPPORT RING
VISUAL SECTION
VORTEX SPIRAL HOUSING
VORTEX SPIRAL
bHr Group
Telephone: (0234) 750422.
FAX. (0234) 750074.
SCALE 1:1
GENERAL ASSEMBLY OF IFV SEPARATOR UNIT FOR COMMINGLING PROJECT.
71660\001
C
THIRD ANGLE PROJECTION - DO NOT SCALE - IF IN DOUBT ASK - FOR ALL QUERIES CONTACT DESIGN OFFICE.

6

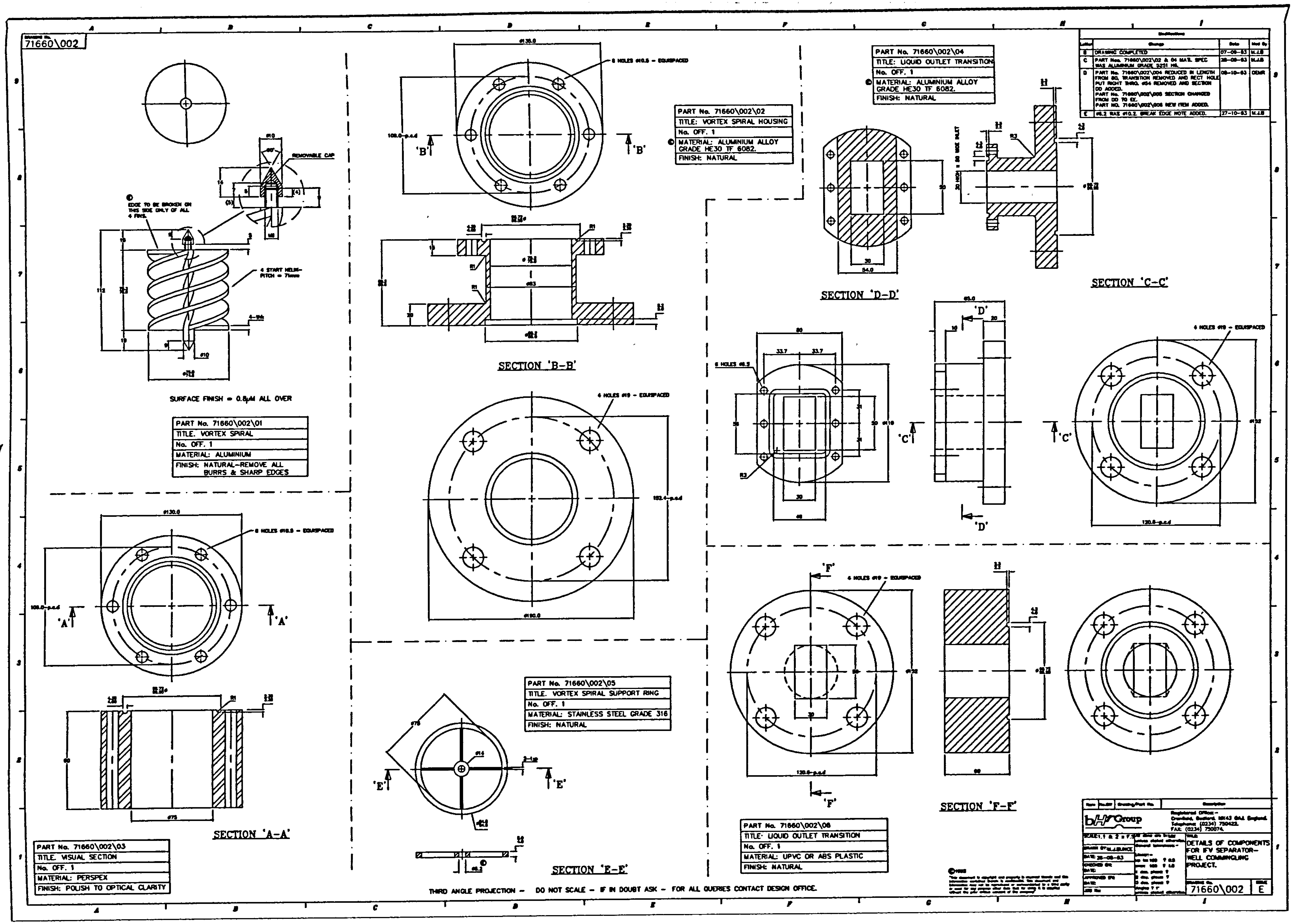
71660\002
REMOVABLE CAP
EDGE TO BE BROKEN ON THIS SIDE ONLY OF ALL 4 FINS.
4 START HELIX– PITCH = 71mm
SURFACE FINISH = 0.8μM ALL OVER
PART No. 71660\002\01
TITLE. VORTEX SPIRAL
No. OFF. 1
MATERIAL: ALUMINIUM
FINISH: NATURAL–REMOVE ALL BURRS & SHARP EDGES
8 HOLES ⌀10.5 – EQUISPACED
SECTION 'A-A'
PART No. 71660\002\03
TITLE. VISUAL SECTION
No. OFF. 1
MATERIAL: PERSPEX
FINISH: POLISH TO OPTICAL CLARITY
SECTION 'B-B'
4 HOLES ⌀19 – EQUISPACED
PART No. 71660\002\02
TITLE: VORTEX SPIRAL HOUSING
No. OFF. 1
MATERIAL: ALUMINIUM ALLOY GRADE HE30 TF 6082.
FINISH: NATURAL
PART No. 71660\002\05
TITLE. VORTEX SPIRAL SUPPORT RING
No. OFF. 1
MATERIAL: STAINLESS STEEL GRADE 316
FINISH: NATURAL
SECTION 'E-E'
PART No. 71660\002\04
TITLE: LIQUID OUTLET TRANSITION
No. OFF. 1
MATERIAL: ALUMINIUM ALLOY GRADE HE30 TF 6082.
FINISH: NATURAL
SECTION 'D-D'
SECTION 'C-C'
6 HOLES ⌀6.5
PART No. 71660\002\06
TITLE: LIQUID OUTLET TRANSITION
No. OFF. 1
MATERIAL: UPVC OR ABS PLASTIC
FINISH: NATURAL
SECTION 'F-F'
C PART Nos. 71660\002\02 & 04 MAT'L SPEC WAS ALUMINIUM GRADE 5251 H8. 28-09-83 M.J.B
D PART No. 71660\002\004 REDUCED IN LENGTH FROM 80. TRANSITION REMOVED AND RECT HOLE PUT RIGHT THRO. ⌀54 REMOVED AND SECTION DD ADDED. PART No. 71660\002\005 SECTION CHANGED FROM DD TO EE. PART NO. 71660\002\006 NEW ITEM ADDED. DEMR
E ⌀6.2 WAS ⌀10.2. BREAK EDGE NOTE ADDED. 27-10-83 M.J.B
bHr Group
Registered Office:- Cranfield, Bedford, MK43 0AJ England. Telephone: (0234) 750422. FAX: (0234) 750074.
DATE: 28-09-83
TITLE: DETAILS OF COMPONENTS FOR IFV SEPARATOR–WELL COMMINGLING PROJECT.
71660\002 E
THIRD ANGLE PROJECTION – DO NOT SCALE – IF IN DOUBT ASK – FOR ALL QUERIES CONTACT DESIGN OFFICE.

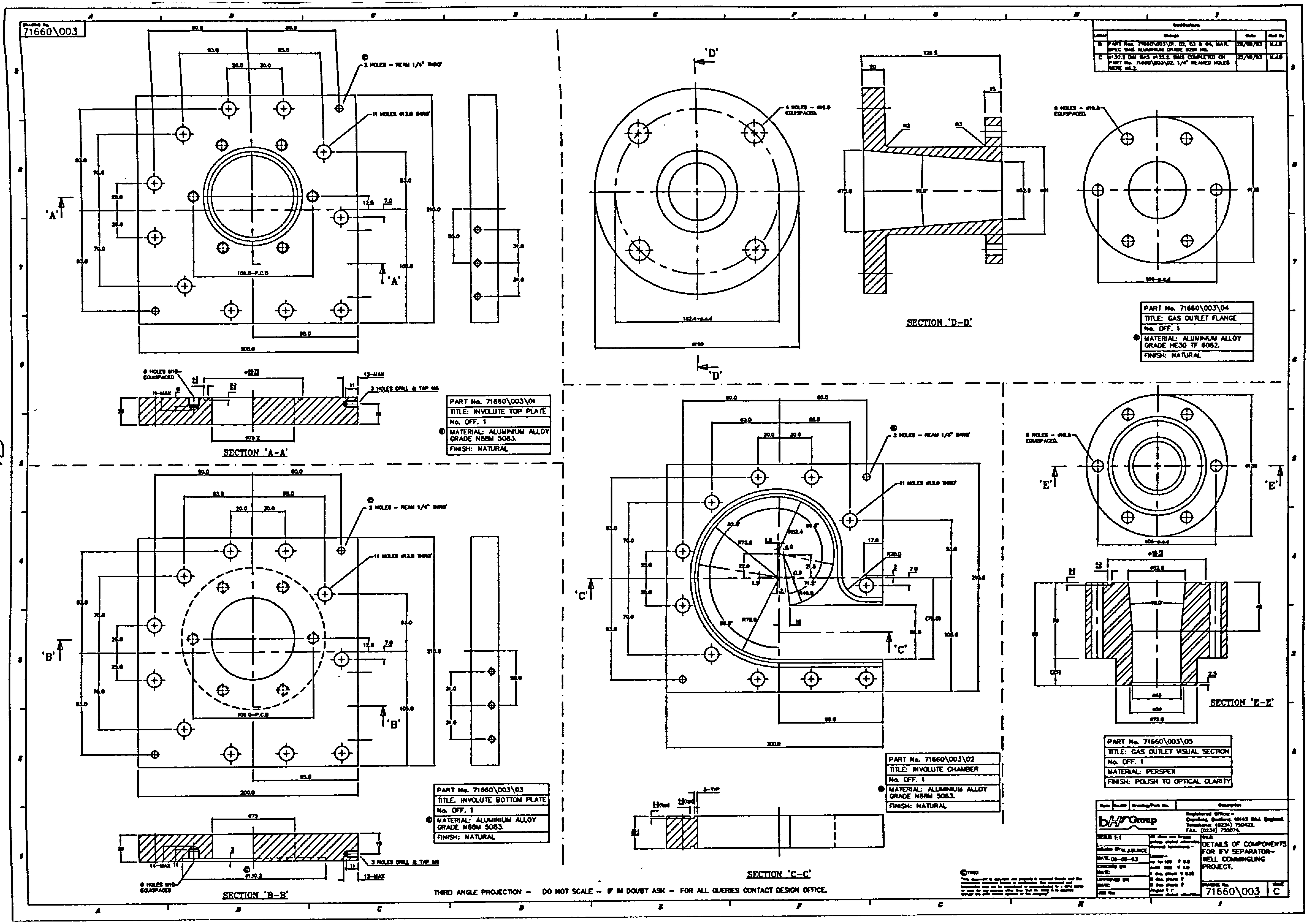
71660\003
SECTION 'A-A'
PART No. 71660\003\01
TITLE: INVOLUTE TOP PLATE
No. OFF. 1
MATERIAL: ALUMINIUM ALLOY GRADE N88M 5083.
FINISH: NATURAL
SECTION 'B-B'
PART No. 71660\003\03
TITLE: INVOLUTE BOTTOM PLATE
No. OFF. 1
MATERIAL: ALUMINIUM ALLOY GRADE N88M 5083.
FINISH: NATURAL
SECTION 'D-D'
PART No. 71660\003\04
TITLE: GAS OUTLET FLANGE
No. OFF. 1
MATERIAL: ALUMINIUM ALLOY GRADE HE30 TF 6082.
FINISH: NATURAL
SECTION 'C-C'
PART No. 71660\003\02
TITLE: INVOLUTE CHAMBER
No. OFF. 1
MATERIAL: ALUMINIUM ALLOY GRADE N88M 5083.
FINISH: NATURAL
SECTION 'E-E'
PART No. 71660\003\05
TITLE: GAS OUTLET VISUAL SECTION
No. OFF. 1
MATERIAL: PERSPEX
FINISH: POLISH TO OPTICAL CLARITY
THIRD ANGLE PROJECTION – DO NOT SCALE – IF IN DOUBT ASK – FOR ALL QUERIES CONTACT DESIGN OFFICE.
bHR Group
DETAILS OF COMPONENTS FOR IFV SEPARATOR-WELL COMMINGLING PROJECT.
71660\003
C

APPENDIX B

RENTAIR
57, Windsor Avenue, Wimbledon, London SW19 2SW **Tel**: 0181 542 8531 **Fax**: 0181 543 3579

More information over leaf

ELECTRIC COMPRESSORS		SL75	SL90	SL110	SL132	SL150
Normal effective working pressure	bar	7	7	7	7	7
	psi	102	102	102	102	102
Actual free air delivery at full load, at max. speed and at normal effective working pressure(l)	m^3/min	13.7	16.2	19.4	22.7	26
	cfm	483.6	571.9	688.7	801.3	917.8
Number of compression stages		2	2	2	2	2
Cooling system		Air	Air	Air	Air	Air
Start up	amps	391	441	678	656	778
Running	amps	170	210	251	274	324
Overall Length (A)	mm	2693	2693	2693	2693	2693
	in	106.1	106.1	106.1	106.1	106.1
Overall Width (B)	mm	1588	1588	1588	1588	1588
	in	62.6	62.6	62.6	62.6	62.6
Overall Height (C)	mm	2370	2370	2370	2370	2370
	in	93.4	93.4	93.4	93.4	93.4
Mass (unit in operating condition) approx.	kg	2430	2580	2650	2800	3000
	lb	5357.2	5687.9	5842.2	6172.9	6613.8
Noise level (acc. ISO 2151 at 7m distance) of the unit running at max. speed and normal working pressure	dB(A)	79	79	79	79	79

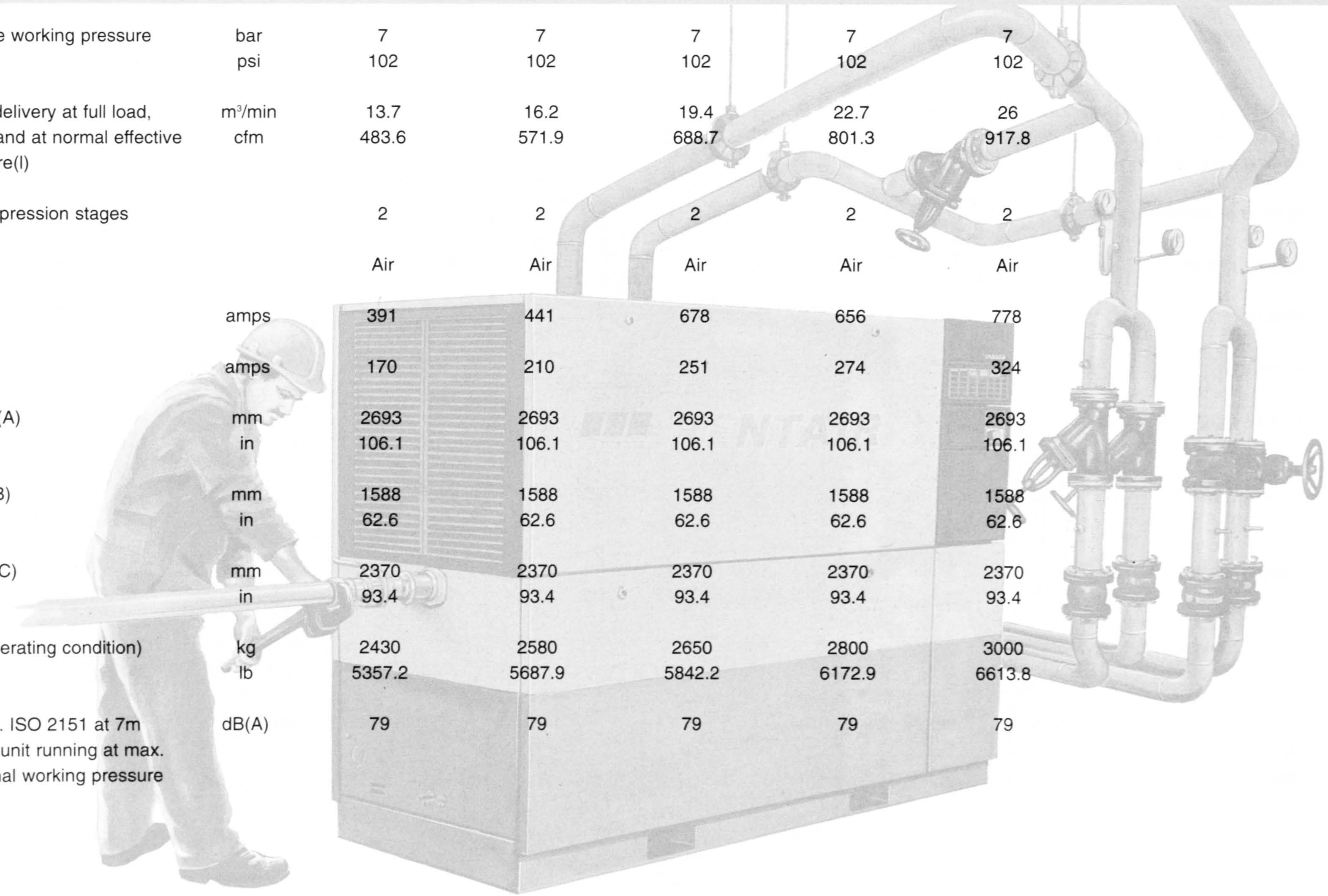

RENTAIR
57, Windsor Avenue, Wimbledon, London SW19 2SW **Tel**: 0181 542 8531 **Fax**: 0181 543 3579

More information over leaf

ELECTRIC COMPRESSORS		ML11	ML15	ML18.5	ML30	ML45	ML55	ML75	ML90	ML110	ML132	ML150
Normal effective working pressure	bar	7.5	7.5	7.5	7.5	7.5	7.5	7.5	7.5	7.5	7.5	7.5
	psi	110	110	110	110	110	110	110	110	110	110	110
Actual free air delivery at full load,	m^3/min	1.64	2.7	2.91	4.3	7.4	9.9	13.3	16.7	20	23	27
at max. speed and at normal effective	cfm	58	80	103	152	262	350	470	590	706	812	953
working pressure(l)												
Number of compression stages		1	1	1	1	1	1	1	1	1	1	1
Cooling system		Air	Air	Air	Air	Air	Air	Air	Air	Air	Air	Air
Start up	amps	63	94	105	161	265	365	395	478	551	776	853
Running	amps	24	32	40	55.2	96	104.7	156	200.8	240	278	309
Overall Length (A)	mm	1210	1210	1210	1460	2590	2610	2610	2770	2770	2770	2770
	in	47.7	47.7	47.7	57.5	102	102.8	102.8	109.4	109.4	109.4	109.4
Overall Width (B)	mm	700	700	700	700	1067	1320	1320	1320	1320	1320	1320
	in	27.6	27.6	27.6	27.6	42	52	52	52	52	52	52
Overall Height (C)	mm	1100	1100	1100	1100	1042	1365	1365	1700	1700	1700	1700
	in	43.3	43.3	43.3	43.3	41.1	53.8	53.8	67	67	67	67
Mass (unit in operating condition)	kg	420	456	456	610	1008	1475	1585	2430	5676	2590	2600
approx.	lb	924	1003	1003	1345	2222	3245	3487	5346	12487	5698	5720
Noise level (acc. ISO 2151 at 7m	dB(A)	70	71	72	73	75	75	76	76	76	77	77
distance) of the unit running at max.												
speed and normal working pressure												

1 INTRODUCTION

All radiation beams are attenuated by material placed in their paths. Attenuation depends mainly on the thickness of the material and its density. The GammaTrol Density Gauge monitors this attenuation to produce an exact indication of density in liquids and gases.

The system is non-invasive. The detector is externally mounted on pipes and vessels; a great advantage in many applications. There are no moving parts. This, combined with the reliability of the latest in electronic components has produced a system which is virtually maintenance free.

The gauge consists of a radioactive source in a shielded container, a Detector and a Signal Processor. The detector is housed in a flameproof enclosure and is suitable for use in Zone 1 areas. The Signal Processor must be mounted in a 'Safe' area. Units are provided for wall, panel or rack mounting.

The Signal Processor interrogates the signal from the detector and computes the density of the process medium. Information is displayed on a small liquid crystal display mounted on the front panel and is transmitted in standard 4-20 mA form or by RS232 link. Integral alarm relays may be set to any density in the operating range and in addition, a watchdog alarm is available. The unit will be normally calibrated via the keypad on the front panel. A calibration mode is selected where information is entered when requested by the display. The RS232 link may be used to calibrate the signal processor remotely.

1.1 Principle of Operation

A narrow beam from the radioactive source is directed through the vessel or pipe to a detector mounted opposite. The beam will be attenuated by the vessel walls and the process medium. As attenuation by the walls is constant any variation in intensity at the detector will be caused by the process medium. During calibration a density to radiation intensity relationship is established which allows the Signal Processor to compute any density from the measured intensity at the detector.

The Detector (PRI 116) comprises a scintillator (crystal) and a high voltage photomultiplier tube. Gamma radiation entering the crystal produces minute pulses of light at a frequency proportional to the intensity of radiation. The light pulses are detected by the photocathode of the photomultiplier tube and converted to small voltage pulses. These are amplified within the tube to a size sensible for further amplification by the detectors electronic circuit.

Pulses of a standard height are then passed via the interconnecting cable to the Signal Processor (PRI 121). This is a computerised unit which counts the incoming pulse-rate. Because of the statistically random nature of this pulse stream an integrating factor (time constant) is applied. This steadier signal is computed into a figure for density. Temperature correction may be made before a final density figure is displayed and transmitted to the plants instrumentation.

2 SPECIFICATION

2.1 PRI 121 Signal Processor

Power Supply	110-120 or 220-240 VAC ± 10% 50-60 HZ 24 VA
Detector Input	6 to 12 volt negative going pulses from a positive supply level. Pulse duration is 4 uS.

Other Inputs

Keyboard	18 keys with tactile feel comprising WATCHDOG RESET, SYSTEM RESET, MODE, ENTER, 1, 2, 3, 4, 5, 6, 7, 8, 9, 0, ., +, - and < (delete).
Analogue Input 1 (temperature correction)	4-20 mA, 56R input resistance. Temperature range -99 to 999°C
Digital Correction (alternative temp correction)	Positive Pulses; 5 to 12V, 10 uS min duration. Selectable frequency/temp range.
RS232 Link	Full Duplex communication port allows remote indication and calibration of the Signal Processor.

Outputs

Analogue Output 1	4-20 mA, galvanically isolated up to 500VDC. May be assigned to density, temperature corrected density or percent concentration.
Analogue Output 2	4-20 mA, galvanically isolated up to 500VDC. May be assigned to density, temperature corrected density or percent concentration.
RS232 Link	The same communication link as described in "Other Inputs" is used to give full on-line information.
Liquid Crystal Display	20 x 4 Alphanumeric characters. Displays current date, time and measurement. Displays information required during calibration and simulation.

Alarm	Three single pole relays as level alarms. May be selected as high or low alarms.. A single pole relay as watchdog alarm to indicate computer failure. Contacts rated at 100VDC, 0.5 Amps. Open on alarm.

Performance

Range	0 to 10 g/ml
Accuracy	Depends on the strength of the radiation field at the detector and the selected response time.
Response Times	Selectable, FIXED or DYNAMIC. Fixed range is 0.1 to 999 seconds. Dynamic response is two state, with automatic selection of short response time for large signal changes and longer response time for small signal changes. Range is 0.1 to 999 seconds.
Data Retention	3 months from removal of power.

Other Data

Operating Temp Range	0 to 50°C
Storage Temp Range	-10 to 50°C
Relative Humidity Range	0 to 95 percent
Electrical Safety	Designed to conform to IEC 348 European Safety Requirements for Electrical Measuring Apparatus.

Mechanical

Wall Mounting (Single Unit) (Figure 1)	Framework clips to wal plate. Wallplate fixing is by 4 holes (5mm dia) on 80mm centres. Electronic module slides and connects into framework. Full plastic body cover provided. Overall dimensions with cover are 179(H) x 163(W) x 207(D)mm excluding 14mm handle projection. Total weight = 3.5 kg.
Panel Mounting (Single Unit) (Figure 2)	Framework fixed to aperture in panel using side clamps. Aperture size 133(H) x 162(W)mm. Depth behind panel = 200mm. Total weight = 3.0 kg.

Sub-Rack Mounting (Figure 3)	Up to 3 electronic modules accommodated in a 19" sub-rack. Sub-rack chassis dimensions are 482(W) x 133(3U high) x 240mm. Note: the 1/0 terminals project 31mm below the sub-rack chassis so a height of 4U must be allowed for when stacking sub-racks. Weight of empty sub-rack = 2.3 kg; weight of full sub-rack = 7.1 kg.

2.2 PRI 116 Detector (Figure 4)

Supply	+ 12VDC nominal
Signal	12V negative going pulse train from a positive potential 4 microsecond pulse width.
Sensor	50mm diameter NaI scintillation crystal with photmultiplier tube.
Operating Temp Range	-20 to 60°C
Storage Temp Range	-20 to 60°C
Sealing	To IP65
Electrical Safety	Flameproof enclosure certified to EExd IIC T6 BASEEFA Certificate No. Ex 88B1105. Suitable for Zone 1 operation.
Size	328 x 122mm tubular stainless steel body, centrally welded to 10 x 170mm square mounting plate.
Weight	18 kg

2.3 Interconnecting Cable

Recommended Armoured	ICI cable CC08BB 0.75mm^2, two twisted pairs - 12mm OD.
Recommended Non-Armoured	ICI cable CC07BB 0.75mm^2, two twisted pairs - 7.4 mm OD. BICC/DELTA/STC cable, DEF 16-12 (16-2-3C) 0.5mm^2 3 core screened - 7mm OD.

4.3 Calibration

4.3.1 Introduction

The system keypad and Liquid Crystal Display are used to input all the set-up information and calibration data. The calibration mode is entered by pressing the MODE key for 5 seconds. The main menu then appears on screen.

Set Time / Date	0
Test	1
Calibrate Hardware	2
Calibrate Software	3

Keypad Number

All these options are used to a greater or lesser degree in the calibration routine.

The set time / date option will be used to register the calibration date in the computers memory so that it may accurately compensate for the gradual decay in source strength with time.

The test option has been described in detail and is used in the calibration routine to contribute the figure for background countrate and also Io, the pulse rate corresponding to a reference density.

The calibrate hardware option is used to select the source type and system deadtime, to calibrate the analogue signals and to set the digital inputs and outputs. These are the RS232 port and the coded pulse input. The latter is an option which may be set if a Coded Pulse Detector type PRI 116C is used.

System equations are chosen, parameters set and functions assigned in the calibrate software option. Most of the effort in calibrating the density gauge will be concentrated here.

Two flowcharts are shown in this calibration routine, one for calibrate hardware and the other for calibrate software. Each column in the chart approximates to a displayed screen. The characters in brackets show the key sequence required to select that option. The first character M stands for the MODE key. The ENTER key may be used to return towards the main menu. A full Menu Listing describing each screen option appears later in this manual.

4.3.2 Calibration Routine (Basic Parameters)

All normal density systems will use a logarithmic equation to calculate density. This equation requires three parameters, a reference (know) density figure, the countrate at this density and the calibration constant K of the process medium. To simply display a density measurement, the only other requirements are the calibration date, source type, system deadtime and background

counts. Source type and system deadtime are entered in the calibrate hardware option of the main menu. The others are described as follows:

Set time and date (main menu)

This is the calibration time stamp which is required when the countrates are first entered or subsequently changed. It allows the computer to compensate for the reduction in countrate due to source decay. This is a natural aging process of known dimension.

enter as DD.MM.YY
and HH.MM.SS

A 24 hour clock is used.

Obtain background count

A figure for background countrate needs to be entered in the calibrate software section. This is the countrate (received from the detector) which is caused by natural or background radiation. When the system is running normally this is subtracted from the total countrate so that the calculated density is based only on radiation resulting from the source.

To obtain a background count select Test from the main menu, then Test inputs and Test detector. With the source container empty of the radioactive source/holder obtain and note the countrate due to background radiation. A 100 second count will suffice.

If nobody is authorised to remove the source holder, a figure of 50 counts/sec may be safely assumed for the PRI 116 detector.

Obtain countrate for a known density (Io)

This figure will also be entered later in the calibrate software section. This known density/countrate relationship is used by the computer in the logarithmic algorithm for calculating measured density (see section 'Calculations - Logarithmic calibration').

There are three methods which can be used to obtain this relationship.

The first and most accurate is to fill the vessel or pipe with the same material as the process medium and then determine its density by sample analysis. Take the temperature into account.

The second is to fill the vessel or pipe with a convenient medium (usually water) at a known temperature. Knowing the temperature the density can be accurately calculated.

The third is to take a countrate with the vessel empty, ie, an air count with an assumed density of .001 g/ml.

Obtain a value for Constant K

This is used in the logarithmic equation for calculating density. If it is known there is not a problem. If it is unknown it can be accurately calculated. Two reference densities are required. Refer to the section on **calculations - calibration constant** for the method of calculating K.

4.3.3 Calibration Routine (Hardware)

The following is a brief explanation of the **calibrate hardware** option in the main menu. For a detailed description of screens in this option consult the **screen menu listing** in this manual.

This calibrate hardware option fixes source type and system deadtime and provides a means of calibrating the 4-20 mA input and outputs. The RS232 communications port may be set if there is to be direct communication with a host computer. If a Coded Pulse Detector (Type PRI 116C) is used the settings required by the signal processor are entered in the last of the sub-options.

These sub-options are presented on screen are:

Source / Dead Time	**0**
Analogue I/O	**1**
RS232 Port	**2**
Coded Pulse Input	**3**

Source / Dead Time

Any reduction in source strength due to natrual decay effects measuring accuracy and needs to be compensated for. The three source types which may be used in this density system decay at different rates. The chosen source type is entered here.

Analogue I/O

The three analogue ports used in a density gauge are calibrated through the keyboard.

To calibrate the current input (temp. compensation) inject a known and steady current in the range 4-20mA between terminals 19 (+ve) and 20. Select input 1 (screen M210). The current measured by the signal processor appears in brackets. If this is inaccurate enter the correct value to one decimal place.

The current outputs may be calibrated by monitoring the current between terminal pins 29 (+ve) and 30 for output 1 and between pins 33 (+ve) and 34 for output 2. Select screen M211 for output 1 and M212 for output 2. If the current of 10.00 mA displayed in brackets does not tally with the monitored current, enter the correct value. Repeat for output 2.

Equations

There are three possible options for converting countrate into a density reading.

The Logarithmic option will be chosen for all standard density systems and this equation requires a figure for the calibration constant K. A guide to arriving at a value for K is given in the following section on calculations. The logarithmic option should be used in all density gauging applications unless Tracerco give specific alternative advice.

The Linear option requires a figure for the slope of the relationship counts per unit density. The unit of density in question is 1 g/ml.

Where neither of these options gives a true density to countrate relationships, co-ordinates should be selected. Here a density relationship over any range may be established with up to 11 density / countrate points. A straight line is assumed between each point. Include background counts.

Units of density need to be entered as g/ml or kg/m^3. 1 g/ml = 1000 kg/m^3.

If a temperature corrected reading or output is required, the temperature co-efficient of the material in units x $10^{-5}/°C$ will be entered. A reference temperature is also required. The measured reading will be normalised to give the equivalent density at the reference temperature.

In addition to straight forward density measurement, the concentration of one medium within another can be calculated and displayed as a percentrage of total weight. The equation for calculating this is true for all imiscible materials and for some soluble ones such as salt in water. For those concentrations where the equation will not give a true result a "look-up table" must be used. If in doubt about which option (equation or look-up table) to use consult ICI Tracerco.

The calculation may be based on the measured density or temperature corrected density.

If the equation option has been chosen for calculating concentration, two reference co-ordinates are required. A co-ordinate in this case is the density at a known percentage concentration. From these two density/concentration relationships any concentration between 0 and 100% is calculated from the measured density or temperature corrected density.

If the concentration is greater at higher density levels the equation gives the concentration of the higher density medium.

If the concentration is less at higher density levels the equation will give the concentration of the lower density medium.

Refer to the following section on calculations for the full equation.

If the look-up table option has been chosen up to 11 density/concentration points can be entered with a straight line assumed between each point. Density is entered in g/ml and concentration as a percentage.

Counts

The background countrate and the Io (known density) countrate are entered. In each case a count period and the total countrate for that period is requested. To obtain these countrates use the test routine from the main menu to test the detector pulserate. It is on these countrates, especially the Io count, that the accuracy of measurement depends. Aim to accummulate at least 10^6 counts on test, the more the better. These counts are used in the log equation for calculating density (see section on calculations).

Input / Output Range

All output ranges are 4-20 mA. The temperature correction input may be 4-20 mA or it may be a digital pulse input with two frequency / temperature points.

For the outputs, decide on a range and select output 1 or 2. Enter the density for 4 mA, then the density for 20 mA. The outputs will be assigned later.

Analogue input 1 (see system wiring diagram) is used for the correction input. It will be ranged to match the plants temperature transmitter. The alternative to an analogue input is a digital (or pulse frequency) input. Here two reference points of frequency to temperature are chosen.

Assign Input / Output

With this option output ranges, the display and the RS232 link (if used) are assigned to one of the three types of measurement. Considering the two analogue outputs available, each may be assigned to a different measurement, eg, output 1 could be assigned to density and output 2 to temperature corrected density or alternatively O/P 1 to TC density and O/P 2 to percentage concentration.

The available temperature correction signal is entered. This may be a 4-20mA analogue signal or a pulse frequency input.

The type of detector is also selected, STD PULSE for the standard detector type PRI 116 which has a pulse output at a random frequency or a CODED PULSE detector type PRI 116C which returns a simplex RS232 signal.

The Liquid Crystal Display is selected to show the main measurement.

Response Time

The response time of the instrument is a compromise between fast response and accuracy. The random pulse rate from the detector is distributed about a mean value. These fluctuations are passed through a digital filter to achieve a more steady mean. For a step change the output of the filter reaches about 63% of its final value in the response time.

For a fixed response time settings can be 0.1 to 99 seconds.

The Dynamic Response is more sophisticated. It will automatically switch between a short response time for large signal changes and a larger respone time for steady state conditions. The two times are fixed values and are chosen as described in the following section on calculations.

Calibration Routine (Test and Parameter Check)

Once calibration is complete the computation of density or concentration by the signal processor may be checked by entering a simulation mode.

Select the Test option from the main menu and then the simulation mode. A simulation count is requested (counts per second). Enter a count expected during operation, preferably one which will give a known density reading then press ENTER. The desired reading should appear on screen. If not, parameters should be checked for correct entry.

A parameter check is provided in the Test menu. Select display parameters. All parameters entered during calibration may be displayed. Use the ENTER key to exit the option.

Then revert back to the main menu and press the ENTER key once more. The display will show:

Saving calibration data
please wait

This process takes about 15 seconds after which the system enters normal running mode.

One note of caution. If the programme fails to run it will most likely put up a detector fail notice. Check that pulses are being received using the Test option. If this, and the simulation are OK the most likely fault is incorrect assignment of detector type in screen M342. Check this.

5 CALCULATIONS

The signal processor computes the density or concentration from the incoming countrate. Several basic algorithms are used, they are described here.

5.1 Response Time

In traditional nucleonic systems, an analogue integrator was used to average the counts. In the PRI 121, an averaging algorithm mimics the action of an analogue integrator and also provides a simple variable to allow the effective time constant or response time to be changed.

The PRI 121 control unit accummulates counts (ie, voltage pulses which are produced by the detector) in successive time increments. The time period over which a count is accummulated is 0.1 seconds.

The smoothed or average count rate I which is subsequently processed to produce a density value is related to the previous smoothed countrate Ip and the current countrate Ic through the algorithm.

$$I = Ip + ((Ic - Ip)/ F)$$

where I is changed every 0.1 seconds and F is a factor whose magnitude determines the weighting to be given to the current countrate. The numerical value of F is the effective time constant or response time in seconds.

F is either a fixed or dynamic and is set during calibration using the response time menu.

If a fixed time constant is selected, then F is fixed at the stored value.

If a dynamic response time is selected, then F is automatically chosen to suit the incoming countrate. A short time constant is applied to large significant changes to give the instrument a fast response time. A long time constant is applied to small signal changes to reduce the statistical noise when the density is steady.

The method used by the computer to test for a step change is to look for new countrates that are more than two standard deviations from the average countrate I. Sometimes this will be noise and so the computer will only switch to a faster time constant if 3 consecutive readings are out of the two standard deviations range. The computer switches back to the slow time constant whenever a new reading (current countrate) is within two standard deviations of the previous averaged countrate.

5.2 Logarithmic Calculation

The equation normally used for calculating density is:

$$I = Io\, e^{-ux(p - po)}$$

where :

I	=	countrate	
Io	=	reference countrate	
u	=	mass absorption co-efficient	in cm^2/gm
x	=	path length	in cm
p	=	density	in g/ml
po	=	density at the reference countrate	in g/ml

re-arranging gives:

$$p = po - Ln \left(\frac{I}{Io} \right) (k) \text{ g/ml}$$

where : K = constant = 1/ux

There is an offset to both I and Io from the natural background countrate Ib. The density equation then becomes:

$$p = po - Ln \left(\frac{I - Ib}{Io - Ib} \right) (k) \text{ g/ml}$$

5.3 Calculating K

The mass absorption figure u, may not be known for some materials. This requires the calibration constant K to be calculated using two known (reference) densities.

First set K to 1 and carry out an Io count with the first reference density as normal. With the process medium at the second reference density observe the indicated density. Apply the following equation to obtain the correct value of K.

$$K = \frac{Pref - Po}{Pind - Po}$$

where :

K	=	correct calibration constant
Po	=	first reference density used for the Io count g/ml
Pref	=	second reference density g/ml
Pind	=	the indicated density of Pref g/ml

5.4 Linear Calculation

The linear equation used for calculating density is:

$$p = po + \frac{(I - Io)}{(C)}$$

where :

I	=	countrate	
Io	=	reference countrate	
c	=	counts/unit density entered by user	
p	=	density	
po	=	density at the reference countrate	

As the equation relies on the difference between I and Io, the background count Ib has no effect and is ignored.

ICI will normally supply figures for a particular source/detector combination if the counts v density relationship is linear, however these figures can be determined experimentally. For a linear calibration, the following parameters must be entered.

Note: counts per unit density (C) are the counts per g/ml or Kg/m^3.

5.5 Concentration Calculation

Two known density / % concentration levels are required for the equation. The concentration by weight is calculated from the measured density as follows:

$$C \text{ (by weight) } \% = \frac{PxCx(Py-Pm) + PyCy(Pm-Px)}{Pm(Py-Px)}$$

where :

Px	=	density for concentration Cx	g/ml
Py	=	density for concentration Cy	g/ml
Pm	=	measured density	g/ml

All concentrations are percentages.

If the concentration rises with density, the percent concentration of the higher density medium is displayed.

If the concentration falls as density increases the percent concentration of the lower density medium is displayed.